Investigation into the Performance of Candle Filter Technology for the Separation of Metal Hydroxide Precipitates from an Aqueous Effluent

Elizabeth Camilla Kuiper

Preface

This study was carried out in association with NTNU and Glencore Nikkelverk. The study combines learning from the subject of filtration at NTNU with practical work at Glencore Nikkelverk in order to understand, gain experience and initiate operational improvements pertaining to filtration in the effluent treatment plant at Glencore Nikkelverk. I thank my NTNU supervisor, Professor Jens-Petter Andreassen, my Glencore Nikkelverk supervisor, Dr. Ing. Ole Morten Dotterud, and my supervisor and assistant in operating the pilot filter rig, Odd Willy Iglebæk, for the guidance in producing this paper.

Declaration of compliance
I declare that this is an independent work according to the exam regulations of the Norwegian University of Science and Technology (NTNU).

Place and date: Kristiansand, 17.06.2014   Signature:

Synopsis

The effluent treatment plant at Glencore Nikkelverk experiences the generation of liquid waste from various areas and processes in the plant. Being primarily a nickel refinery, but also producing copper and cobalt, the effluent contains significant concentrations of heavy metals. Such effluents are harmful to the environment. The effluent treatment plant thus operates to limit the discharge of harmful elements from the plant to the effluent, to allow the plant to comply to discharge limits set by authorities and to recover valuable elements from effluents for reprocessing. This is currently performed by means of metal hydroxide precipitation followed by solid-liquid separation.

The solid-liquid separation is carried out by manual chamber filter presses that require heavy manual labour and have thus been classified as a health hazard by the health, safety and environment department. An investigation is therefore done to assess the suitability of DrM Fundabac$^®$ candle filters as an alternative filtration technology by use of a DrM Fundabac pilot filter rig. The investigation analyses filtration performance while also exploring variations in general filtration behaviour. This is done by carrying out initial filter cloth screening tests in the laboratory to choose a suitable range of filter cloths for further testing. Filtration tests are then performed on the pilot filter, employing the chosen filter cloths. Operating parameters including filtration time, applied pressure and feed flowrate are evaluated. The feed to the filter varies continually and cannot be controlled. It is thus investigated how variations in feed affect variations in filtration in order to understand why filtration performance can change. Samples from the feed slurry, filtrate and filter cake are taken and analysed. Measurements from online data systems are recorded. These enable an overview of some of the primary particle properties, the state of the system and the secondary properties that together govern filtration.

The study shows that the pilot filter operates effectively and through the use of either DrM N 11 U 030 or Markert PPV 2737 filter cloth qualities, good filter cake release and production of filtrate of equal clarity to that of the currently employed filter presses is enabled. For optimal throughput of filtrate and good cloth-cake adhesion during filtration, the filtration time should be set to at least 40 minutes and the applied pressure to 4 bar. An increase in the pH in the range of 9 to 10 during the precipitation process is beneficial for filtration as it results in a higher concentration of solids in the feed to the filter. Both an increase in the solution pH and an increase in the feed solids concentration result in a decreased specific cake resistance and decreased filter cake moisture content. An increase in the feed solids concentration also results in an increase in the mass of filter cake produced. Further information on the particle size distribution in the solution is required in order to conclude on its effect on filtration. An increased concentration of nickel hydroxide precipitate and a decreased concentration of iron hydroxide precipitate in the feed appear to result in a lower specific cake resistance. It is recommended that the study continues whereby the mentioned filter cloths are operated on for a longer duration of time while also investigating the benefit of setting an even longer filtration time. The next stage of investigation will be to design a full-scale filter such that potential candle filter performance can be evaluated and compared to chamber filter press performance.

Table of Contents

List of Tables

List of Figures

Nomenclature

Symbol	Description	Units
V	cumulative volume of filtrate filtered in time (t)	[m^3]
t	time corresponding to point V	[s]
A	face area of filter bed	[m^2]
Δp	pressure drop over filter	[Pa]
μ	filtrate viscosity	[PaS]
c	concentration of solids in suspension	[kg/m^3]
α	specific filter cake resistance	[m/kg]
R_m	filter medium resistance	[1/m]
T	temperature	[°C]
pH	pH	[-]
δ	specific weight	[kg/m^3]
m	mass	[kg]
t_s	time elapsed from start of filtration to constant dP period	[s]
V_s	volume of filtrate passed through at t_s	[m^3]

Glossary

dP	Pressure drop experienced over the filter
Filter cake moisture content	Percentage of filter cake taken up by water
Filter cake filter capacity	Cumulative mass of filter cake produced during filtration
Filtrate filter capacity	Cumulative volume of filtrate passed through the filter during filtration
Medium resistance	Resistance to the flow of liquid experienced by the filter cloth
Specific cake resistance	Resistance to the flow of liquid experienced by the filter cake
PSD	Particle size distribution
SEM	Scanning electron microscope

1. Introduction

1.1. Background to Study

The industrial process at Glencore Nikkelverk experiences the generation of liquid waste. This waste contains metal impurities as a result of chemical processing, thus rendering it harmful to the environment. The effluent treatment plant at Nikkelverk performs three critical tasks; it limits the discharge of harmful elements from the plant to the effluent, it allows the plant to comply to discharge limits set by authorities and it recovers valuable elements from effluents for reprocessing. All effluent liquid streams from the plant enter the effluent treatment plant. Here, the waste is processed by means of chemical precipitation followed by solid-liquid separation.

Currently, solid-liquid separation is performed by chamber filter presses. These filter presses are more than 30 year old, are operated manually and require heavy manual labour for filter cake emptying. They have thus been classified as a health hazard by the health, safety and environment department. This study is an attempt to test the suitability of alternative filtration technology, namely the DrM Fundabac$^®$ candle filter. Due to the concentration of solids and the size of particles in the feed (which tend to be between 1 μm and 40 μm), the process is identified as requiring solids separation through surface filtration by means of pressure filtration. Fitting such criteria, the candle filter is a good alternative to the existing filter press installation: it is a mechanically simple system with a closed chamber that can provide good filtrate throughput and cake discharge using minimum floor space for large filtration areas. It is necessary to operate the filter for maximum efficiency. This includes evaluating the optimal operation parameters such as applied pressure, feed flowrate and filtration time. Critical to filtration performance is the employment of the correct filter cloth.

The feed to the effluent treatment plant varies continually and such variations are not controlled. It is therefore expected that filtration performance will vary. Analysis of how the change in feed affects filtration enables an understanding of why performance variations occur. There are three types of parameters that fully characterise the solid/liquid system and should be regarded when designing the filtration system. These are the primary properties, the state of the system and the macroscopic or secondary properties. The primary particle properties include description of the particle size and effect of pH on the surface properties of particles. The state of the system includes analysis of the concentration of particles in solution. Together, the primary properties and the state of the system govern the secondary properties that are measured in the application of the separation programme. These include analysis of the specific cake resistance and medium resistance. Filtration theory proposes a method of measuring the specific cake and medium resistances for a constant pressure filtration operation, and this theory can be applied to measurements obtained practically. Overall, filtration performance can be evaluated with respect to the extent of separation achieved, the throughput of filter cake and the moisture content of the cake formed.

1.2. Problem Statement

The separation of metal hydroxide precipitates from an aqueous effluent at Glencore Nikkelverk is carried out currently by use of a bank of manually operated chamber filter presses. The use of candle filter technology as an alternative technology is to be investigated through trials on a DrM Fundabac pilot filter. In addition to assessing filtration performance, an understanding of what affects filtration performance is to be gained.

1.3. Scope of Study

The purpose of this study is three-fold. Firstly, an appropriate filter cloth for operation should be obtained. Secondly, optimal set operation parameters should be found. And lastly, it should be understood how variations in the feed to the filter affect filtration. This will be done by carrying out primary filter cloth screening tests in the laboratory to select a range of appropriate filter cloths for testing on the DrM Fundabac pilot candle filter rig. The filter rig will be operated using the chosen cloths. Regular sampling of the inlet slurry feed, filtrate and filter cake will be performed from tests run at the same set parameters. Information pertaining to the changes of pressure in the chamber and flowrate with time will also be recorded. Additionally, the operation parameters (feed flowrate and filtration time) of some tests will be varied in order to assess optimal operation parameters. Filtration performance and filtration capacity will be evaluated continually. The study contains an isolated investigation into the performance of the DrM Fundabac pilot candle filter rig and does not address full scale design or operation. It therefore does not involve a comparative study of candle filter technology to the existing filter press technology.

1.4. Project Objectives

i. To find the appropriate filter cloth for filtration and to assess the suitability of laboratory filtration tests as indicative of pilot filter operation. This will be done by carrying out laboratory filtration tests to screen cloths and then select a range of cloths to be used for pilot filtration tests. The cloths will be evaluated with reference to the clarity of filtrate obtained and the cake release enabled by the cloths. Laboratory filtration results will be compared to pilot filtration results.

ii. To identify the ideal operating parameters for optimal filtration capacity – namely filtration time and inlet feed flowrate. The applied pressure will be set to a maximum for all tests to evaluate whether this is effective. Tests will be carried out where the duration of the filtration part of the cycle is varied, and separately, where the feed flowrate is varied.

iii. To understand how variations in the feed affect filtration. Variations in properties including solution pH, concentration of solids in solution, particle size distribution and concentration of elements in the filter cake will be investigated. Such properties will be analysed with reference to the specific cake resistance, mass of filter cake produced and moisture content of the filter cake.

1.5. Key Questions

The key questions resulting from the aims and objectives are:

- What is the ideal filter cloth in terms of producing a clear filtrate and enabling good filter cake release?
- Do laboratory filtration tests reflect pilot filter operation?
- What is the ideal applied pressure, filtration time and feed flowrate for operation?
- How does the pH of the solution affect filtration?
- How does the solids concentration in the feed affect filtration?
- What is the particle size distribution and how does this affect filtration?
- How do the concentrations of precipitated metals in the feed affect filtration?

2. Literature Review and Theory

2.1. Removal of Heavy Metals from Effluent Streams in Industrial Processes

Heavy metals are metals that, when in significant concentration in the liquid stream, may pose detrimental effects to the surrounding environment (Ayres, et al., 1994). From an industrial perspective, the increase in consumption of metal in different forms, such as galvanised steel and other electroplated items, has resulted in the generation of huge amount of liquid wastes. The large build-up of acidity and metal impurity in liquid wastes in, for example, the electrolysis industries, such as in waste acid pickle liquor (an acid solution used to treat formed steel), spent electrolyte, wash water and rinse water renders the waste as complex and hazardous in nature (Agrawal, et al., 2009). Its toxic nature is harmful to the environment – be it on land, in water or in air (Djedidi, et al., 2009). The treatment of such effluents is thus critical.

The conventional process for the removal of heavy metals from industrial waste water usually involves a chemical precipitation process followed by solid-liquid separation (Zhou, et al., 1999); (Cavaco, et al., 2007). Other notable technologies include ion exchange, adsorption or biosorption, physical separation, electrochemical separation, solvent extraction, membrane separation, flotation and cementation (Coman, et al., 2013); (Djedidi, et al., 2009); (Cavaco, et al., 2007); (Isamoglu, et al., 2006). The method used for effluent treatment tends to be dependent on the concentration of heavy metals in solution and the cost of treatment (Richardson, et al., 2002).

2.2. Separation Technology

Knowledge plays a vital role in effective application of separation technology in many process industries. Issues relating to waste management and disposal, efficient mineral benefaction and resources recovery, and the manufacture of new classes of materials and the production of fine chemicals and pharmaceuticals can often be resolved through effective filtration technology. This demands a thorough understanding of the various aspects of the filtration process (Tien, 2002). In solid-liquid separation, the solid and liquid phases are separated from a suspension. This is necessary for either the recovery of valuable solids, liquid recovery, solid and liquid recovery or the recovery of neither phase such as when, for example, a liquid is being cleaned before discharge.

The design of a separation system must consider the stages of pre-treatment, solids concentration, solids separation and post treatment. Pre-treatment involves slurries that are difficult to filter. They thus require the addition of a filter-aid to alter the chemical or physical nature of the solid suspension to increase the permeability of the cake under subsequent filtration. Another application is the reduction of liquid volume in a suspension by thickening or hydrocycloning. This then reduces the load on the filter by reducing the liquid volume and thus mass of the suspension (Wakeman, 2011). The separation of solids

and liquids by filtration can be performed by two means: surface filters, which are used for cake filtration, and depth filters, which are used for deep bed filtration (Perry & Green, 1984). To further categorise, filters operate by means of either pressure, vacuum, centrifugal or gravitational forces (Svarovsky, 2000). Post treatment processes improve the quality of the solid or liquid products. Regarding the filtrate, this can involve using micro or ultra-filters to remove fine substances or the use of reverse osmosis, ion exchange or electrodialysis for the removal of ionic and macromolecular species. Regarding the cake, post-treatment can involve the washing of soluble impurities and removal of excess liquid from the cake voids (Wakeman, 2011). The equipment and processes encompassed in the various stages of the separation system are shown in the table below.
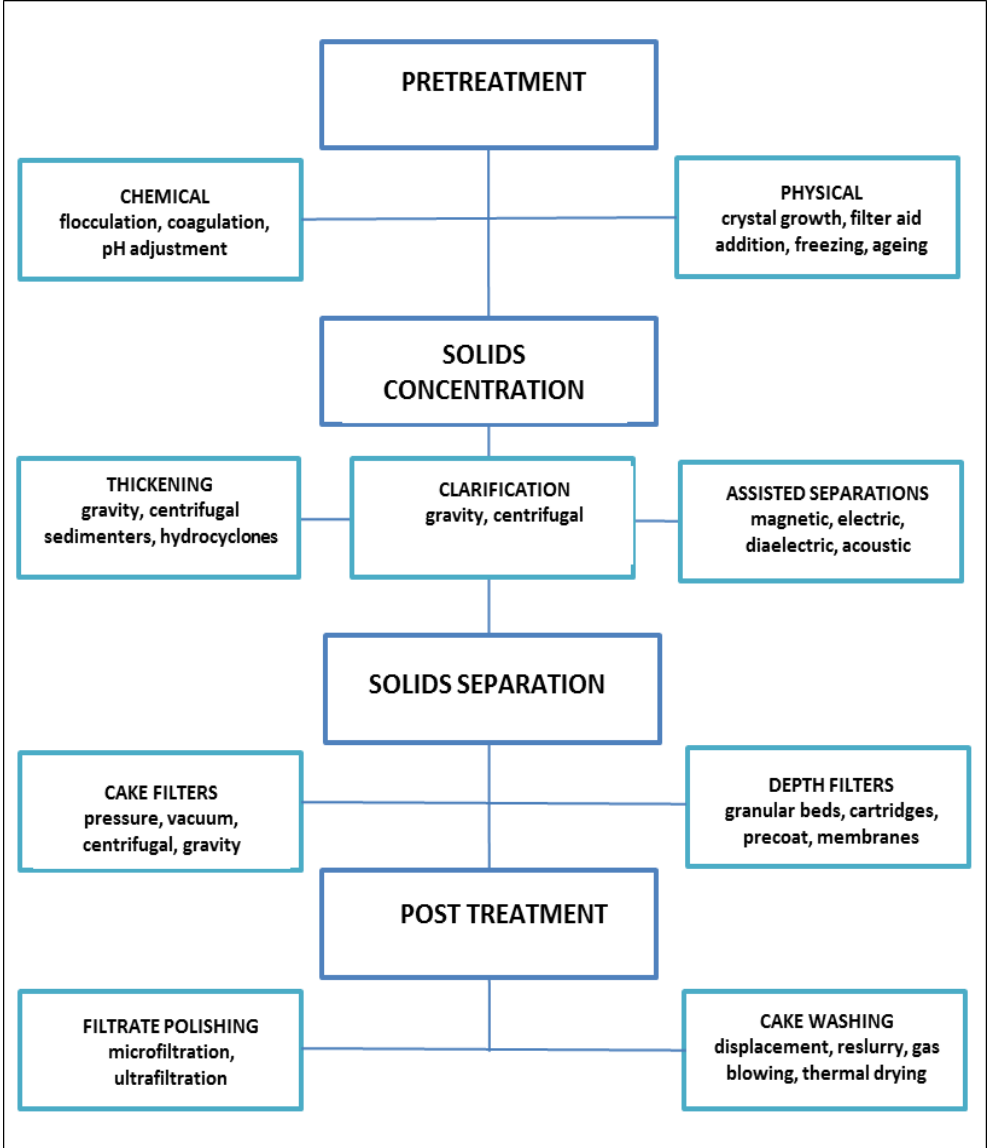
Figure 2.1: Schematic of the possible components of the solid/liquid separation process (Wakeman, 2011)

2.3. Filtration Mechanisms

Filtration occurs when the separation of particles from slurry happens by means of a medium that is permeable to liquid flow while blocking the passage of particles (Stamatakis & Tien, 1991). Fluid flows through the filter medium if a pressure drop is maintained over the medium during filtration. As mentioned, particle removal can either occur by means of surface filters (which are used for cake filtration) or depth filters (which are used for deep bed filtration). The filter medium thus retains particles in two principal ways. When the particles are predominantly larger than the sizes of the filter medium pores, solids are deposited on the up-stream side of the thin filter medium during what is referred to as surface filtration. The filter medium itself has a relatively low initial pressure drop. During deep bed filtration, particles are generally smaller than the sizes of the filter medium pores and are deposited inside the internal structure of the medium (Svarovsky, 2000). In deep bed filtration applications, the concentration of solids in the feed tends to be very low, enabling particles to pass unhindered into pores by following the flow of fluid streamlines. Such technology is used for deep bed sand filters and some types of cartridge filters (Wakeman, 2007).

At the microscopic scale, cake filtration occurs by a combination of two primary mechanisms – complete blocking and bridging. Complete blocking occurs when the particles are larger than the filter medium pore sizes while bridging occurs when the particles smaller than the filter medium pore sizes form a cake. Bridging is enhanced when the concentration of particles in the feed is higher. Several particles then attempt to pass simultaneously into a singular pore at the surface of the filter medium but fail to pass, instead forming a bridge over the pore entrance. This arch is stabilised by the flow environment around the pore entrance and can be destabilised if flow velocities or directions are changed significantly (Wakeman, 2007). The smaller passages created by particles becoming wedged in the filter medium openings then remove smaller particles from the fluid. A filter cake is thus formed which behaves as the new medium for the filtration of suspension (Svarovsky, 2000). Surface filters are usually used for suspensions with a higher concentration of solids (from approximately 1 % to greater than 40 %) and are thus more commonly used in the chemical industry (Perry & Green, 1984).
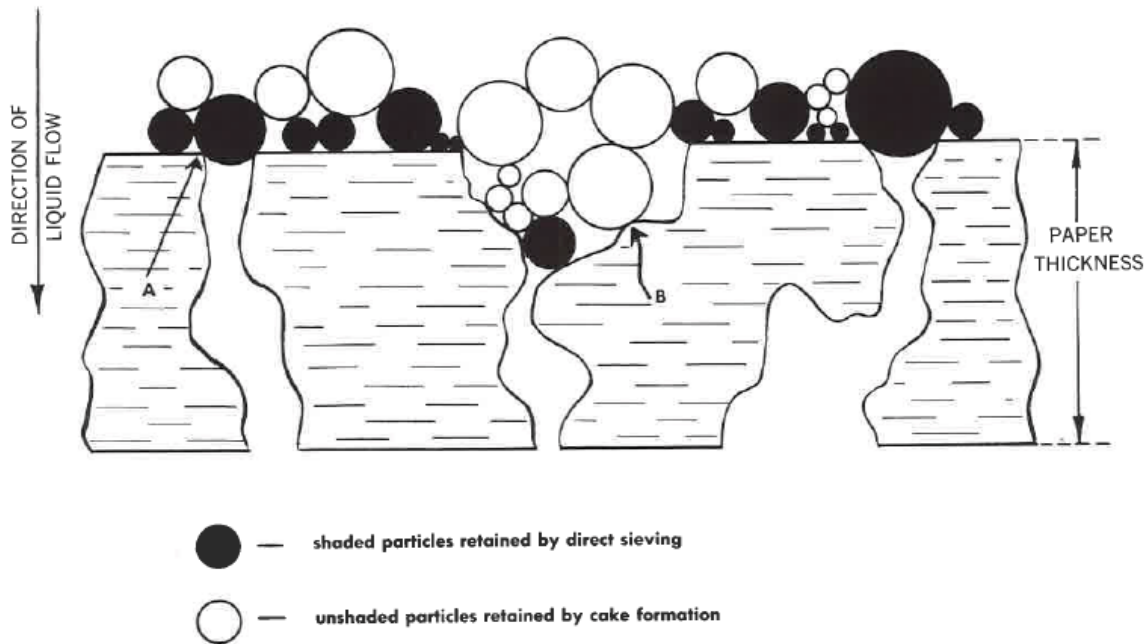
Figure 2.2: Illustration of direct sieving and cake formation (Eaton-Dikeman Company, 1960)

2.4. Comparison of the Driving Forces for Solid/Liquid Separation

The driving force for solid/liquid separation by surface filtration can be divided into four groups: gravity, vacuum, pressure and centrifugal force.

2.4.1. Gravity filters

Gravity filters use atmospheric pressure to force solids through the filter medium that results in a simple process with zero direct running cost. The equipment, however, tends to be bulky and fairly coarse solids will still contain a large amount of liquid after separation, thus increasing the overall running costs. The slurry is fed into the top of the filter and the clear filtrate emerges from the filter medium below (Svarovsky, 2000). Gravitational filtration tends to be used to reduce large quantities of solution to more manageable proportions. It is usually operated continuously and only a limited amount of washing of solids is possible (Perlmutter, u.d.). Gravity filters include sand filters, traveling belt filters and rotary drum gravity filters (Svarovsky, 2000).

2.4.2. Vacuum filters

Vacuum filters obtain vacuum forces via the suction of an ordinary liquid pump or by a gas displacement device. The effect is to find a driving force of up to 0,81 bar, which can be sufficient to obtain vastly improved filtration rates for all except the finest solids. The vacuum is created behind the filter medium while atmospheric pressure in front of the filter medium drives the slurry through the medium (Svarovsky, 2000). Vacuum filtration enables a mechanically simple driving force and can be batch operated, however is normally continuously operated. The cake thickness here can be controlled within close limits and some vacuum filters offer the best solids washing possibilities (Perlmutter, u.d.). Belt, horizontal pan, vertical disc and drum filters all fall into this category (Svarovsky, 2000).

2.4.3. Pressure filters

Pressure filters enable a greater output per unit area thus permitting smaller equipment to fit easily into the process circuit and allowing easier handling of volatile liquids. The continuous discharge of solids, such as cake, is however not always easy. The feed slurry is introduced into the filter under pressure and forced through the filter medium (Svarovsky, 2000). Most conventional pressure filters are batch operated (with the exception of the BHS rotary pressure filter). Cake washing is highly effective and the obtained filter cake is usually as dry as can be expected without heat input (Perlmutter, u.d.). The two basic designs used in pressure filtration are plate-type filter presses that contain a series of plates with a filter medium between them, and case-enclosing pressure filters, which consist of the filter medium enclosed in a pressure tank. Pressure filters can handle feed concentrations of up to and over 10% solids by weight and can handle fine particles. Pressure filtration tends to be preferable over vacuum filtration when 10% of the solid particles in the feed are larger than 10 µm (Svarovsky, 2000).

2.4.4. Centrifugal filters

Centrifugal filtration can sometimes offer a compromise between vacuum and pressure filtration. Such filters can be continuously operated or operate in a continuous batch mode. The effectiveness of operation and of cake washing is greatly dependant on the nature and behaviour of solids (Perlmutter, u.d.). The liquid is passed through the filter medium or perforated plate under a centrifugal force. Filtration occurs when the liquid passes through the interstices of the solid particles that have been built up on the filter medium. Such filtration can occur in cyclones or centrifuges. Cyclones have a simple and compact construction with low running costs, however with low separating efficiency for very small particles (approximately less than 10 µm). The solids are discharged in the form of slurry. Centrifuges enable higher separating efficiencies, even for such fine particles, and discharge occurs in a cake or slurry form. The high capital cost of centrifuge equipment can often be justified by the high throughputs achieved relative to the equipment size (Svarovsky, 2000).

2.5. Batch Pressure Filtration

A further elaboration is given on pressure filtration as an effective means of solid/liquid separation and dry solids recovery in surface filter operations. Pressure filtration occurs when liquid penetrates the filter medium upon application of either hydraulic or mechanical pressure that is greater than atmospheric pressure (Svarovsky, 2000). The batch wise pressure filtration operation involves a cyclic process of cake formation and cake consolidation followed by cake washing or cake dewatering with the final cake being discharged at the end of the cycle (Tien, 2002). This enables continuous discharge of cake and filtrate products (Svarovsky, 2000). It is necessary to understand how filtration can be optimised by assigning the appropriate amount of pressure during filtration and the appropriate length of time for each part of the cycle.
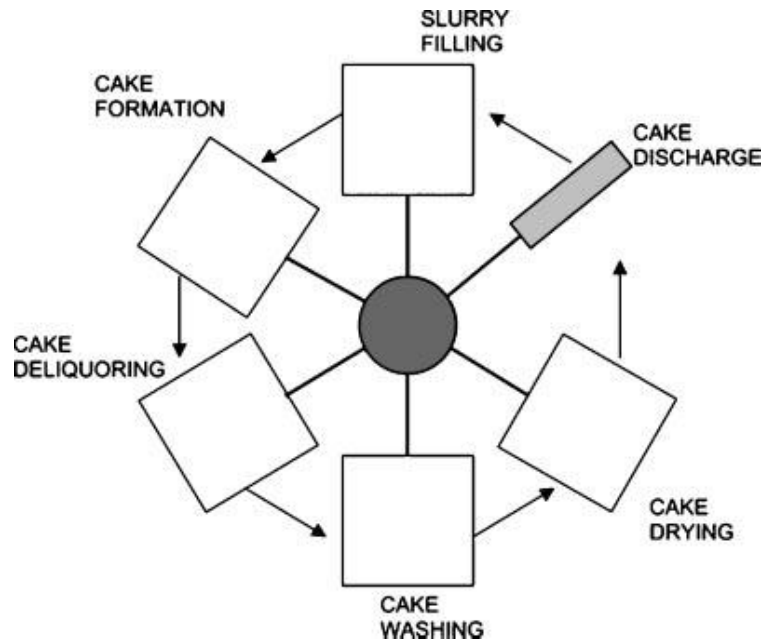
Figure 2.3: Schematic of the different phases of the filtration cycle (Seidel, 2007)

2.5.1. The filtration stage of the cycle

Pressure filters that use hydraulic pressure as a driving force can be distinguished from vacuum filters in that they can exceed the theoretical pressure drop limit over the filter medium for vacuum filters (1 bar). In some instances, a high pressure drop is advantageous in that it leads to higher outputs, drier cake or cleaner filtrate. For compressible cakes, however, increasing the pressure drop can lead to a decrease in the permeability of the cake due to cake consolidation or collapse. A lower filtration rate is therefore achieved. Derivation of Darcy's law and neglecting filter medium resistance leads to the fundamental case for pressure filters whereby the dry cake production capacity can be found.

$$Y = (\frac{2\Delta p f c}{\alpha \mu t_c})^{1/2}$$ [2.1]

Where:

Y solids yield (dry cake production in kg/m^2/s
Δp pressure drop
c concentration of solids in the feed
α specific cake resistance
μ liquid viscosity
f ratio of filtration time to cycle time
t_c cycle time

From this relationship, it can be seen that if the pressure drop is increased by a factor of four, the dry cake production will double. Thus, the filtration area can be halved for the same capacity if the specific cake resistance is constant. The relationship also shows that if the specific cake resistance increases with pressure drop, the increased pressure drop may not enable much higher capacity. For the filtration of most minerals, the increase in specific

9

cake resistance with increased pressure drop is not significant and thus pressure filtration is advantageous over vacuum filtration as it enables better filtration rates (Svarovsky, 2000).

2.5.2. The dewatering stage of the cycle

During dewatering, there is a minimum moisture content (called irreducible saturation) in the filter cake that cannot be removed by air displacement at any pressure. There is also a threshold pressure that must be exceeded so that air can enter the filter cake. The capillary retention forces in the pores of the filter cake are affected by the size of the particles forming the cake and by the deposition of particles upon cake formation. Theoretically, the particle systems could produce closely packed deposits. Practically, however, filter cakes have large voids and are more loosely packed due to the lack of particle relaxation time. According to capillary-pressure diagrams drawn up by Svarovsky (2000), the moisture content of the produced cake can be obtained during a shorter dewatering time if higher pressure is applied. If, however, the dewatering time is not decreased, the moisture content is reduced at higher pressure with a parallel increase in cake production capacity (Svarovsky, 2000).

2.5.3. Optimisation of cycle times

A critical part of batch filtration design is allocating the appropriate amount of time to the different filtration operations. The different stages of the cycle, such as filtration, displacement, dewatering or cake washing and cake discharge all occur within a cycle time. It is important to ascertain how long the filtration time should be relative to the other operations. A long filtration time can result in a thick cake, however the filtration rates can rapidly decrease towards the end of filtration. On the other hand, filtration can be stopped early while the filtration rate is still reasonably high. According to a derivation by Svarovsky (2000) that relates the non-filtration operations (downtime) to the optimal filtration time by optimising the average dry cake production, the optimal filtration time should always be set to at least equal to the sum of time of the other non-filtration stages (Svarovsky, 2000).

2.6. The Influence of Particle Properties on Filtration

There are three types of parameters that fully characterise the solid/liquid system and should be regarded when designing the filtration system. These are the primary properties, the state of the system and the macroscopic or secondary properties. The primary properties refer to the primary particle properties as well as the liquid properties (Wakeman, 2007). The primary particle properties describe the particle size, the particle size distribution, the particle shape and the surface properties of the particles in their solution environment while the primary liquid properties refer to viscosity and density (Svarovsky, 2000). These properties can be measured independent of the other components of the system. The state of the system refers to the porosity, concentration and the homogeneity and extent of dispersion of particles. Together, the primary properties and the state of the system govern the macroscopic or secondary properties that are measured in the application of the separation programme. These measurements include the permeability or

specific resistance of a filter medium or filter cake, the terminal settling velocity of the particles or the bulk settling rate of particles in suspension (Wakeman, 2007). Further analysis of the determination of the specific resistance of the filter medium and filter cake is given in section 2.7 and of the solution environment in section 2.8.

2.6.1. Particle size measurements

The effect of the particle size on the performance of solid/liquid separation is notable. Solids are therefore evaluated in order to predict their behaviour in the separation process. This assists in the initial choice between different separation methods. The interaction of particles with their surrounding fluid is particularly significant for small particles (<10 µm) as the net attractive or repulsive forces between the particles become as influential as the gravitational or hydrodynamically induced forces (Wakeman, 2007). Figure 2.4 shows the different solid-liquid separation equipment suitable for various particle sizes (Svarovsky, 2000).
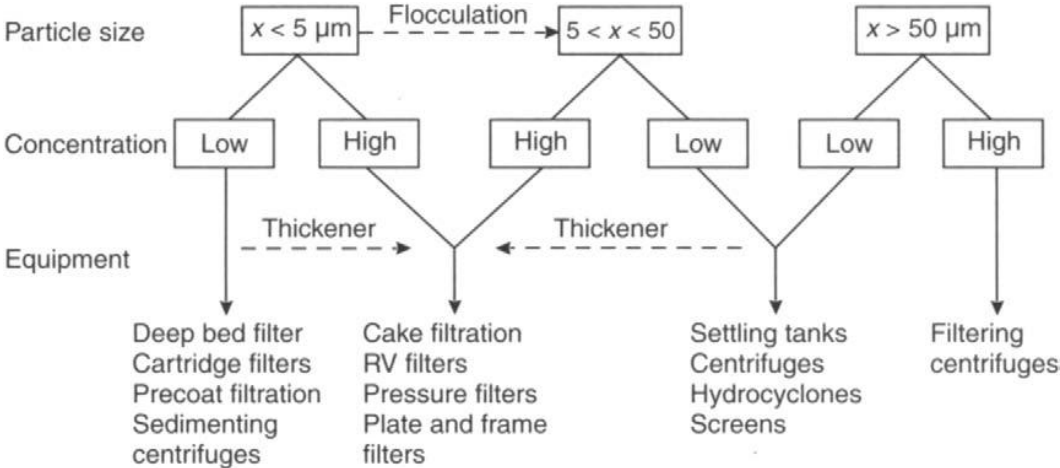
Figure 2.4: Particle size as a determining factor in the selection of solid-liquid separation equipment (Svarovsky, 2000)

The particle size that is measured in calculating filter cake formation, deliquoring or washing calculations is the volume mean diameter (x_{sv}). Particularly for small particles, the surface area provides a more appropriate characteristic for analysis than some size based on an equivalent diameter (Mullin, 2001). The volume specific surface area, which provides the total surface area of the solid per unit volume (m^2/m^3) is related to the surface-volume mean diameter as follows (Wakeman, 2007):

$$S_0 = \frac{6}{x_{sv}}$$

Given that the specific surface of the particles comprising the bed is inversely proportionate to the particle size, the particle size (x) affects the specific resistance ($\propto$) of the packed bed during filtration through the following relationship:

$$\propto \sim \frac{1}{x^2}$$

Analysis of the particle size therefore enables a qualitative assessment of the permeability of the packed bed (Svarovsky, 2000).

2.6.2. Particle size distribution

The feed to the filter is normally characterised by the mean particle size. This disregards the range of particle sizes which is of importance given that the smallest particles in the size distribution have the largest effect on filtration. The smallest particles in the suspension bleed through the filter cloth during the initial part of cake formation. They also move through the voids in the cake that is forming, thus making the cake layers close to the filter cloth more concentrated. As shown in the relationship between specific surface area and particle size, the smallest particles contribute most to the specific surface of the particles and thus to the specific filter cake resistance. Because smaller particles lead to the formation of smaller size pores in the filter cake, higher deliquoring pressure is required to displace liquid from the cake. Filtration of smaller particles thus leads to higher cake moisture content. The rate of filtration, washing and deliquoring is thus decreased by the presence of smaller particles (Wakeman, 2007).

2.6.3. Particle shape

The particle shape is determined from the conditions of crystallisation under which the particles are formed. The particle shape mainly affects the volume and surface area of the particles, and in turn their specific surface. This then affects the flowrate of liquid through the filter cake. The cake porosity is also affected by the particle shape with, for example, the porosity of cakes of fibrous particles tending to be much higher than those of cubic particles (Wakeman, 2007). The particle shape can also determine whether the particles are retained on a screen/cloth as shown in the figure below
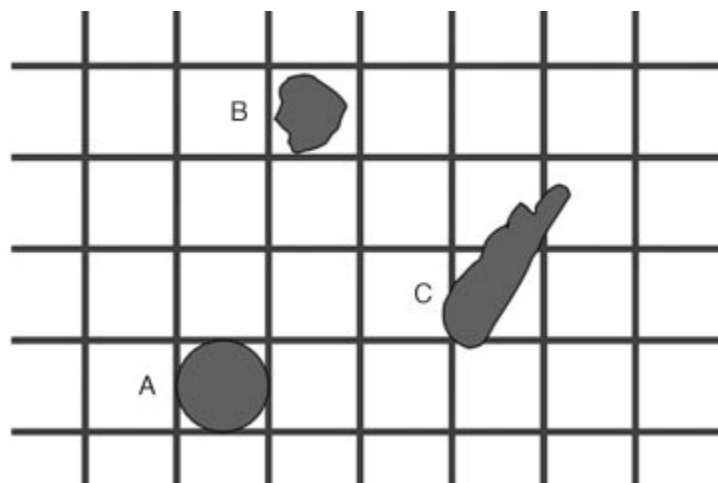
Figure 2.5: Representation of how particles of different shapes can pass through or remain on a screen (Seidel, 2007)

2.7. Theory of Filtration for the Calculation of Macroscopic Properties

Filtration theory attempts to quantify the relationship:

$$Rate = \frac{driving\ force}{resistance}$$

where resistance is the sum of the filter cake resistance and medium resistance. This theory is valuable in interpreting laboratory tests, in evaluating optimal conditions for filtration and in predicting the effects of changes in operating conditions. The limitations of filtration theory are such that filtering characteristics must be determined on the slurry in question and therefore data from one slurry is not transferrable to data from another (Perry & Green, 1984).

At the start of batch cake filtration, the pressure drop (which is the driving force for filtration) is across the filter medium itself, as no cake has yet been formed. The medium pores are normally small and the flowrate of filtrate low, and thus laminar flow conditions are usually obtained (Svarovsky, 2000). The basic equations to describe cake formation use Darcy's law and the constitutive equations relating cake structure (solidosity, permeability or specific resistance) with the compressive stress on the solid particle (Stamatakis & Tien, 1991). Darcy's law assumes the pressure loss only to be due to friction between the solid and liquid under streamline flow conditions (Reynolds, et al., 2003).

Darcy's basic filtration equation is:

$$Q = K\left(\frac{A\Delta p}{\mu L}\right) \qquad\qquad [2.2]$$

Where:

Q flowrate of filtrate
K filter bed permeability constant
A face area of filter bed
Δp driving pressure
μ filtrate viscosity
L filter bed thickness

Introducing R as the medium resistance (which is equal to L/K), equation 2.2 can be written as:

$$Q = \left(\frac{A\Delta p}{\mu R}\right) \qquad\qquad [2.3]$$

(Svarovsky, 2000)

Once a layer of solid particles have formed on the filtering medium, this new surface becomes the new filter medium with solids being deposited and adding to the cake thickness while clear liquor is passed through (Perry & Green, 1984). A larger amount of the pressure drop is therefore taken up by the cake itself which results in an effective increase in the cake

resistance and thus a gradual decrease in flow rate. The volume of filtrate accumulated over time slows down (Svarovsky, 2000).

2.7.1. Medium with cake formation

When a cake forms on the filter medium, the filtrate flowrate at a constant driving pressure becomes a function of time. This is because the liquid experiences two series of resistances – the filter medium resistance (R_m), which is assumed constant, and the cake resistance (R_c), which increases with time.

Equation 2.3 becomes:

$$Q = \frac{A\Delta p}{\mu(R_m + Rc)}$$
[2.4]

The filter medium resistance is, however, rarely constant because penetration and blocking of the medium tends to occur when particles settle on the medium. The resistance of the cake is assumed to be directly proportional to the amount of cake deposited on the medium, and therefore:

$$R_c = \alpha w$$
[2.5]

Where:
w mass of cake deposited per unit area [kg/m^2]
α specific cake resistance [m/kg]

Equation 2.4 therefore becomes:

$$Q = \frac{A\Delta p}{\alpha\mu w + \mu R_m}$$
[2.6]

The pressure drop can be constant or variable with time, depending on the pump characteristics or driving force. The face area of the filter medium is usually constant (however can vary with a large cake build up on a tubular medium or rotary drum). The liquid viscosity is constant when the temperature is constant and the liquid is Newtonian. The medium resistance is usually constant but can vary with time when solids penetrate the medium or when applied pressure compresses the medium fibres.

Specific cake resistance

The specific cake resistance should be constant for incompressible cakes, but can change with time because of flow consolidation of the cake and if the flowrate is changing. Most cakes are compressible meaning that their specific resistance will change with the pressure drop across the cake.

Mass of cake deposited per unit area

The mass of cake deposited per unit area (w) is a function of time in batch filtration processes and can be related to the cumulative volume of filtrate filtered during a certain time:

$$wA = cV \qquad [2.7]$$

Where:
c concentration of solids in suspension [kg/m^3]
V cumulative volume of filtrate filtered in time (t)   [m^3]

Medium resistance

The medium resistance (R_m) should be constant, however can vary with time as solids penetrate the medium. The applied pressure during filtration can also compress the fibres in the medium, thus altering its resistance (Svarovsky, 2000).

2.7.2. Filtration operations - basic equations for incompressible cakes

In order to determine the specific cake and medium resistance, the pattern of filtration concerning the variation of the flow rate and pressure with time must be known. The pumping mechanisms generally determine the filtration flow characteristics, giving rise to three possible categories: constant pressure filtration, constant rate filtration and variable pressure, variable rate filtration (Perry & Green, 1984).

Substituting the relationship for the mass of cake deposited per unit area (equation 2.7) into the determining relationship for the flow rate (equation 2.6):

$$Q = \frac{A\Delta p}{\alpha \mu c (\frac{V}{A}) + \mu R_m} \qquad [2.8]$$

The total flow volume is an integral function of the flow rate, therefore:

$$Q = \frac{dV}{dt} \qquad [2.9]$$

Inverting the form of equation 2.8 in combination with equation 2.9 gives:

$$\frac{dt}{dV} = \alpha \mu c \frac{V}{A^2 \Delta p} + \frac{\mu R_m}{A\Delta p} \qquad [2.10]$$

Constant pressure filtration

The case of constant pressure filtration is further elaborated given that it is relevant to both laboratory and plant scale investigation. A continuation of the basic equations derived from the above filtration operations for incompressible cakes gives involves integrating equation 2.10:

$$\int_0^A dt = a_1 \frac{V^2}{2A^2 \Delta p} \int_0^V V dV + \frac{b_1}{A\Delta p} \int_0^V dV \qquad [2.11]$$

which results in:

$$t = \alpha \mu c \frac{V^2}{2A^2 \Delta p} + \mu R_m \frac{V}{A \Delta p} \qquad\qquad [2.12]$$

A plot of $\frac{t}{V}$ against V will thus give a straight line with:

$$slope = \frac{\alpha \mu c}{2A^2 \Delta p}$$
and $intercept = \frac{\mu R_m}{A \Delta p}$

For filtration experiments operating at a constant pressure, these relationships can thus be used to calculate the specific cake resistance and the material resistance (Svarovsky, 2000).

Increasing pressure drop to attain a constant pressure drop

In industrial application, the constant pressure period is often preceded by a period in which the applied pressure drop is increased from a low value. If the solids are non-homogeneous, high initial filtration rates are often detrimental to the filtration performance. If there is a high initial pressure, colloidal particles will be forced into the interstices of the filter cloth which results in plugging and therefore a decrease in the filtration rate. Filtration can instead be operated such that the pressure is slowly increased, allowing the filter cake to develop a more open structure. In filters where the cross sectional area is not too large, this results in a higher overall filtration rate and easier cake release from the filter medium at the end of the filtr ation cycle (Reynolds, et al., 2003).

Equation 2.10 is integrated from a point t_s, V_s which is the start of the constant pressure period, which results in:

$$\frac{t-t_s}{V-V_s} = \frac{\alpha \mu c}{2A^2 \Delta p} (V + V_s) + \frac{\mu R_m}{A \Delta p} \qquad\qquad [2.13]$$

When $\frac{t-t_s}{V-V_s}$ is plotted against V, the slope $(\frac{\alpha \mu c}{2A^2 \Delta p})$ and the intercept $(\frac{\mu R_m}{A \Delta p} + \frac{\alpha \mu c}{2A^2 \Delta p} V_s)$ can be calculated from the part of the graph that corresponds to constant pressure operation, i.e. for $V \geq V_s$. These relationships can thus be used to calculate the specific cake resistance and the material resistance (Svarovsky, 2000).

2.7.3. Relationship between specific cake resistance, porosity and specific surface
The Kozeny-Carman equation relates the permeability to the porosity, specific surface and the density of a packed bed. The equation was derived upon considering the flow of clean liquid through a packed bed. The pore space of the packed bed was taken as equivalent to a bundle of parallel capillaries each with an equivalent radius and with the cross sectional shape representing the average shape of the pore cross section. The relationship is shown:

$$\alpha = (\frac{K_0 S_0^2}{\rho_s})(\frac{1-\varepsilon}{\varepsilon^3}) \qquad\qquad [2.14]$$

Where:

K_0 Kozeny constant (approximates to a value of 5 in lower porosity ranges)

S_0 Specific surface of particles making up the bed ($S_0 = \frac{surface\ area\ of\ solids}{volume\ of\ solids}$)

ε Porosity ($\varepsilon = \frac{volume\ of\ voids}{volume\ of\ cake}$)

ρ_s Density of solids

By combining equation 2.14 with equation 2.4, the pressure drop is related to the cake porosity as such:

$$\Delta p \propto \frac{1-\varepsilon}{\varepsilon^3}$$

(Svarovsky, 2000)

Therefore an increase in the delta pressure results in a less porous cake.

2.7.4. Effect of the feed concentration on filtration

It is usually the case that higher feed solids concentration leads to improved filter performance through higher capacity and lower cake resistance. The relationship given in section 2.5.1., equation 2.1, shows that a four-fold increase in solids concentration will result in a doubled production capacity. Another benefit of a higher feed solids concentration can be seen in the resultant reduction in specific cake resistance. When there are few particles in the feed, they tend to pack together more tightly. When there are more particles that approach the filter medium simultaneously, they can form bridges over the pores thus reducing penetration into the forming filter cake or cloth. This can be explained by the particle relaxation time; when a higher concentration of particles approaches the filter at the same approach velocity, less time is available for a stable cake to form. There is not time for the particles to orientate themselves in an ordered manner (this is particularly pronounced for irregularly shaped particles). The resulting cake is therefore more permeable leading to a lower specific cake resistance (Svarovsky, 2000).

2.7.5. Effect of viscosity and temperature on filtration

The rate equations show that the filtrate flow rate should be inversely proportionate to the filtrate viscosity. The effect of temperature on filtration is seen primarily through its effect on the viscosity. For most liquids, an increase in temperature causes a decrease in viscosity which thus leads to higher filtration rates (Perry & Green, 1984).

2.8. The Solution Environment

2.8.1. Point of zero charge, zeta potential and isoelectric point

It is beneficial to start this section with a definition of point of zero charge, zeta potential and isoelectric of a suspension as they will be referenced in the different studies examined henceforth. When insoluble oxides are present in aqueous solutions, they form surface electrical charges from the charge transfer that occurs in order to establish electrochemical

equilibrium between the solid surface and the solution. Negative charge arises from an acidic dissociation of surface hydroxyl groups while positive charge arises from proton addition to the neutral surface. The magnitude of potentials in such suspensions is affected by small changes in the concentration of acid or base and therefore H^+ and OH^- are considered potential-determining ions. The point of zero charge (pzc) is the pH where the suspension has zero net charge (Tewari & Campbell, 1976). Because the inter-particle forces are inactivated, the particles flocculate and do not experience motion when an electric field is applied (Pansu & Gautheyrou, 2006).

The distribution of solution ions around the charged surface of the particle lead to inter-particle repulsive forces and a resultant electrical charge that is dependent on the chemical species at the surface. The magnitude of the net repulsive force between particles is called the zeta-potential (ξ) (Wakeman, 2007). The zeta potential is also defined as the electrical potential at the shear plane with respect to the surrounding liquid (CMC, 2014). The dependency of the sign and magnitude of the oxide on the pH of the solutions is defined as follows:

$$\xi = k(pzc - pH) \qquad\qquad [2.15]$$

Where k is a constant (Tewari & Campbell, 1976). The pH at which the surface charge is zero, i.e. at the pzc, is termed the isoelectric point. Here the extent of adsorption of positively charged species equals that of negatively charged species (Birdi, 2009)

2.8.2. The effect of the solution environment on filter cake properties

A cake formed from the same suspension but with different pH values will experience significantly differing solidosity and permeability (Wakeman, 2007). For fine particle suspensions, the nature of the filter cake is controlled by colloidal forces which arise from the interaction between suspended particles (Iritani, 2003). Colloidal particles are microscopic solid particles that are suspended in a fluid (Lu & Weitz, 2013). The primary colloidal forces are van der Waals forces, electrostatic forces, and in some cases hydration forces (Tien, 2002). The attractive van der Waals forces are caused by fluctuating dipoles as a result of the outer electrons on the interacting suspended particles while the repulsive electrostatic forces are caused by the presence of like charges on the interacting particles and a dielectric medium. The van der Waals forces for a system are essentially constant but the electrostatic forces vary in accordance with the surface charge of the particles which vary with the solution environment. It is in this way that the solution properties such as pH and electrolyte strength effect the filtration of colloids (Iritani, 2003).

Iritani (2003) conducted particulate microfiltration experiments on titanium dioxide particles to investigate the effect of pH on the specific filtration resistance (α) and the average porosity (ε). The titanium dioxide particles were in the rutile form with an original mean specific surface area size of 0,47 µm and an isoelectric point of 8.1 (Iritani, 2003). The result was that the specific filter resistance value went through a minimum around the isoelectric

point, indicating that the highest filtration rate is obtained when the particles carried no charge. In contrast, the average porosity was higher around the isoelectric point. Because the titanium dioxide particles are hydrophobic colloids, they are destabilised around the isoelectric point where the van der Waals forces dominate. The particles are therefore attracted to each other (i.e. the flocculate) causing the formation of porous flocs. The resulting filter cake often has a loose and wet structure making it more permeable and thus decreasing the specific filter resistance around the isoelectric point (Iritani, 2003). In order to investigate the particle-particle interaction effect in cake filtration, the fluid-particle and particle-particle interactions on the particle level should therefore be analysed for each individual system (Tien, 2002).

A general summary of the effect of a low zeta-potential on filtration by Wakeman (2007) further reiterates the findings of Iritani (2003). When the zeta-potential is close to 0 mV, faster settling rates, a higher filter cake formation rate and filter cakes with slightly higher moisture content prior to dewatering can be expected. This is because the particles aggregate in the suspension when the inter-particle repulsion forces are low. For a constant cake bulk volume, the wash liquid flowrate and deliquoring rate can also be slightly higher. The wash liquid changes the ion species distribution in the cake pores which can lead to reduced cake porosity (Wakeman, 2007).

2.8.3. *Point zero charge of nickel hydroxide*

Tewari and Campbell (1976) performed an investigation into the temperature dependence of the pzc of nickel hydroxide. The pH for the primary equilibrium distribution of H^+ and OH^- ions was measured by adding 20 cm^3 of a KNO_3 solution of a set pH and ionic strength (*method I*). The solution was then allowed to reach equilibrium at the desired temperature. A set amount of the nickel hydroxide (which had no excess acid or base on its surface) was then added to the solution and the change in pH with time was recorded. The addition of nickel hydroxide to fresh solutions occurred until a point was found where the pH did not change upon such addition. This pH was taken as the pzc of the nickel hydroxide.
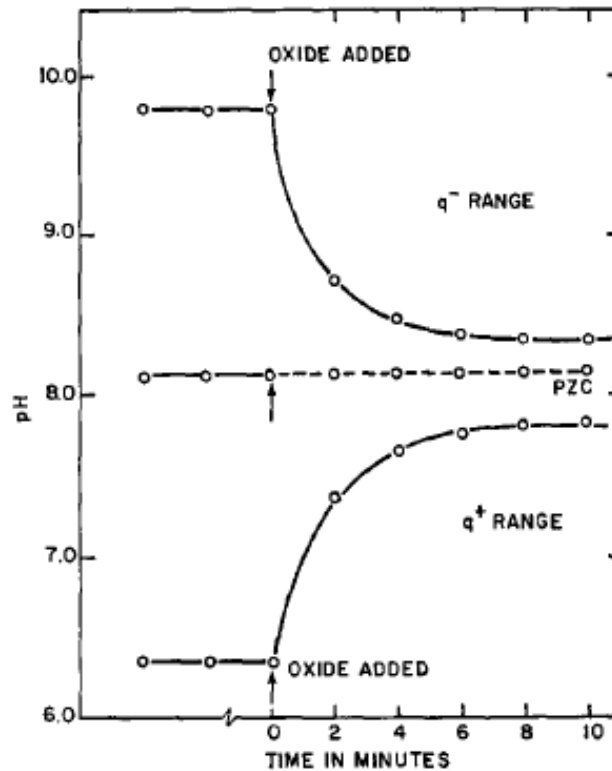
Figure 2.6: Variation of pH with time pre and post addition of Ni(OH)₂ (Tewari & Campbell, 1976)

Tewari and Campbell (1976) also determined the effect of temperature on the pzc of Ni(OH)$_2$ by means of electrometric titration (*method II*) and by electrophoretic mobility (*method III*). The results from all three methods are given below.

Table 2.1: The variation of pzc with temperature for Ni(OH)₂ (Tewari & Campbell, 1976)

	Method I		Method II		Method III
$Temperature$ $(°C)$	pzc	$pzc - \dfrac{1}{2}pK_w$	pzc	$pzc - \dfrac{1}{2}pK_w$	pzc
25	8,12	1,12	11,2	4,2	11,1 +- 0,1
40	7,75	1,05	11,02	4,32	
60	7,19	0,68	10,7	4,19	
80	6,80'	0,5	10,5	4,2	

The pzc values determined by electrometric titration and by electrophoretic mobility (em) were significantly higher. The reason that the different methods obtained different results was likely due to the time allowed for experiments. The contact of an oxide with an electrolyte solution results in the distribution of the potential determining H$^+$ and OH$^-$ ions between the solution and the oxide-solution interface. The equilibrium distribution can, for many oxides, occur within a short time (around 8 minutes). The rapid primary equilibrium is,

20

however, followed by a slow change and it can take many days or weeks to achieve final equilibrium. This can be because of the dissolution of the oxide and the hydrolysis of the dissolved metal ions and the subsequent structural arrangement. The titration and em methods were carried out over longer equilibrium times which may therefore have resulted in the higher pzc. The overall results therefore do not give a clear indication of the pzc for nickel hydroxide. However, what is clear for all methods used is that the pzc decreased with an increased temperature (Tewari & Campbell, 1976).

2.8.4. The properties of filter cakes composed of mixtures

The calculation of the pzc of nickel hydroxide in previous literature is only relevant for solutions of pure nickel hydroxide. Any variations in the degree of hydration or impurity content in the material will, however, alter the pzc (Tewari & Campbell, 1976). The interaction between two or more types of particles can strongly affect the filterability of a feed fluid (Iritani, 2003). Iritani et al. (2002) investigated the filter cake properties upon dead-end microfiltration of binary particulate mixtures of titanium dioxide and silicon dioxide. The isoelectric point for each material was different. It was found that in the pH range where two particles had opposite electrical charges, the particles came together as a result of coulombic attractive forces and London-van der Waals forces. The particles aggregated in very porous flocs. The filter cake was therefore very permeable which resulted in lower resistance to flow. In a pH range where both particles were charged with the same sign, the particles were very dispersed by repulsive electrostatic forces. This resulted in the formation of compact cakes and thus a higher filtration resistance (Iritani et al., 2002; Iritani, 2003). The large effect of inter-particle interactions on the pH at which filterability is improved makes it difficult to predict the optimum range of pH for a feed solution whereby the composition of elements is constantly changing.

2.9. Classification of the Treatment Process Prior to Filtration

It is necessary to understand the precipitation process prior to filtration in order to understand how changes in operation may affect the filtration process.

2.9.1. Precipitation

Precipitation can be described as 'very fast crystallisation'; however it can also refer to an irreversible process. Many precipitates produced by a chemical reaction are virtually insoluble substances. This differs from the products of most crystallisation processes which can usually be re-dissolved if the original solution conditions (temperature and concentration) are restored. The precipitation process usually occurs at very high supersaturation, meaning fast nucleation which then results in many very small primary crystals. There are three basic steps defining crystallisation: supersaturation – where the solution contains more dissolved solid than is represented by equilibrium saturation: nucleation – where minute solid bodies formed act as the centre of crystallisation; and growth – where a stable nuclei grow into crystals. In addition to this, the precipitation process has two steps. Agglomeration occurs where small particles in a liquid suspension

cluster together (Mullin, 2001). Flocculation can then occur whereby these destabilised particles conglomerate into larger aggregates (Armenante, u.d.). The other defining step is ageing, whereby the larger particles in a suspension grow, and which refers to the irreversible changes that take place after the precipitate is formed.

Direct mixing by the addition of chemicals to the solute or by mixing two solution streams can result in a chemical reaction between components in the liquid, resulting in the formation of a product or products exhibiting low solubility. Precipitation then occurs because the liquid phase becomes supersaturated with respect to the solid component (Mullin, 2001).

2.9.2. Selective Precipitation of Metal Hydroxides

The metals precipitation process involves the addition of alkaline reagents to adjust the pH of the solution so that the metals exhibit low solubility and therefore precipitate (Marchioretto, et al., 2005). The selective precipitation of metal hydroxides by controlled changes in pH is the most common precipitation technique for the removal of certain metals from impure leach liquors (Monhemius, 1977). It is the most widely used method because of the relative low cost of hydroxide salts (Djedidi, et al., 2009) and simplicity of technique (Baltpurvins, et al., 1996). Soluble metals can be precipitated as hydroxides using different alkaline reagents such as CaO, $Ca(OH)_2$, $Mg(OH)_2$, NaOH and NH_4OH. The representative reaction is:

$$M^{2+} + 2(OH)^- \leftrightarrow M(OH)_2 \tag{2.16}$$

Where M refers to the metal in solution (Djedidi, et al., 2009).

Theoretical considerations for obtaining solubility data – hydroxide precipitation

The solubility of metal hydroxides is defined by equations relating the metal hydroxide solids in equilibrium with the soluble free metal ion or metal hydroxide species and by solubility products (K_s). The solubility of divalent metal hydroxide can be described by the following equations, in addition to equation 2.16 referenced above (Patterson, et al., 1977):

$$M(OH)_{2(s)} \Leftrightarrow M^{2+} + 2OH^- \qquad K_{s0} \tag{2.17}$$

$$M(OH)_{2(s)} \Leftrightarrow M(OH)^+ + OH^- \quad K_{s1} \tag{2.18}$$

$$M(OH)_{2(s)} \Leftrightarrow M(OH)_2^0 \qquad K_{s2} \tag{2.19}$$

$$M(OH)_{2(s)} + OH^- \Leftrightarrow M(OH)_3^- \quad K_{s3} \tag{2.20}$$

$$M(OH)_{2(s)} + OH^- \Leftrightarrow M(OH)_4^{2-} \quad K_{s4} \tag{2.21}$$

The solid phase is represented by $M(OH)_{2(s)}$ and the soluble metal species is represented by M. The solubility product can then be used to describe the equilibrium position of the reactions:

$$K_{s0} = [M^{2+}][OH^-]^2 \qquad\qquad [2.22]$$
$$K_{s1} = [M(OH)^+]\,[OH^-] \qquad\qquad [2.23]$$
$$K_{s2} = [M(OH)_2^0] \qquad\qquad [2.24]$$
$$K_{s3} = [M(OH)_3^-]/[OH^-] \qquad\qquad [2.25]$$
$$K_{s4} = [M(OH)_4^{2-}]/[OH^-]^2 \qquad\qquad [2.26]$$

To define the metal hydroxide solubility curve, each of these equations would be plotted (after taking the logarithmic form) using appropriate solubility constants. The total soluble metal concentration is given as the sum of all the soluble metal species (Patterson, et al., 1977).

2.9.3. *Observing Solubility Diagrams for Evaluation of Metal Precipitation*

Solubility diagrams illustrate the solubility behaviour of metal salts and are used in order to predict precipitation efficiency. It can be impossible to determine all the present species in solution, and therefore a general 'solubility domain' is defined that encompasses the main species of interest (Guillard & Lewis, 2001).
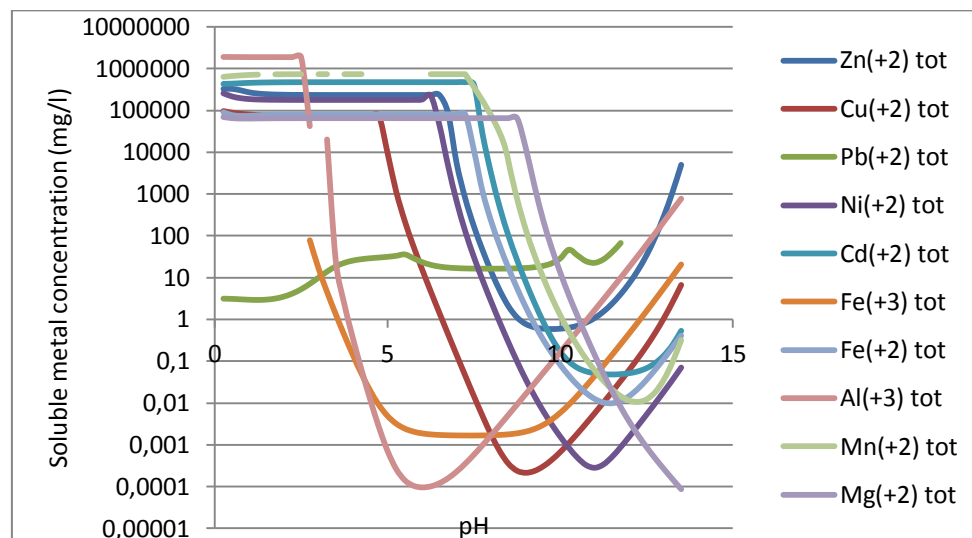
Figure 2.7: The pH dependency of metal hydroxide solubilities (Lewis, 2010)

Figure 2.7 represents data from Lewis (2010) that was calculated using Stream Analyser, using the revised Helgeson-Kirkham-Flowers (HFK) model for calculation of standard thermodynamic properties of aqueous species and the frameworks of Bromley, Zemaitis, Pitzer, Debye-Huckel and others for the excess terms (Lewis, 2010).

This diagram enables an overview of the theoretical solubility trends of nickel (and various other elements) using hydroxide precipitants. It provides an outline of the possible solubility domain for various elements which enables a prediction of the amount of precipitation to be expected at different pH levels. It is to be noted that the results in industrial processes can vary significantly due to the effects of temperature, solution concentration, impurities and precipitation ageing.

2.9.4. Structural Characteristics of Nickel Hydroxide

This study does not involve investigation into the structural characteristics of nickel hydroxide. The following references to previous studies therefore only give an outline of the structural characteristics *possible* upon precipitation of nickel hydroxide with while mentioning the length of time it *can* take for nickel hydroxide to change from an amorphous form.

Previous studies on precipitation of nickel hydroxide

The formation of precipitate depends not only on pH, but also on the solution concentration, precipitation rate, temperature, formation of poly-nuclear complexes and duration of precipitation ageing. These conditions could either lead to the formation of an active (fresh) form of precipitate which is amorphous or crystalline with a disordered lattice, or the formation of an inactive (aged) form of precipitate which has larger and more ordered crystals (Patterson, et al., 1977).

Ramesh and Vishnu Kamath (2005) carried out a study into the synthesis of nickel hydroxide by precipitation from a solution containing dissolved Ni^{2+} ions. Strong alkali induced precipitation was observed by the addition of NaOH (2 M) to a solution of nickel nitrate (1 M). The effect of systematically varying the precipitation conditions on the formation of nickel hydroxide was observed and samples were studied by powder X-ray diffraction (PXRD) and infrared spectroscopy (IR). The results showed the bonding in nickel hydroxide to be anisotropic (Ramesh & Vishnu Kamath, 2005). This means that their mechanical, electrical, magnetic and optical properties can vary according to the direction in which they are measured (Mullin, 2001). Intra-layer bonding in nickel hydroxide is strongly iono-covalent in nature, while bonding between layers is of the weak van der Waal's type. This results in the layers losing orientation with respect to each other thus displaying disorder.

Nickel hydroxide exists in two polymorphic forms, α- and β-Ni(OH)$_2$ (Song, et al., 2002). Nickel hydroxide obtained by alkali precipitation from a nickel salt solution followed by hydrothermal treatment forms what is known as β-nickel hydroxide. In this structure, the OH^- ions are hexagonally paced and the Ni^{2+} ions occupy alternate rows of octahedral sits which leads to a layered structure. This can be described as an ordered stacking of charge neutral layers of composition Ni(OH)$_2$. Nickel hydroxide obtained by precipitation using ammonia or by electrosynthesis is a poorly ordered material and is known as α-nickel hydroxide. Nickel hydroxide obtained by ambient temperature alkali precipitation from a nickel salt solution gives and XRPD pattern similar to that of β-nickel hydroxide, however it is poorly ordered. This is referred to as β$_{bc}$-nickel hydroxide (where bc refers to badly crystalline) (Rajamath , et al., 1999). The disorders of β$_{bc}$-nickel hydroxide are incorporated during the crystallisation process and cannot be eliminated by ageing at different temperatures at ambient pressure (Ramesh & Vishnu Kamath, 2005).

Precipitation will take place when two solutions having different free energies are mixed. Ostwald's law states that the solid obtained immediately on precipitation is disordered as well as thermodynamically unstable, with a free energy similar to that of the reactants. Through a step wise process, the disordered phase transforms into a more stable phase of lower free energy. Previous tests by Ramesh and Vishnu Kamath (2005) show that during the precipitation of nickel hydroxide at low temperatures (4 °C) and moderate pH conditions by ammonia induced precipitation or by stoichiometric strong alkali addition, the solid formed immediately on precipitation is in the α amorphous phase. This phase is metastable (meaning that it can exist in this state for a long period of time, though it is not the most stable state) and transforms into other phases of progressively greater order and thermodynamic stability. Observations in the study show that the following transformation takes place:

$$\alpha, amorphous \rightarrow \beta_{bc} \rightarrow \beta, nickel\ hydroxide$$

In strong alkali, once the first step is completed, the secondary transformation becomes very slow and can be accelerated only at high alkali concentrations (> 10 M) or at high temperature (> 80 °C). A duration of 18 to 96 hours is needed to complete the transformation. The second step likely occurs by the dissolution – re-precipitation mechanism. Nickel hydroxide is not very amphoteric, and this transformation therefore requires harsh conditions (Ramesh & Vishnu Kamath, 2005).

2.10.   Particle Classification

As discussed previously, the particle size and shape affect filtration. There are various different ways to obtain more detailed information about the size and shape of the particles. The techniques for gaining Malvern particle size distributions and scanning electron microscope images are detailed below.

2.10.1. Malvern particle size distributions

Particle sizing techniques aim to provide a single number that represents the particle size. Most sizing techniques assume the particle to be spherical in order to provide a complete description of the particle size, which includes length, breadth and height. Particle sizes are therefore reported as the diameter of an *equivalent sphere* which would give the measured response. For the laser diffraction technique, the diameter of the sphere that gives an equivalent light scattering pattern to the particle that is measured is reported. The corresponding physical property here is the average cross sectional area.

After calculation of the particle size for the sample, the distribution of particle sizes within the sample is displayed. The laser diffraction system is configured such that equal volumes of particles of different size give a similar scattering response. The size is therefore reported by a volume distribution which gives the percentage of particles of that given size. This corresponds to a mass distribution if the particle density is the same for all particle sizes (Malvern(a), 2013).

Laser diffraction particle sizing

This technique is based on the theory that when particles pass through a laser beam, they will scatter light at an angle that is directly proportional to their size. The smaller the particle size, the larger the scattering angle (this increases logarithmically). The scattering intensity is related to the particle size such that it decreases according to the cross sectional area of the particle. A large particle will scatter light at a small angle with high intensity, while a small particle will scatter light at a large angle with low intensity (Malvern(a), 2013). The laser diffraction technique therefore involves capturing the light scattering data from the particle using a laser, a presentation system and a series of detectors. The laser is used to provide an intense light of fixed wavelength. A sample presentation system ensures that the material passes through the beam as a homogeneous stream of particles in a known state of dispersion. And finally, a series of detectors measure the ligh t pattern produces over the range of angles (Malvern(b), 2013).
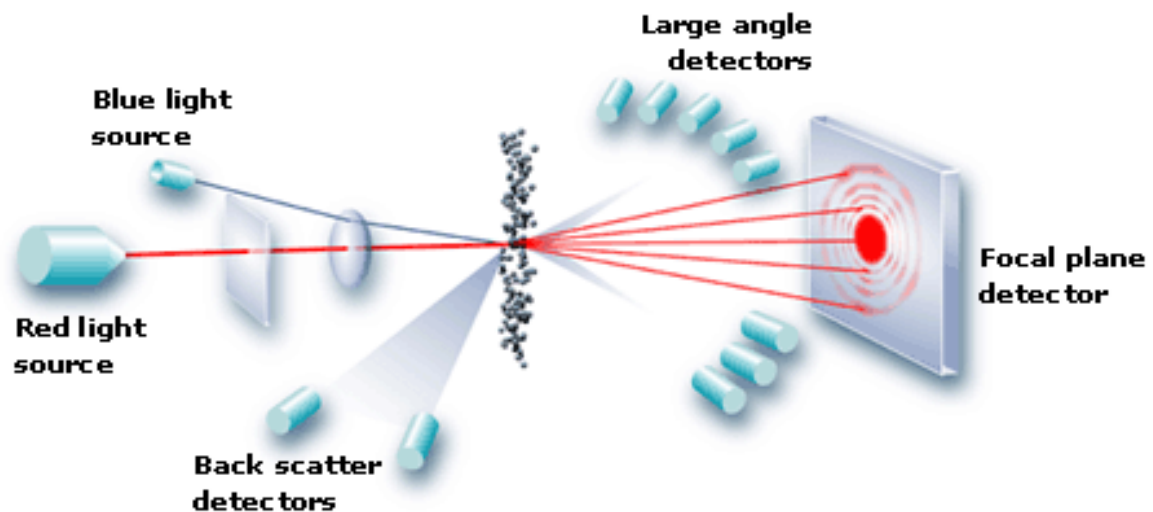
Figure 2.8: The instrumental setup showing the light source and back scatter and angle detectors (Malvern(b), 2013)

To analyse light scattering data in laser diffraction, particle size distributions are calculated by comparing the scattering pattern of a particle to an optical model. This is done using a mathematical inversion process, using either the Fraunhofer Approximation model of the Mie Theory model.

Mie Theory predicts scattering intensities for all particles, with the following assumptions:

- The measured particles are spherical
- The suspension is dilute, meaning scattered light is measured before being scattered by other particles
- The particles and the medium that the particles contain known optical properties
- The particles are homogeneous

26

This theory predicts the primary scattering response that is seen from the surface of the particle while the intensity is predicted by the refractive index difference between the particle and the medium it is dispersed in (Malvern(c), 2013). The refractive index is the measure of the bending of a ray of light as it passes from one medium into another (Encyclopædia-Britannica, 2013). The theory will also predict how the absorption of the particle will affect the secondary scattering signal that is caused by light refraction inside the particle. This is very relevant for particles below 50 microns in size, and especially relevant for transparent particles.

The Fraunhofer Approximation is based upon similar assumptions to the Mie Theory, however assumes additionally that:

- The measured particles are opaque discs
- Light is scattered only at narrow angles
- Particles of all sizes scatter light with the same efficiency
- The refractive index is infinite

These assumptions are most relevant for particles above 50 microns in size, while they hold error for fine particles (Malvern(c), 2013).

2.10.2. Scanning electron microscope (SEM)

The SEM technique uses a focused beam of high energy electrons to generate signals at the surface of a solid particle. These signals are formed from electron-sample interactions and provide information about the sample including particle morphology, particle composition, the crystalline structure and the orientation of materials that make up the sample. The accelerated electrons carry a high amount of kinetic energy and are decelerated in the solid sample, thus providing the signals from the electron-sample interactions that occur. Imaging samples are created by signals from secondary electron and from backscattered electrons. Secondary electrons are used to show morphology and topography on samples while backscattered electrons are used to show the contrasts in composition in multiphase samples.
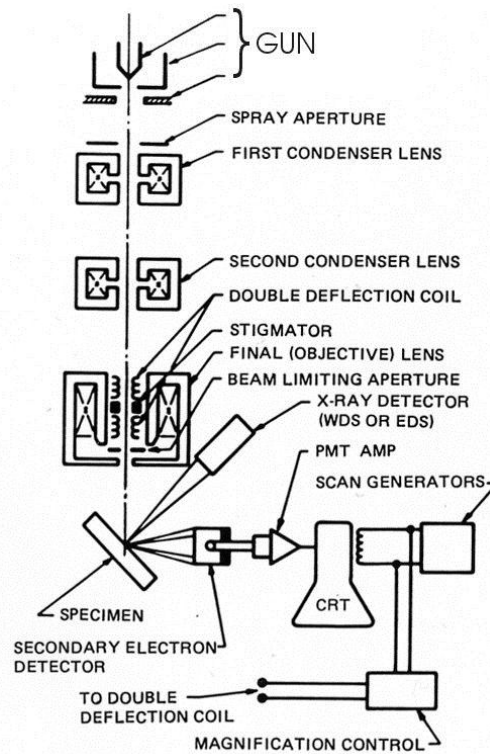
Figure 2.9: Schematic drawing of the electron and x-ray optics of a SEM (combined with an electron probe micro-analyser) (Swapp, 2013)

The components of the SEM include an electron source (electron gun), electron lenses, a sample stage, detectors for all signals and a display output device (Swapp, 2013).

2.11. **Selection of Filtration Equipment**

The choice of an ideal filter is based on that which will fulfil all filtration requirements at a minimum overall cost. The cost of equipment tends to be relative to the filtration area, and thus a high overall filtration rate is desirable. This requirement calls the use of relatively high pressures, though the maximum pressure is often limited by mechanical design considerations. Other concerns are that filter cake should also be easily discharged in a convenient form and the quality of filtrate should be as to requirements. The most common types of filters are filter presses, leaf filters and continuous rotary filters. The most important factors that determine the choice of the correct filter are the specific filter cake resistance, the concentration of solids in the feed and the quantity to be filtered (Richardson, et al., 2002). Figure 2.2. (shown in section 2.6.1.) indicates that for particle sizes up to 50 µm, and where the concentration of particles in the feed solution is high, cake filtration should be employed. For this means, rotary vacuum filters, pressure filters and plate and frame filters give a suitable selection of options. A description of plate-and-frame and candle filters, both of which operate batch-wise, is given below as they are the equipment types to be compared in this study.

2.11.1. Plate-and-frame presses

In the early years of the chemical industry, the filter press was one of the most frequently used filter types (Perry & Green, 1984). Plate-and-frame filter presses are the most versatile of filters because the effective area for filtration can be varied simply by removing or blanking of plates. Full mechanisation of filter presses began in late the 1950s, enabling further developments such as plate-shifting mechanisms for the vibration of cloths and filter cloth washing on both sides of the plates. Automation also enables a reduction in down-time, thus increasing capacities (Svarovsky, 2000).
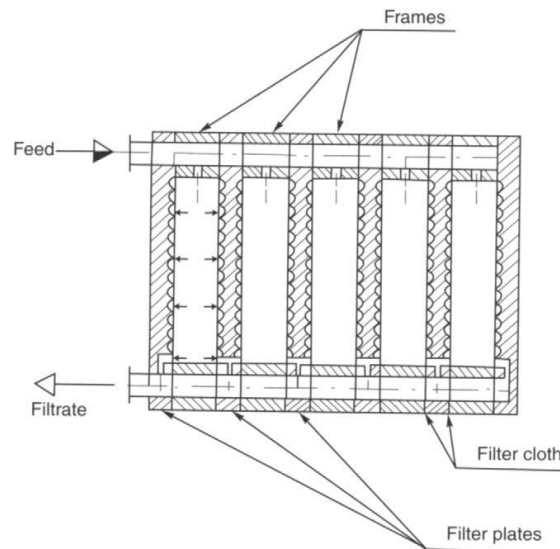
Figure 2.10: The principle of plate-and-frame filter presses (Svarovsky, 2000)

The plate-and-frame press consists of an alternative plates covered with a filter cloth and hollow frames that permit cake build up. The frames have feed and wash ports where the slurry and wash water are pumped through and the plates have filtrate drainage ports (Perry & Green, 1984). The designs encompass many different possible combinations of inlet and outlet location (top, centre, bottom, corner or side feed/discharge) (Svarovsky, 2000). Top feed and bottom discharge to and from the chambers is especially suitable for heavy and fast settling solids. Such an arrangement allows for maximum recovery of filtrate and maximum mean cake dryness. To achieve quick air displacement and a more uniform cake, bottom feed and top filtrate discharge are optimal (Perry & Green, 1984). Washing can be performed by simple washing (where the washing occurs in the same direction as the filtration process) or by thorough washing (where the wash liquid is introduced through a separate port and passes through the thickness of the cake in the chamber).
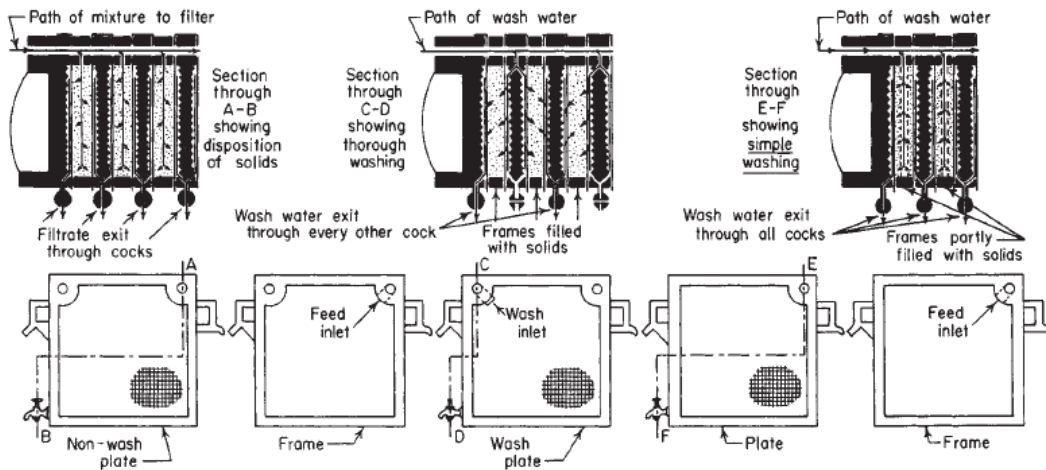
Figure 2.11: Schematic representing the filling and washing flow patterns in a filter press (Perry & Green, 1984)

The size of plates ranges from 150 mm^2 to 2 m^2 enabling filtration areas of up to 200 m^2. The number of chambers tends to vary up to 100, but in exceptional cases up to 200. The typical operating pressure is around 6 to 7 bar, though presses operating at up to 20 bar of higher are also manufactured.

Richardson et al., (2002) list the advantages and disadvantages of filter presses:

Advantages

- Simple design enables more versatility and may be used for a wide range of materials under varying operating conditions of cake thickness and pressure
- Low maintenance cost
- Large filter area on small floor space
- Most joints are external enabling leakage detection
- Can operate at high pressure
- Suitability is independent of whether the cake or liquid is the main product

Disadvantages

- Operation can be irregular and continual dismantling leads to wear on the cloths
- Fairly labour intensive despite improvements in automation

2.11.2. Candle filters

Candle filters (otherwise known as cylindrical element filters) have cylindrical elements (or candles) mounted in parallel, vertically. The diameter of the tubes is usually between 25 – 75 mm and the length is usually up to 2 m (Svarovsky, 2000). The larger types can contain 250 or more sleeves and filtration areas of up to 200 m^2. The three major components of the candle filter are the vessel, the filtering elements and the cake discharge mechanism (Halberthal, u.d.). The tubes are usually made of metal or cloth-covered metal, but can be

made of stoneware, plastics, sintered metal or ceramics (Svarovsky, 2000). The slurry is fed into the vessel under pressure and filtration takes place with solids being deposited on the outside of the tubes. The liquid passes through the drainage system and out of the filter. The filtration cycle time is determined by the pressure available, cake capacity or batch capacity (Richardson, et al., 2002).
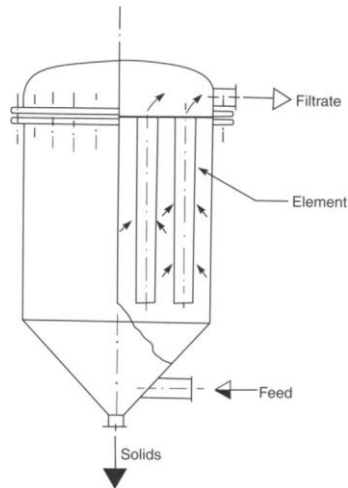
Figure 2.12: The principle of the candle filter (Svarovsky, 2000)

The slurry is fed in to the bottom of the filter such that it flows upwards in the vessel. This is necessary to prevent solids from settling and maintain a homogeneous suspension, thus allowing for even filter cake formation. An uneven cake thickness reduces the effective possible volume of the filter cake. A suitable pump must be selected so that it enables the required upflow velocity. The filtrate outlet from each row of individual sleeves is connected to a horizontal header. The headers deliver the filtrate through valves so that they are collected for further processing. The candles consist of a bundle of perforated tubes or ball shaped packing material inside a coarse mesh screen and are covered by the filter medium (such as a filter cloth). The cake is discharged by means of blowing (blowback pressure) or by a vibrating mechanism (Halberthal, u.d.).

Figure 2.13: Image of the cylindrical candles, each covered with a filter cloth (Halberthal, u.d.)

Candle filters are more applicable when cake washing is not required. The inherent advantage of candle filters is that as the cake grows on the cylindrical elements, the filtration area increases and the thickness of a given volume of cake is thus less than it would be on a flat surface. One of the operational issues with candle filters is that there is a portion of unfiltered slurry left in the vessel at the end of the filtration period. Compressed air cannot be used to complete the filtration of this slurry as the air would preferentially escape through the top of the leaves. This means that either a separate filtering element should be installed at the bottom of the filter, or recycle of slurry must occur (Svarovsky, 2000). Other advantages and disadvantages of candle filters are given:

Advantages

- Minimum floor space for large filtration areas provided
- Good cake discharge
- Can deal with toxic, flammable or volatile cakes without being environmentally hazardous as cake formation occurs in a close chamber
- Cake discharge can be in the form of a dry or thickened slurry
- Mechanically simple as no complex sealing glands or bearings

Disadvantages

- High headroom required for dismantling filtering elements
- For thick and heavy cakes, pressure available may not be sufficient to hold the cake on to the elements (Halberthal, u.d.)

A more detailed explanation of the filtration cycle related to DrM Fundabac candle filter equipment is given in chapter 4.

2.11.3. Filter media

The filter medium acts as a support for the filter cake of which the initial layers then provide the true filter. The medium should be mechanically strong, resistant to corrosive fluids and offer minimal resistance to the filtrate flow (Richardson, et al., 2002). Categorisation of the types of media available is given in the following table.

Table 2.2: Types of filter media and the typical size range of the smallest captured particles (where known) (Seidel, 2007)

Type	Examples	Effective smallest particle retained (μm)
Solid fabrics	flat wedge-wire screens	100
	wire bound tubes	100
	stacks of rings	5
Rigid porous media	ceramics and stoneware	1
	carbon	
	plastics	
	sintered materials	3
Cartridges	sheet fabrics	3
	yarn wound	2
	bonded beds	2
Metal sheets	perforated	100
	woven wire	5
Plastic sheets	woven monofilaments	
	fibrillated film	
	porous sheets	
	membranes	0,1
Woven fabrics	textile fabrics	10
Non-woven media	felts and needle felts	10
	paper	2
	bonded media	10
	meltblown	<2
	nanofibre sheets	<1
Loose media	fibers	<1
	powders	<1

The life-time of the medium must be long enough to justify its cost. It should therefore withstand the pressure and mechanical stress upon it, the temperature of the slurry and be resistant to the chemical in the slurry (i.e. be acid or base resistant) (Eaton-Dikeman Company, 1960). A balance must be struck between a medium that has weave pattern open enough so that plugging does not occur, but also be tight enough to prevent bleeding of fine particles. The weave pattern enabling the highest retention of fine solids is chains (broken twills), then twills then satins. The tendency for plugging decreases in that order. Plugging tends to occur more with thick, stiff cloths than with thin, pliable ones, and a longer cloth lifetime is invariably achieved when plugging is minimised (Perry & Green, 1984).

Markert Gruppe, which is a supplier of filter cloths (MarkertGruppe, 2014), classifies their cloths by filaments and yarns (which include either staple fibers, multifilaments or monofilaments) or needle felts that the fabric is made of, and then by the cloth weave (which include either satin weave, twill weave or plain weave).

Table 2.3: Relationship between the filter cloth yarn and filtration characteristics and the filter cloth weave type and filtration characteristics based on the supplier experience

Yarn (weft/warp)	Flow rate	Separation rate	Cake release	Cleaning properties
Staple fibre	3	1	4	4
Staple fibre/multifilament	2	1	3	3
Multifilament	2	2	2	2
Mono/multifilament	2	2	1	1
Monofilament	1	3	1	1
Weave type	Flow rate	Separation rate	Cake release	Cleaning properties
Plain	3	1	2	3
Twill	2	2	2	3
Satin	1	2	1	2

1=excellent, 2=good, 3=moderate, 4=poor (MarkertGruppe, 2014)

2.11.4. Study into the comparative performance of centrifugal and pressure filtration (using DrM Fundabac® technology)

Collins and Pickering (1997) carried out an investigation to compare the performance in filtering, washing and deliquoring of a centrifuge to that of a DrM Fundabac candle filter. Details focusing on the operation and performance of the DrM Fundabac during the study are given henceforth.

The basket centrifuges used are versatile, batch-operated equipment that perform cake filtration by use of a spinning, perforated bowl. The disadvantages of this technology are that it offers limited surface for the filtrate to pass which can restrict the capacity for filtration. The DrM Fundabac filter was chosen for comparison due to its unique ability among candle filters to spray wash deposited solids, deliquor them and discharge a dry cake. It is mechanically a more simple equipment than the centrifuge and provides very good containment and filtering surface area at a lower unit cost. Operation at or above the boiling point is possible with candle filtration. Results from the comparative findings showed the candle filter to be competitive with the centrifuge in most categories for fine filtration. It had excellent throughput and could deliquor solids as well as the centrifuge filter. For details on the design and operation of the DrM Fundabac filter, see chapter 4.

Findings concerning the DrM Fundabac filter

In operating the candle filter, it was found that it was critical to maintain a positive pressure drop (of minimum 0,3 – 0,7 bar) across the cake and medium at all times. This was in order to prevent the cake being released from the candles before the filtration cycle had finished. The higher achieved operating pressure enabled higher average specific flow rates to be achieved for the candle filter. The specific flow rate declined throughout filtration in correspondence with an increase in cake deposition. A decrease in the particle size in the feed resulted in a decrease in the average specific flow rate because the smaller particles packed closely together leaving less void space. A higher average specific flow rate was achieved for a feed where the shape of the particles was globular (almost spherical), as

opposed to platelet, needle or irregular in shape. Spherical particles pack together closely and are independent of orientation; however because of physical constraints, they enable a relatively high void fraction. This leads to higher cake permeability, enabling faster flow rates (Collins & Pickering, 1997).

2.11.5. Evaluation of filter performance

There are certain factors that are necessary to evaluate in order to evaluate the performance of the filter in question. The mass fraction of the solids recovered indicates the separation efficiency or degree of clarification. If a dry cake is desired, the moisture content in the recovered solids should be found. The rate of filtration (i.e. the volume of filtrate collected per unit time) should be determined as this affects the filtration time and thus the filter capacity (and consequently the cost of operation) (Reynolds, et al., 2003).

2.12. Previous Studies on Effluent Treatment Plant Solutions

Prior to this study, a pre-study was carried out to investigate the solubility trends of the main metals precipitated in the effluent treatment plant. Some results relevant to this study are shown below (Kuiper, 2013).

2.12.1. Solubility curves of nickel, cobalt, copper and iron

Experiments were performed on solution from T-1410 (the first tank in the precipitation series) whereby 200 g/l NaOH was added to the solution which was maintained at 32 °C. In separate experiments for each pH point, the pH was raised from 7 to 11 and stirred for 20 minutes. After fine filtration, the concentrations of metals in the filtrate were analysed. The results are shown below and then compared with theoretically predicted values shown in the literature.
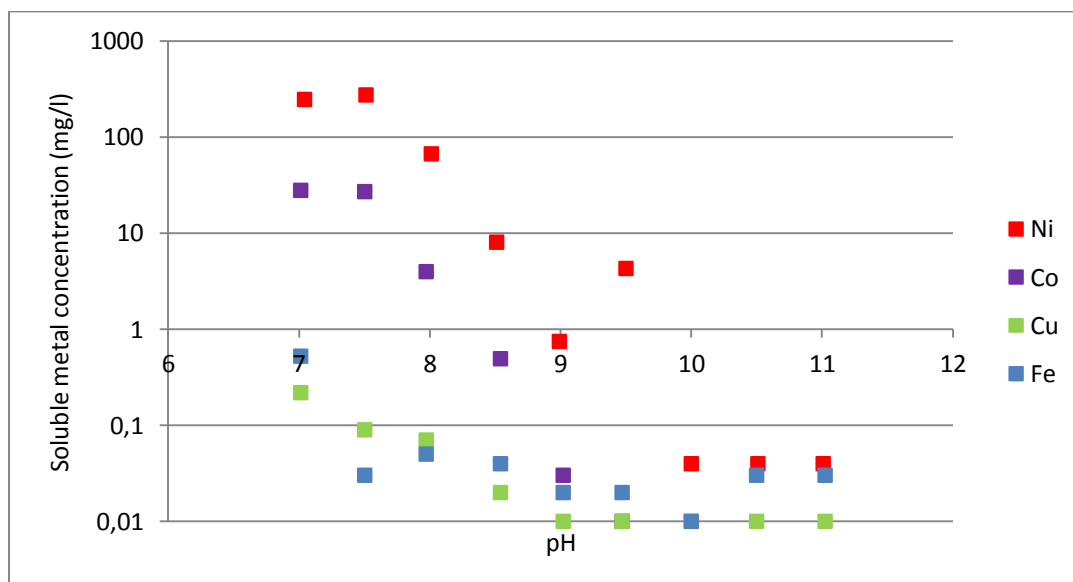
Figure 2.14: Soluble metal concentrations for nickel, cobalt, copper and iron in the pH range of 7 to 11 (Kuiper, 2013)
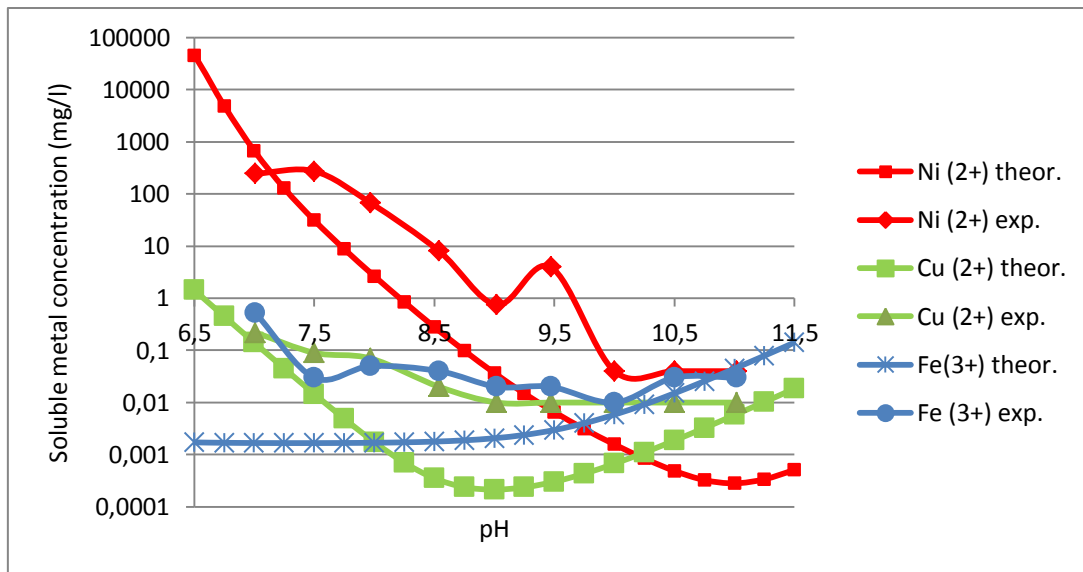
Figure 2.15: Comparison of the theoretical soluble metal concentrations to those achieved experimentally for nickel, copper and iron (Lewis, 2010); (Kuiper, 2013)

The data presented for the comparison between theoretical and experimental soluble metal concentrations is for nickel, copper and iron. The theoretical values are taken from the study by Lewis (2010) as seen in the literature. Nickel and copper are present as two-valent ions, while it is assumed that iron is present as three-valent. The theoretical soluble metal concentration is lower than the experimental concentration for nickel, copper and iron. The comparison is done on solutions obtained at 32 °C because this is likely the temperature that is most representative of plant operation. Cobalt is not presented; however two-valent cobalt and two-valent nickel display similar behaviour in water chemistry (see figure 2.15 for soluble cobalt concentration measured experimentally).

The theoretical soluble metal concentration is for an ideal solution. The experimental data varies from the theoretical data and does not achieve as low soluble metal concentrations. The formation of a precipitate is not only pH dependent, but also depends on the solution concentration, precipitation rate, temperature, formation of polynuclear complexes ($M_m(OH)_n$) and duration of precipitate ageing (Patterson, et al., 1977). The presence of impurities can also affect the precipitation. These factors may result in less effective precipitation than achieved theoretically for an ideal solution. Deviations from the theoretical data can also occur when the soluble metal species do not have sufficient time to establish equilibrium with the precipitated metal, such as is proposed for this system. This shows that the theoretical data cannot be used to accurately predict the behaviour in the plant. The theoretical data does, however, give a correct indication of which metals will achieve the lowest soluble metal concentration in the pH range of 8-10. As shown both theoretically and experimentally, copper achieves the lowest soluble metal concentration, then iron and then nickel.

The deviation from theoretical solubility also reinforces the likelihood that the experimental system has not yet reached equilibrium and therefore a system of *pseudo solubility* may be represented. The theoretical system is based on an ideal solution that may consist of different anions (i.e. not chlorides), and even though the experimental system is studied is dilute, it is not ideal. It is therefore expected that it would deviate from the theoretical system; however the large deviation is indicative of the system not having reached equilibrium. This point re-iterates the results of the previous studies referred to in section 2.9.4. (structural characteristics of nickel hydroxide).

The relevance of these findings is two-fold. Firstly, the findings indicate that care should be taken when using theoretical findings in industrial applications. As evident, the many variations in a system lead to large deviations from what might be theoretically predicted. Proper investigations should therefore be done in order to gain information about the particular system in question, with theoretical findings only being used as a guideline. Secondly, the experimental findings give an indication of the variation in the concentration of solids that may appear in the slurry feed to the filter with varied pH. As the pH is changing continually (usually within a range of 9 to 10), the concentration of metals that have precipitated out may change. The solubility diagrams also indicate the potential concentrations of metals to be expected at which pH. For instance, the ratio of nickel to iron may change. This is useful when observing filtration performance as it can help to explain the link, if there is any, between variations in pH and variations in filterability.

2.12.2. Variation of specific cake resistance with pH

An investigation was set up whereby the precipitation tanks in the effluent treatment plant were simulated in the laboratory. This was to study which conditions in the reactor were optimal for the precipitation of metals.

Two continuously stirred tank reactors (CSTRs) of 1,75 litres (liquid volume) each were set up in series in the laboratory. The reactors were set up to simulate T-1411A and T-1411B. Solution obtained from the effluent treatment plant was fed into the first reactor with overflow into the second reactor and the pH was controlled in the first reactor by means of 200 g/l NaOH addition. The temperature in the first tank was kept constant at 32 °C by means of heating. At the end of the each experiment, as well as sampling to analyse the filtrate concentrate, 500 ml of sample was taken from reactor 2 to perform a filtration test. Here the specific filter cake resistance was calculated (following a similar procedure as outlined in the experimental section).
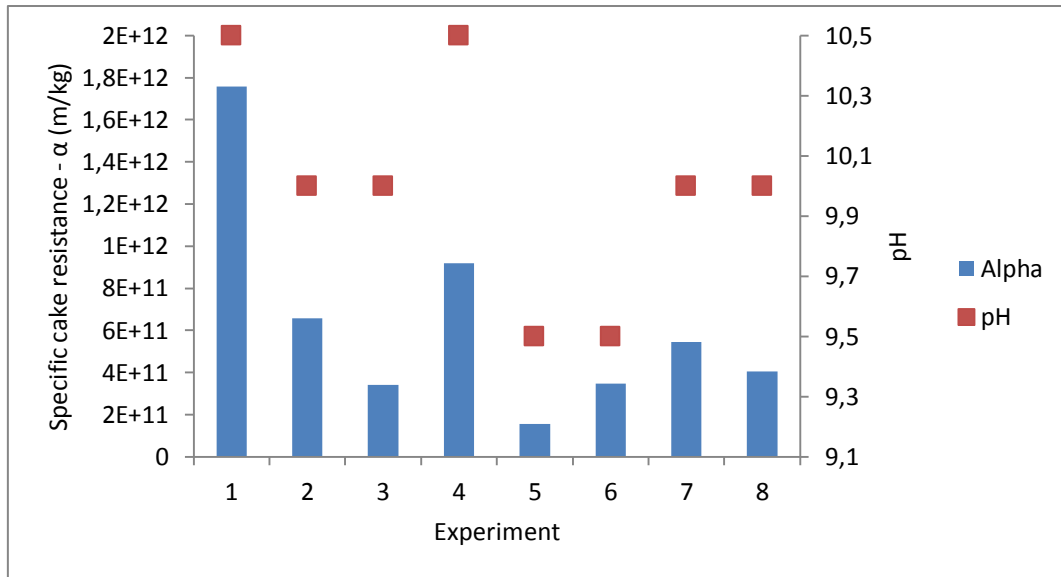
Figure 2.16: The variation of specific cake resistance with varied pH (Kuiper, 2013)

The pH in the different tests varied between 9,5 and 10,5 as this was the range found optimal for the precipitation of metals. Results from the precipitation tests showed that all metals (nickel, cobalt, copper and iron) achieved the highest level of precipitation at a pH of 10 and all metals achieved the lowest level of precipitation at a pH of 9,5. This meant that the solids concentration in the samples taken were lowest at a pH of 9,5 and highest at a pH of 10. The results from the filtration tests varied from test to test, however there is a general trend showing that the lowest specific cake resistance was achieved at a pH of 9,5 while the highest was achieved at a pH of 10,5.

As discussed earlier in the literature review, the solids concentration in the feed to the filter can effect filterability because of the way the particles fall and form a packed or loose arrangement, depending on the relaxation time available. It is predicted that filter cakes formed from a higher concentration of solids in the suspension will form a more loosely packed cake due to the lack of time available for particles to pack closely, thus offering less resistance during filtration. These results do not, however, show a clear relationship between the concentration of solids in the suspension and the specific cake resistance. It is thus possible that the effect of pH on the zeta potential of the suspension plays a more significant role in affecting the interactions between particles and therefore the cake formation.

2.13.   **Conclusions from Literature and Previous Studies**

Chemical precipitation, followed by an appropriate solid/liquid separation process, is an effective way of separating out solids from an aqueous effluent while also enabling the recovery of valuable solids. Due to the concentration of solids in the feed and the particle size range, the particular effluent treatment process in question is identified as requiring solids separation through surface (cake) filtration by means of pressure filtration. For a cake that is not highly compressible, operating at a high pressure drop is optimal as it enables higher capacity for dry cake production. The candle filter is a good alternative to the existing filter press installation in that it is a mechanically simple system with a closed chamber that can provide good filtrate throughput and cake discharge using minimum floor space for large filtration areas. If constant pressure is achieved during operation and the appropriate measurements are made, theoretical relationships derived from Darcy's basic filtration equation should enable the calculation of specific cake resistance and medium resistance which can be used to evaluate filterability.

It is expected that the large variations in types of feed to the filter will result in variations to the filterability. Filtration of very fine particles is not optimal as they result in the formation of small pores which then require higher pressure in the deliquoring process. Filtration of fine particles can thus result in a decreased filtration and deliquoring rate and in the production of a more moist filter cake. Concurrently, a higher concentration of solids in the feed results in particles orientating themselves in a more disordered form (due to the 'relaxation effect' and lack of time for orientation time) causing the formation of a more porous cake which offers less resistance to filtration and provides a less moist cake. As well as this, the concentration of elements in the solution coupled with the solution pH affects filtration. Optimal filtration occurs at the pH where the solution has a zero net charge but given that this is dependent on the inter-particle attractive/repulsive forces, this point will change with differing compositions of differing particles.

It is necessary to understand the precipitation process prior to filtration in order to understand how changes in operation may affect the filtration process. In terms of nickel hydroxide (which is the predominant metal hydroxide in the precipitate), literature and previous tests on the solution in question show precipitation to be optimal (in a pH range of up to 11) after a pH of 9,5. This is where the highest concentration of solid nickel hydroxide in the feed may be expected. Particle images obtained by SEM showing particle morphology and particle size analyses by Malvern analysis should enable further understanding of the types of particles to be filtered and consequently of the filterability to be expected.

3. Process Description Glencore Nikkelverk A/S

Glencore Nikkelverk A/S in Kristiansand produces nickel as a main product with cobber, cobalt, precious metals (gold, silver, platinum, palladium, iridium, ruthenium and rhodium) and sulphuric acid as by-products. It has the capacity to process 92000 tonnes of nickel, 39000 tonnes of copper and 5200 tonnes of cobalt annually. The refinery was built in 1910 in order to process nickel-containing ore from mines in Evje, Setesdal, through the so-called Hybinette-process. In 1975, this pyro-metallurgical process began to be changed to the KLA (chlorine-leach-autoclave) process that is used today. This technology is based on hydrometallurgical principles. By 1975, the conversion to electrowinning had been completed (Stensholt, et al., 1985).
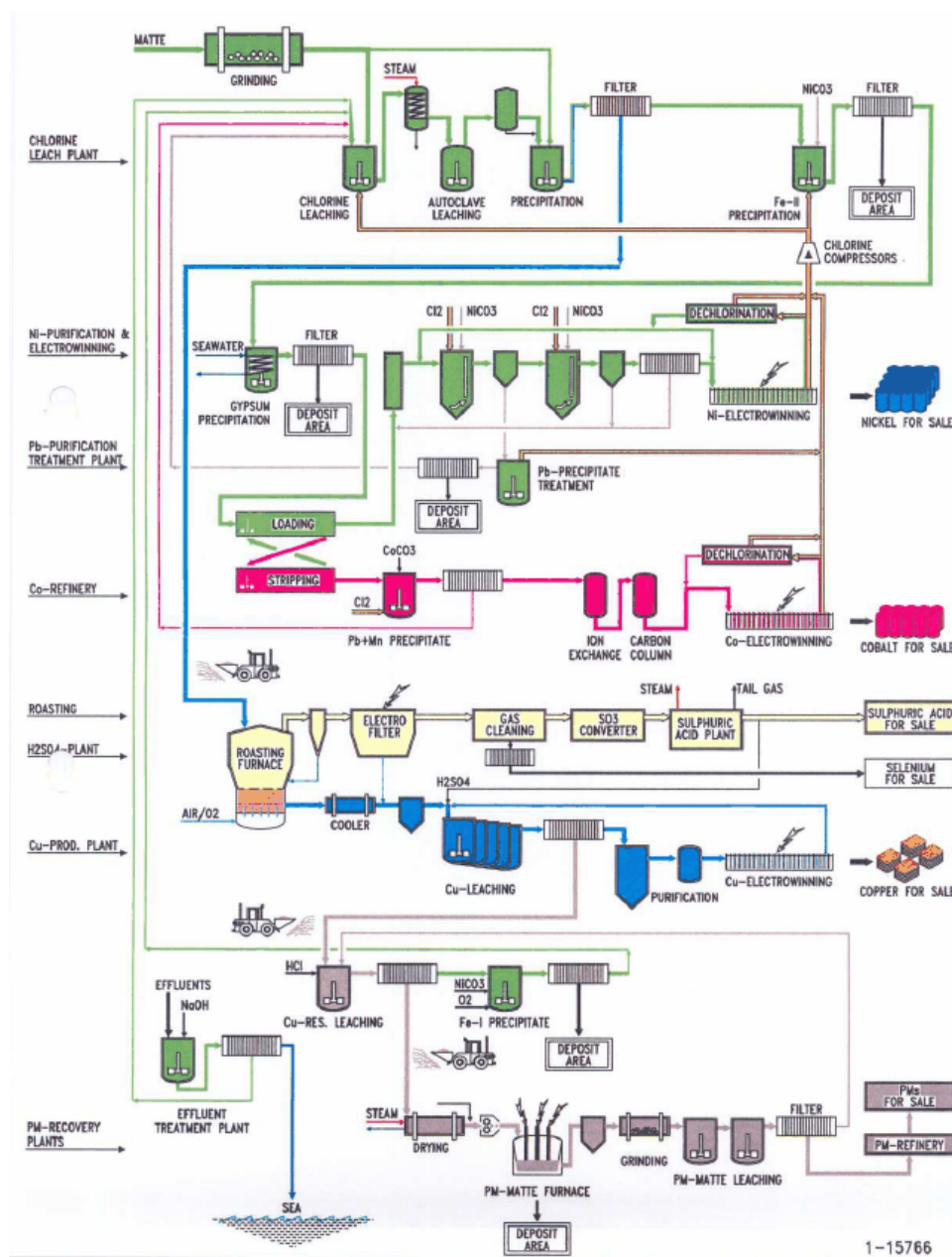
Figure 3.1: Flow sheet of the Glencore Nikkelverk production process

The raw material that is fed to the process is a concentrated sulphide ore on which flotation, roasting and smelting has been performed at smelters principally in Sudbury, Canada and Selebi-Phikwe, Botswana. The composition of raw material feed to Glencore Nikkelverk is approximately 40-45% Ni, 25-30% Cu, 20-22% S, 2-3% Fe and 1.0-1,5% Co. The raw material is dry-crushed to a particle size <0,4 mm through a crusher and ball mill. The particle size is significant for affectivity in the following matte chlorine leach process whereby the matte is mixed with recycled electrolyte from the system. Nickel is dissolved selectively in a three stage process consisting of chlorine leach, autoclave and cementation processes. Chlorine is used to control the redox potential in the slurry so that nickel and cobalt are dissolved while copper appears in the residue as CuS.

The strong nickel chloride electrolyte solution which is recovered from the filter presses is then purified. The first step is to precipitate iron, whereby ferrous iron is recovered as ferric iron through redox and pH control via the addition of chlorine and nickel carbonate. The filtrate recovered from filter press filtration is then cooled which results in the precipitation of gypsum, which is consequently separated from the solution by filtration on filter presses.

Cobalt is thereafter separated from nickel electrolyte through solvent extraction with TIOA (triisooktylamin) dissolved in an organic solvent called Solvesso 100. Cobalt is stripped from the organic phase. Impurities, including lead, manganese, iron and zinc are removed through precipitation and subsequent iron-exchange processes and filtered to obtain cobalt anolyte which is then sent to the cobalt electrowinning plant for recovery of cobalt metal via electrolysis.

Through the addition of nickel carbonate and chlorine for pH and redox control, the remaining impurities (Co, Cu, Fe, Pb and Mn) are removed as oxides/hydroxides from the nickel electrolyte. The nickel solution is then fed to the tank house where nickel is produced on the cathode. In both the cobalt and nickel electrowinning processes, chlorine gas is released and recycled back to the chlorine leach process.

The copper sulphide leach residue is dead-roasted in fluidised bed roasters. Through the addition of oxygen at a temperature up to 900°C, the metal sulphide is converted to an oxide while releasing sulphur dioxide gas. The gas is then purified through an electro-filter and scrubbing process and then sent to the sulphuric acid plant where sulphuric acid is produced for sale. The calcine recovered from the roaster is leached in sulphuric acid whereby copper sulphate is dissolved. After the solution is separated from the residue by filtration, it is sent to the electrowinning house where copper is produced on the cathode. Sulphuric acid is produced on the anode and recycled back to the copper leach step.

The residue that is separated from the copper electrolyte is exposed to several process steps, which include hydro-chloric acid leaching and separation and smelting of the residue. The precious metals are thereafter produced in their pure form through respective processing.

3.1. Description of the Effluent Treatment Process at Nikkelverk

The effluent treatment process performs three critical tasks:

- It limits the discharge of harmful elements from the plant to the effluent
- It allows the plant to comply to the discharge limits set by authorities
- It recovers valuable elements from effluents
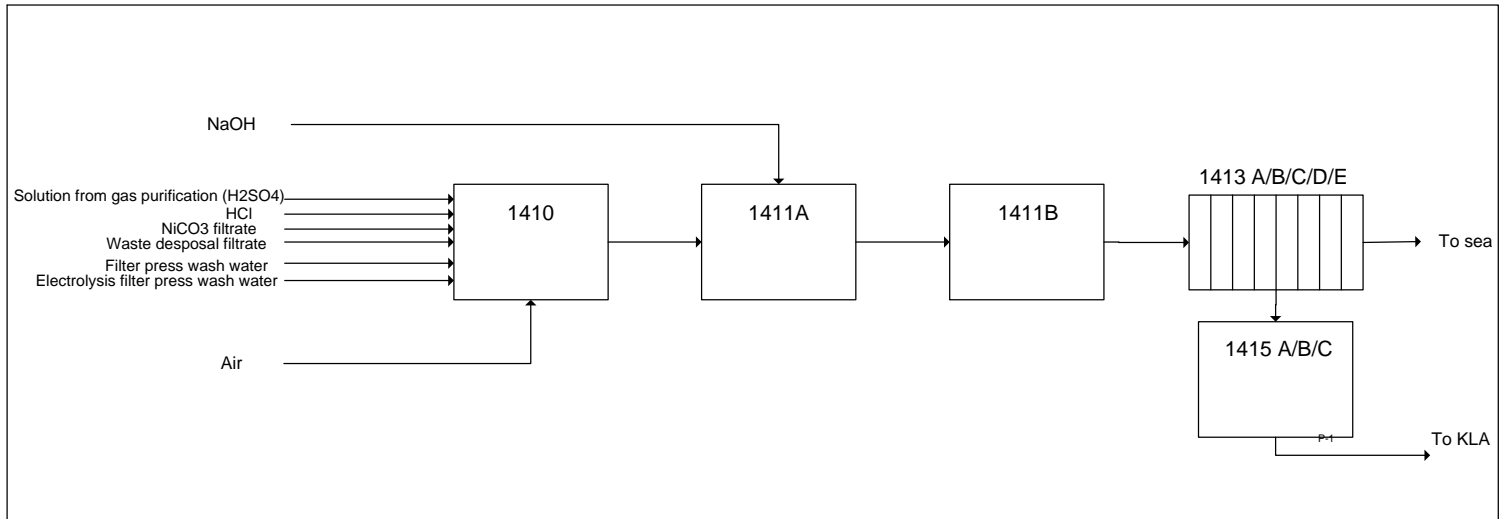
Figure 3.2: Block diagram representation of the Glencore Nikkelverk effluent treatment plant

All effluent liquid streams are sent to the effluent treatment plant, which consists of three agitated tanks in series. The feed streams first enter T-1410, which is a carbon dioxide stripping tank, and the overflow flows to T-1411A and then to T-1411B which are precipitation tanks. T-1411B is used as a pumping tank. The solution is then sent to the filter presses (1413 A-E), after which stage the filtrate is diluted with water and, if it meets the requirements set by CPA (Climate and Pollution Agency), is discharged to the sea. Air is added to T-1410 to strip of CO2, HCl is added to T-1410 to lower the pH and NaOH is added to 1411A for metal precipitation.

The flowrate into T-1410 varies greatly as the streams do not all flow on a regular basis. The residence time in the tanks therefore varies accordingly, however is approximately 30 minutes for T-1411A and T-1411B.

CO_2 stripping – T-1410:

Solution from the KL (chlorine leach) plant contains sodium bicarbonate ($NaHCO_3$) from nickel carbonate ($NiCO_3$) precipitation. This solution operates as a buffer – i.e. it is able to neutralise acid from the gas purification plant. Through mixing, the bicarbonate is converted to CO_2 gas which will be sparged off:

$$2NaHCO_3 + H_2SO_4 \leftrightarrow Na_2SO_4 + 2H_2O + 2CO_2 \qquad\qquad [3.1]$$
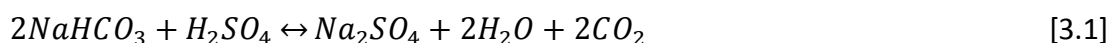
Precipitation tank – T-1411A:

In T-1411A, the metal ions precipitate as metal hydroxides through the addition of 600 g/l NaOH:

$$NiCl_2 + 2NaOH \leftrightarrow Ni(OH)_2 + 2NaCl \qquad [3.2]$$

$$CuCl_2 + NaOH \leftrightarrow Cu(OH)_2 + NaCl \qquad [3.3]$$

$$CoCl_2 + 2NaOH \leftrightarrow Co(OH)_2 + 2NaCl \qquad [3.4]$$

$$Fe^{3+} + 3NaOH \leftrightarrow Fe(OH)_3 + 3Na^+ \qquad [3.5]$$

By addition of NaOH, the pH increases to approximately 9.5 (though often ranging between 9 and 10) and nickel, copper and cobalt precipitate out as hydroxides. Iron from the caverns is partially in the form of precipitated ferric hydroxide and partially dissolved. Usually NaOH is not added to T-1411B which serves as a mixing/pump tank that can be used if T-1411A should be temporarily substituted.

The hydroxide residue that is formed is filtered off through filter presses, dispersed and pumped to the KL plant for re-processing. The filtrate, which mostly contains sodium chloride (NaCl) and sodium sulphate (Na_2SO_4) is diluted with sea water as well as various other water streams, analysed to ensure it meets discharge requirements and sent to the sea. Additional information regarding the chemistry pertaining to tank 1410 (stripping of CO_2 and air stripping prior to purification is given in appendix A).

3.2. Design Specifications of Existing Filter Presses in the Effluent Treatment Plant

The specifications of the existing filter presses, medium for filtration and operation are given in the following table.

Table 3.1: Filter, medium and filtration operation specifications for existing filter presses

Filters		
Type	Chamber presses	
Number of units	5	
Frame dimensions	4 units: 1,2 x 1,2; 1 unit: 1 x 1	m^2
Chamber thickness	0,05	m
Effective volume	1 - 2,1	m^3 (per unit)
Effective filter area	50 - 85	m^2 (per unit)
Filter cloth	Polypropylene, multi-multi filament	
Medium		
Type of residue	Metal hydroxide precipitate	
Temperature	25 - 40	°C
Filtrate pH	9 - 10	
Filtrate density	1 - 1,05	g/cm^3
Filtrate viscosity	1	cp (at 30°C)
Residue density	3 - 4	g/cm^3 (dry)
Particle size	10 - 30	μm
Cake bulk density	1,1 - 1,2 (wet); 0,2 - 0,3 (dry)	g/cm^3 (wet)
Cake moisture	80 - 85	% (H2O)

Max. flowrate	180	m^3/hr
Typical flowrate	140	m^3/hr
Solid content in slurry	2 - 10	g/l
Max. pump pressure	5 - 6	bar
Number of presses emptied	30 - 50	number per day
Total cycle time	4 - 8	hrs
Effective filtration time	>80% of total cycle time	
Filter press load	100 - 200	kg dry solids/press
Specific filter cake resistance	2 x E^12 - 5 x E^12	m/kg
Cake treatment	Repulped in stirred tanks	
Target	No solids in filtrate - effluent to the sea	

Table 3.1 indicates the typical range of parameters experienced by filter press operation, though variations do occur.

4. DrM Fundabac Candle Filtration Equipment

"DrM, Dr. Mueller AG is a privately held enterprise with its headquarters in Männendorf, Switzerland where it develops, designs and fabricates filtration systems for solid/liquid separation in the processing industries." (DrM, 2014)

4.1. Description of Equipment

The DrM Fundabac filtration system consists of a vertical chamber with filtration candles placed inside. The filter cloth is fitted around the outside of the candles. The feed (containing solids and liquid) is fed in to the bottom of the chamber and is fed until the chamber is full. The solution is then filtered through the candles so that a cake forms on the outside of the candles while the filtrate flows out the top of the chamber. In some cases, this is followed by a washing step. The excess solution in the chamber is then drained out from a valve in the bottom. Blowing thereafter occurs by an air supply in order to dry the cake. A back flush of air then results in the cake being released from the candles and falling into a container situated below the chamber.

The filter is designed to enable safe filtration while ensuring adherence of the filter cake to the cloth and thereafter for effective cake discharge. The filtration elements contain a clover leaf cross-section which enables adherence of the cake during filtration. This occurs because the concave parts of the filter element cause the cake to adhere during compression, ensuring that it remains in place during the filtration cycle. The filtrate passes through the filter cloth and flows into the peripheral tubes through slots and then down to the bottom of the candle before flowing upwards in the central tube toward the registers. The multi-channelled candles enable downward flow by gravity and thereafter upwards flow hydraulically in the central tube.

The cake discharge occurs by counter-current flow and pressure in the interior of the candle. The clover leaf interior structure of the filter accentuates the effects of this counter-current force. It enables an extreme outward billowing of the filter cloths, particularly at the zone where the cake adheres, causing vertical cracks in the cake. The quick-pulse gas blow-back into the filter hose instantly releases the cracked cake which then falls into the chamber below (DrM, 2014).
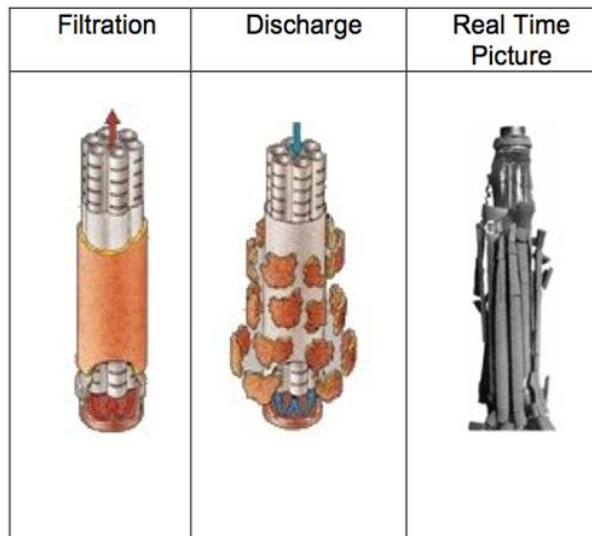
Figure 4.1: Image showing the filter cake build-up and release during filtration and discharge (DrM, 2014)
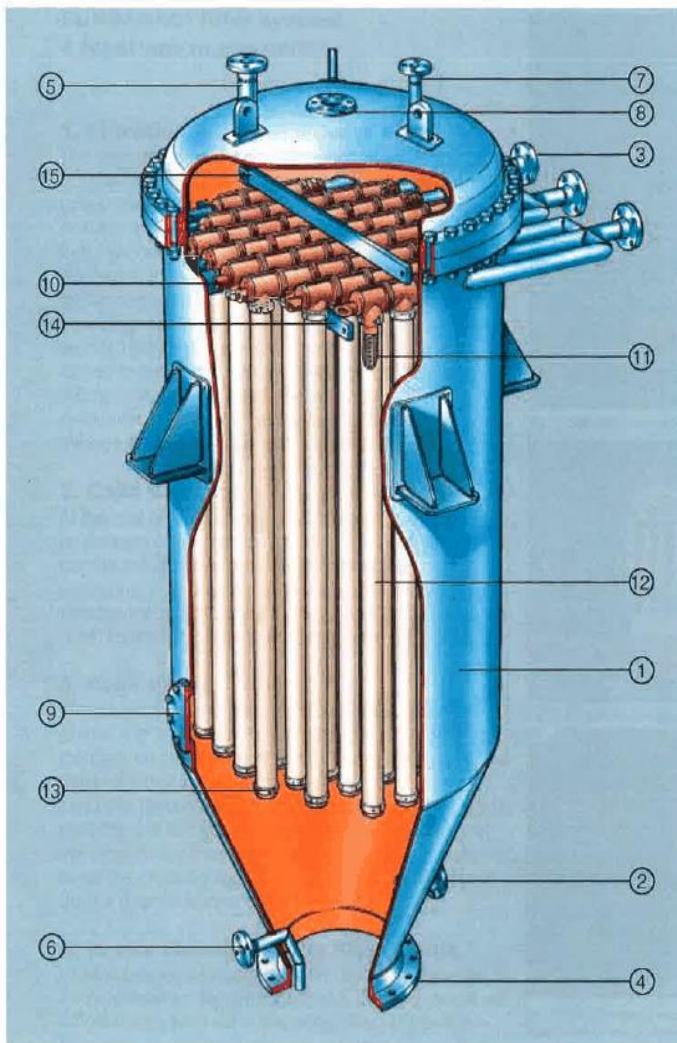
1	Pressure vessel
2	Product feed nozzle
3	Filtrate nozzles
4	Solid-residue discharge nozzle
5	Overflow and vent nozzle
6	Heel volume nozzle
7	Instrumentation nozzle
8	Saddle and flange for heel filtration spray jet nozzle
9	Inspection port
10	Register
11	Filter element
12	Filter medium (cloth)
13	Cloth clamp ring
14	Lower register for support bar (only for synthetic internals)
15	Upper register support bar (only for synthetic internals)

Figure 4.2: Illustration of the DrM Fundabac filter design with an accompanying index (DrM, 2014)

4.2. Operation of DrM Fundabac Pilot Filtration Rig in the Effluent Treatmant Plant

A pilot filter rig of this technology is used for investigation in this study. The dimensions and operating restrictions are given below.

Table 4.1: Description of the DrM Fundabac pilot filter rig used for testing in the effluent treatment plant

Number of candles	3	
Filter area per candle	0,33	m^2
Total filter area	1	m^2
Length of candle	138	cm
Diameter of candle	8,5	cm
Distance between candles (from edge to edge)	9	cm
Maximum width of cake	3,5	cm
Maximum flowrate of feed	5	m^3/hr
Maximum pressure of feed	4,5	bar
Maximum pressure during blowing	4,5	bar
Maximum pressure during blow-back	4,5	bar
Design pressure of the chamber	7	bar
Pipe diameter	2,5	cm
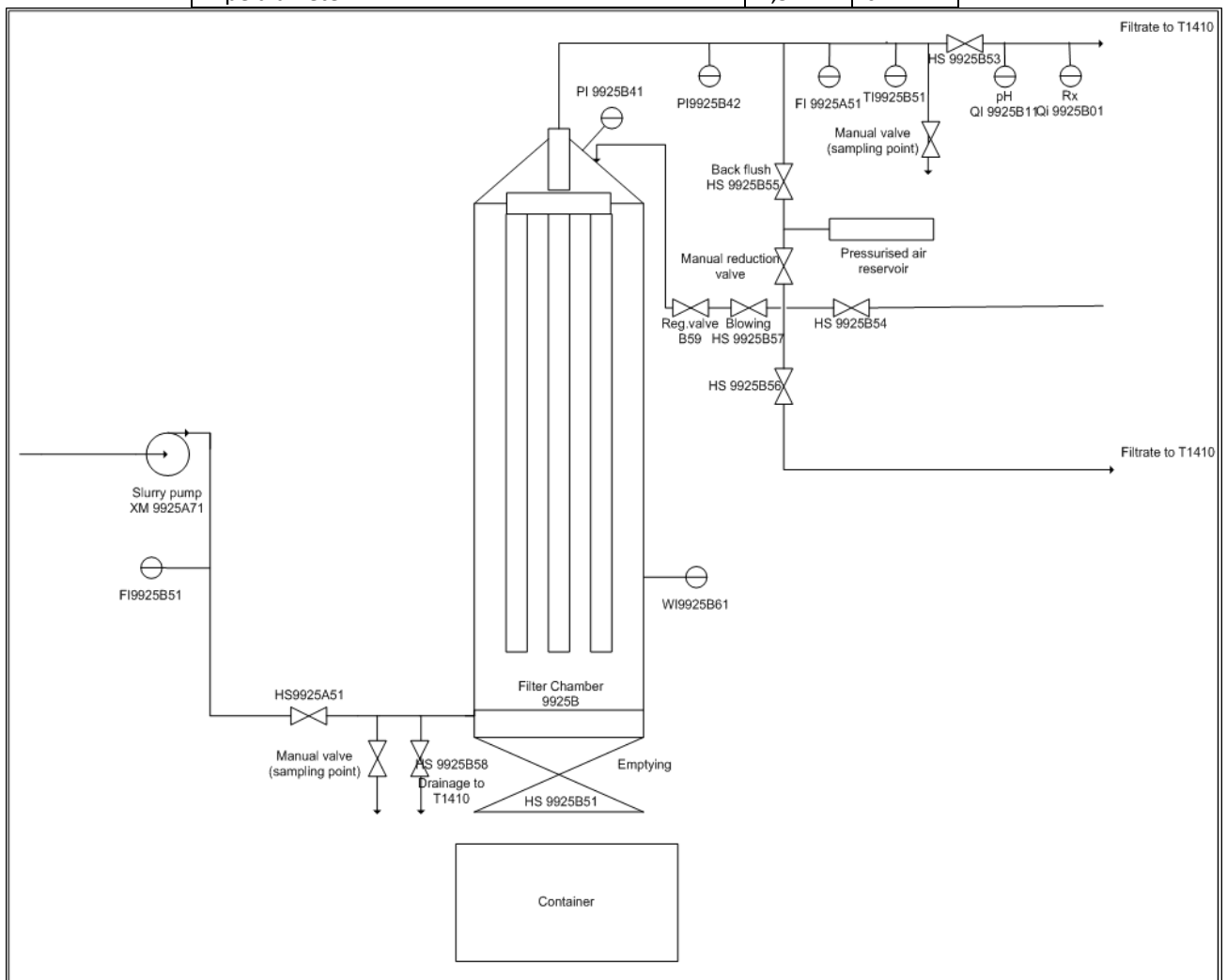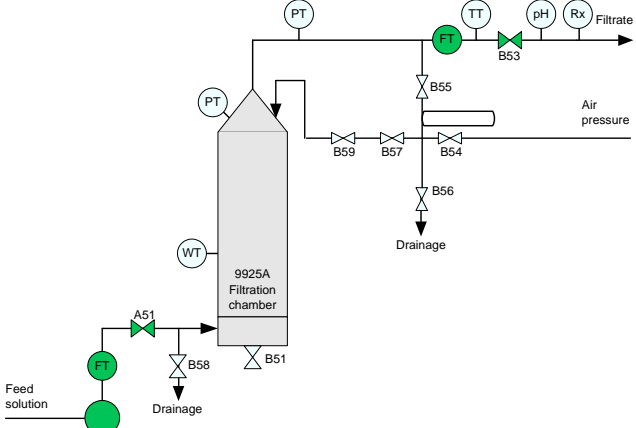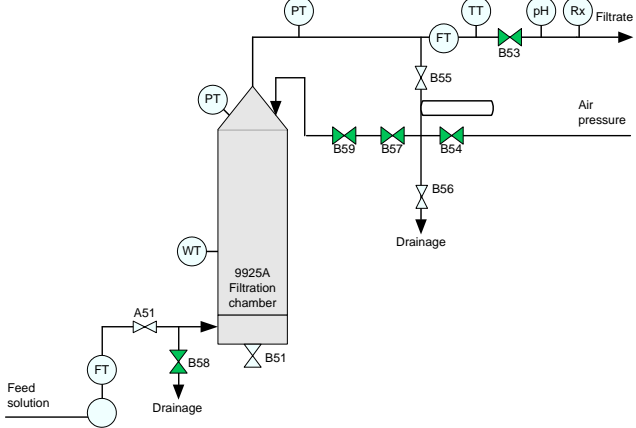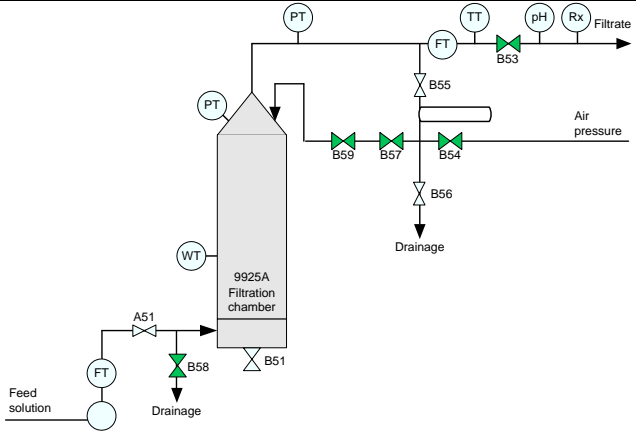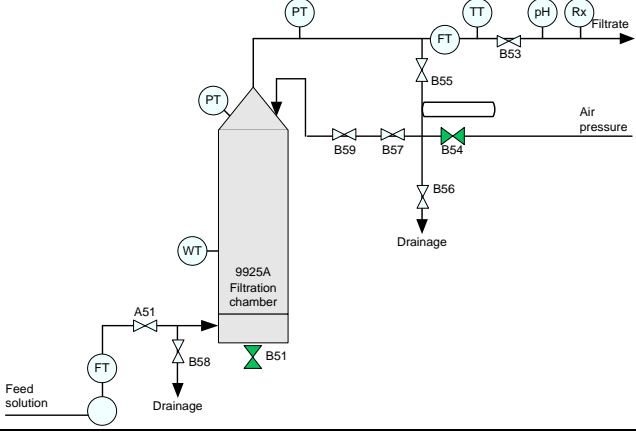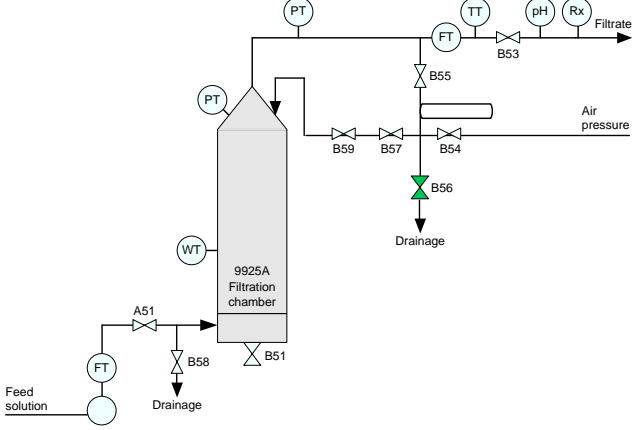
Figure 4.3: Schematic of the DrM Fundabac filter rig showing the filter chamber, pumps, pipelines, valves and control regulators

The filter rig is set up so that solution from T-1411B is fed to the filter, while filtrate is returned to T-1410. The filter cake is removed manually and discharged along with the cake from the filter presses.

The filter is programmed to operate automatically once started. Samples are taken manually by opening the valves at the sampling points. The programmed sequence for filtration, drainage, blowing and cake release is given below. Green valves indicate those that are open.

Table 4.2: Detailed filtration sequence

Step 1. Filling candles with solution, filtration	
1. Open A51 to allow feed solution in Open B53 to allow filtrate out 2. Start the feed solution pump *The pump is regulated to the desired flow until the pressure in the chamber is larger than the desired pressure set point. The pump is thereafter regulated by the pressure in the chamber.* 3. Set the filtration time	
Step 2. Filtration time	
4. Start countdown of filtration time 5. Time expired	
Step 3. Drainage	
6. Stop feed solution pump Close A51 to stop feed solution in 7. Open B53 to allow feed solution out Open B54 to allow air supply Open B57 to allow air blowing Open B59 (regulating valve) Open B58 to drain solution	
Step 4. Drainage time	
8. Start countdown of drainage time 9. Time expired	
Step 5. Blowing	

10. Close B58 5 seconds after blowing begins
11. Open B53 to allow filtrate out
    Open B54 to allow air supply
    Open B57 to allow air blowing
    Open B59 (regulating valve)
    Open B58 to drain solution	

Step 6. Blowing time	
12. Start countdown of blowing time 13. Time expired	
Step 7. Back flush	

14. Close B57 to prevent air blowing
    Close B59 (regulation valve)
    Close B58 (drainage)
15. Open B51 to enable cake release from chamber
    Open B54 to allow air supply	

Step 8. Back flush time	
16. Start countdown of back flush time 17. Time expired	
Step 9. End of filtration sequence	

18. Close B51 (bottom valve)
    Close B53 (filtrate out)
    Close B54 (air supply)
    Close B55 (back flush)
    Close B58 (drainage)
19. Open B56 to allow draining of exit pipe
20. Filtration sequence finished	

Figure 4.4: The left image shows the candle filter vessel. The right image shows of the demounted candles taken out of the container. The top candle is without a filter cloth while the bottom two candles are covered by a filter cloth.

5. Experimental Methods and Materials

The study involved different stages of experiments starting from laboratory filtration experiments which then led to filtration experiments on the filtration rig.

5.1. Primary Cloth Screening Trials

5.1.1. Filter cloth screening tests

Upon description of the nature of the slurry for filtration (table 3.1), four filter cloth suppliers supplied cloths for trials. These were DrM, Markert, Clear Edge and Septek. After an initial round of testing, feedback was given and the suppliers sent more cloths for trials. The filter cloth screening tests involved performing a simple Labox vacuum filtration test using the filter cloth and a concentrated sample of solution taken from T1411B. The filtration time, clarity of filtrate and cloth release was observed. The procedure and materials are outlined as follows:

Solution

Solution was fetched using plastic containers from out of tank 1411B, which feeds to the filter presses in the effluent treatment plant. The concentration of solids in the solution is usually between 2 to 10 g/l (this varies due to variation in feed to the effluent treatment plant). In order to obtain filtration tests with a sufficiently thick filter cake on the cloth, the solids concentration was increased. The container was left still allowing the solids to settle and the top layer of liquor was decanted from top of the container. The remaining solids concentration was then measured by taking 100 ml of solution, filtering the solution (see figure 5.3), drying the cake and then weighing the dry cake. The solids concentration was 28,1 g/l. It was important to have the same solution used for every cloth screening test to give comparable results.

Experimental

The experimental setup is show in figure 5.1.

1. The solution was heated in a water bath to 35 °C (the solution in the precipitation tanks varies between approximately 25 °C and 40 °C)
2. Vacuum was enabled by opening the vacuum tap
3. 500 ml of solution was added to the Larox filter which uses vacuum as the driving force for filtration
4. The time taken for the filtrate to fill 8 volumetric intervals and the pressure at such intervals was recorded [min]
5. Filtration was finished upon a decrease in pressure, and the pipe connecting to the vacuum disconnected
6. The volume of filtrate was measured from the measuring cylinder inside the flask [ml]

51

7. The filtrate was filtered using a Nutsche filter and Millipore filter paper (see figure 5.3)
8. The residue recovered was then placed on a glass (the filter paper and glass previously weighed), set inside the oven to dry, and then weighed on a scale once dry [g]
9. After opening the sealing, the compartment holding the filter cloth and cake was tilted from the horizontal to see at which angle the cake would fall
10. The cake was weighed, dried in an oven and weighed again once dry to obtain moisture content [%]

5.1.2. *Specific filter cake resistance and medium resistance tests*

The cloth screening tests gave an indication of which cloths should be tested further to obtain data for specific cake resistance and specific cloth resistance. Six cloths were chosen for these tests.

Experimental

The experimental setup is shown in figure 5.2

1. The solution was heated in a water bath to 35 °C
2. 80 ml of the solution was added to the Nutsche filter apparatus which uses vacuum as a driving force for filtration
3. The time taken for the filtrate to fill 7 volumetric intervals was recorded [min]
4. The filter area was recorded (this is a standard area and the same for all tests) [cm]
5. The filter pressure was recorded from the pressure gauge attached [bar]
6. The temperature of the solution was recorded [°C]
7. The total filtrate volume was measured using the measuring cylinder filled during filtration [ml]
8. The cake and cloth were placed on a glass (the glass and cloth had been weighed) and then weighed using a scale [g]
9. The cake was then set in a drying oven to dry, and the mass recorded when dry, using a scale [g]
10. The viscosity of the filtrate was calculated. The filtrate was sent through a glass capillary (U-tube) viscometer which was placed in a beaker that was kept at the desired temperature and the time taken to move between the two points (above and below the bulb) was recorded. This was done three times and an average reading recorded. The viscosity was then calculated (see data analysis). [cp]
11. The specific weight was measured using a density hydrometer [g/cm^3]

All values were then converted to S.I. units during data analysis.

5.2. DrM Fundabac Filter Rig Trials

The sequence of operation of the DrM Fundabac equipment is detailed in chapter 4. The filter cloths used for trials were:

- DrM G 11 U 010
- DrM F 11 U 020

- DrM N 11 U 030
- Markert PPV 2737
- Clear Edge 98080F

See appendix B for filter cloth technical data.

5.2.1. Trial Schedule

The initial daily programme of operating the rig with each cloth consisted of two cycles with three runs each. The slurry flowrate (5 m^3/hr) and applied pressure (4 bar) were set constant for each run, while the filtration time was either 20 minutes, 30 minutes or 40 minutes. This was in order to obtain comparable data and to see how the cloth handled the variations in feed at constant flowrate and pressure. The programme was repeated for between two and three days. Because the rig is set up in a currently-operating part of the plant, plant conditions (relating to factors such as other operations in the vicinity or pressure availability, for example) in some cases prohibited operation of the rig. It was therefore aimed to operate the rig for at least two days at set parameters.

Table 5.1: Test schedule for operating the filter

Cycle	Run	Slurry flowrate	dP	Filtration time
(-)	(-)	(m3/hr)	(bar)	(mins)
1	1	5	4	20
1	2	5	4	30
1	3	5	4	40
2	1	5	4	20
2	2	5	4	30
2	3	5	4	40

Having operated the filter rig at set parameters, the final day of cloth testing involved operating each run at varied flowrate, pressure and filtration time. The purpose of these trials was to obtain an idea of which parameters would enable optimal filtration with regards to capacity of filtrate filtered for that specific cloth. The parameters were not set but were varied upon the results of the previous trials (for instance, if a thin cake was achieved during one trial, the filtration time or flowrate may have been increased during the next trial).

The time allocated to draining, blowing and emptying was set upon recommendation from the manufacturer. The time for filtration was varied.

Table 5.2: Time allocated for filtration, draining, blowing and emptying

Filtration	20 minutes/30 minutes/40 minutes
Draining	1 minute
Blowing	5 minutes
Emptying	2 minutes

5.2.2. Sample Preparation

Samples were collected in order to analyse the slurry feed to the filter and the filtrate and cake from the filter. Samples were taken once per cycle (during the first run of each cycle) and it was assumed that the measurements obtained applied to all runs during that cycle. The samples taken and measurement obtained from each sample is outlined in the table below.

Table 5.3: Sample taken and measurement required

Cycle	Sample	Measurement
1	Slurry	Solids concentration
		Filtrate element analysis
		Cake element analysis
	Filtrate (0 minute)	Solids concentration
	Filtrate (5 minute)	Solids concentration
		Element analysis
	Filter cake	Moisture content
2	Slurry	Solids concentration
	Filtrate (0 minute)	Solids concentration
	Filtrate (5 minute)	Solids concentration
	Filter cake	Moisture content

The slurry sample (approximately 400 – 500 ml) was obtained at the beginning of the filtration cycle. The filtrate (0 minute) sample (approximately 700 – 1000 ml) was obtained immediately after the first volume of filtrate exited the filter. The filtrate (5 minute) sample (approximately 700 to 1000 ml) was obtained after filtration had occurred for 5 minutes. The filter cake sample (approximately 100 to 200 g) was taken at the end of the filtration cycle. All liquid samples were taken to the laboratory and placed in a warm bath set to the temperature of filtration operation. A short description of the steps used for sample preparation followed by a more detailed description of the laboratory process is given below.

Slurry sample

1. The slurry was filtered using a Buchner funnel and filter paper
2. The filtrate volume was measured using a measuring cylinder [ml]
3. A 10 ml sample of filtrate from the first cycle was taken using a pipette
4. The sample was placed in a sealed flask with 10 ml of 37 % HCl (to prevent precipitation of metals) and sent for element analysis
5. The residue sample was placed on an hour glass (the mass of the hour glass and filter paper having been weighed on a scale) and set in the oven at 50 °C

6. Once dry, the dry mass was recorded [g] and the dry mass concentration in the filtrate calculated [g/l]
7. The sample was then crushed into a fine powder using a mortar and pestle, placed in a zip-lock bag and sent for element analysis

Filtrate (0 minute) and filtrate (5 minute) samples

1. A 10 ml sample of the filtrate (5 minute) sample from cycle one was taken with a pipette prior to laboratory filtration
2. The sample was placed in a sealed flask with 10 ml of 37 % HCl (to prevent precipitation of metals) and sent for element analysis
3. The filtrate (0 minute) and filtrate (5 minute) samples were filtered individually using a Nutsche filter and 0,65 μm Millipore filter paper
4. The filtrate volume was measured using a measuring cylinder [ml]
5. The residue sample was placed on an hour glass (the mass of the hour glass and filter paper having been weighed on a scale) and set in the oven at 50 °C
6. Once dry, the dry mass was recorded [g] and the dry mass concentration in the filtrate calculated [g/l]

Filter cake sample

1. The wet filter cake was placed on an hour glass (mass previously recorded), weighed and set in the oven to dry
2. Once dry, the mass was recorded in to obtain the filter cake moisture content [%]

5.2.3. Viscosity determination

The viscosity of the filtrate of one slurry sample was determined and this value was assumed constant for all trials. The viscosity was determined as described in section 4.1.2. and a sample calculation is given is appendix D1.

5.2.4. Analysis of elements in the analytical laboratory

The filtrate and residue samples were analysed in the analytical laboratory for nickel, copper, cobalt and iron concentrations. ICP-OES (inductively coupled plasma optical emission spectrometry) was used for analysis of the metals. The residue samples were analysed using either X-ray, for high concentrations, or FAAS (flame atomic absorption spectrometry) for low concentrations.

5.3. Particle Characterisation and Moisture Content Comparison

Trials were done using cloth Markert PPV 2737 to obtain samples which were then sent for Malvern particle size analysis as well as to obtain scanning electron microscope pictures. Filtration was performed thrice throughout one day. For all trials, the flowrate was 2,5 m^3 per hour, the applied pressure was 4 bar and filtration time was 40 minutes. Samples were taken and analysed as described in section 5.2.2.

Three additional filter cake samples were taken and prepared for element analysis, Malvern analysis and SEM. The samples for element analysis and for SEM were weighed, set in the oven to dry and once dry, weighed again to obtain the moisture content. The two dried samples were then crushed into a fine powder using a mortar and pestle, placed in a zip-lock bag and sent for element analysis and for SEM analysis. The sample for Malvern analysis was left in the form of a moist residue (four samples were sent for Malvern analysis).

5.4. Apparatus
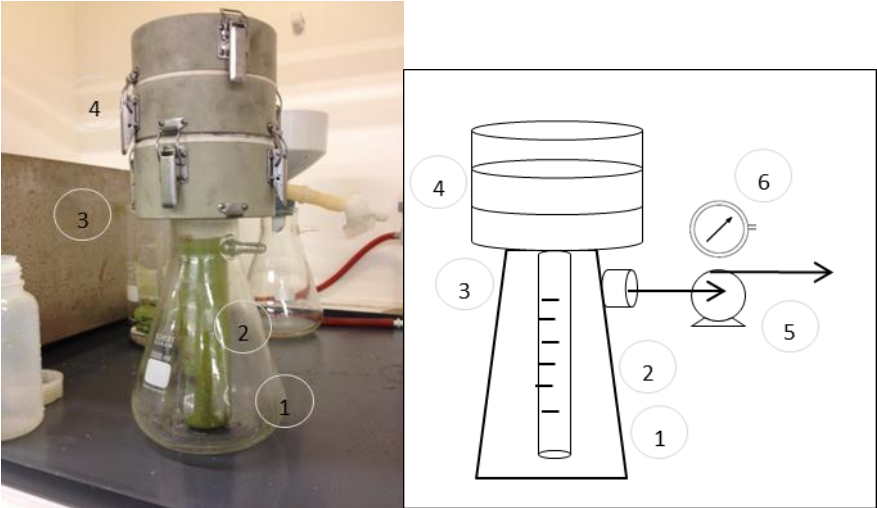
Figure 5.1: Primary cloth screening filtration apparatus
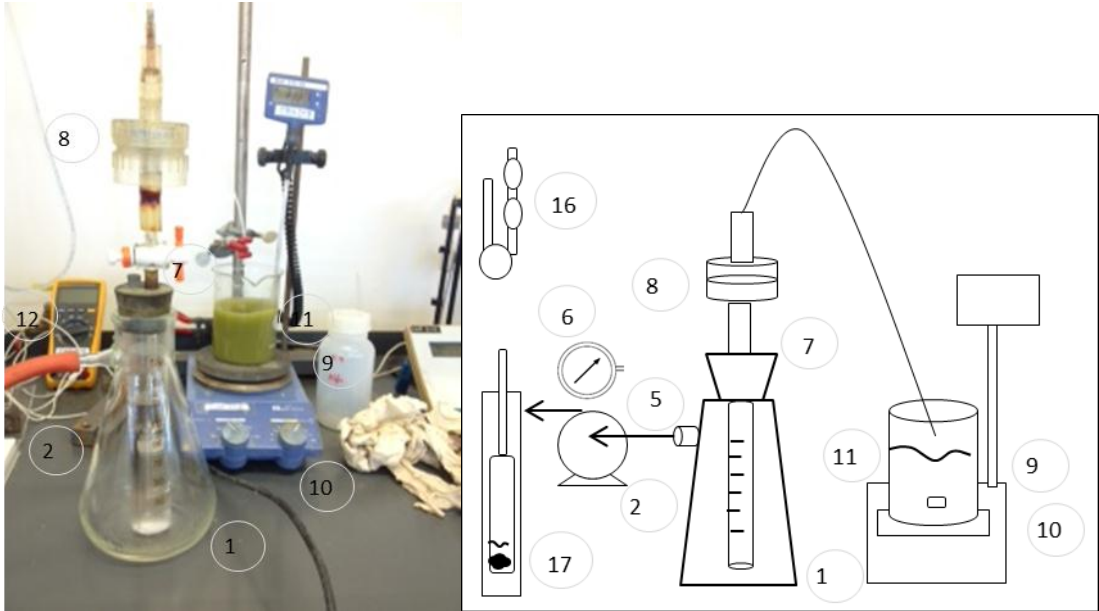
Figure 5.2: Specific cake resistance and medium resistance filtration apparatus
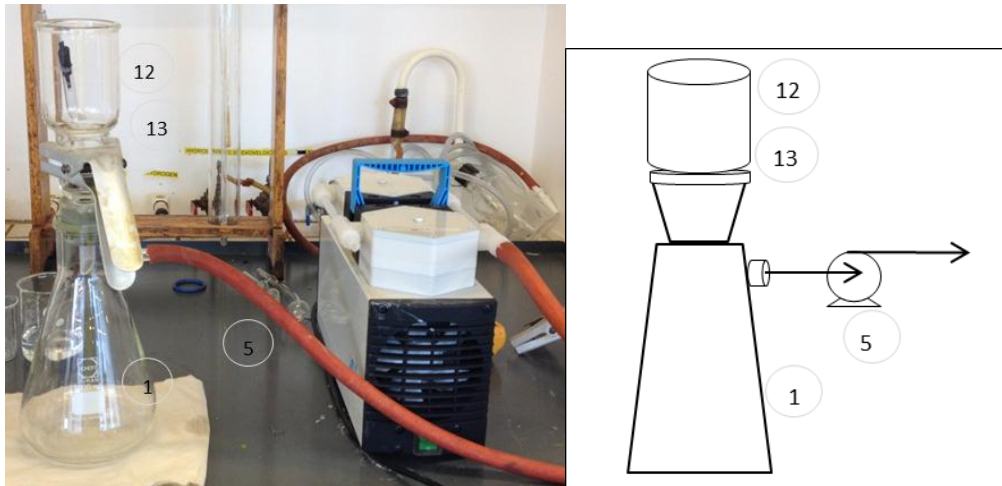
Figure 5.3: Apparatus for filtration of samples from filter rig (filtrate samples)
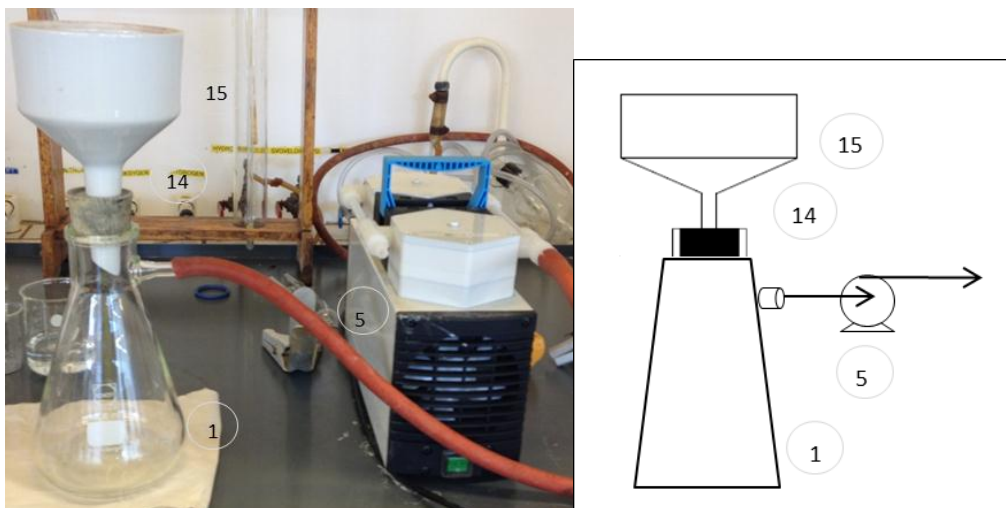
Figure 5.4: Apparatus for filtration of samples from filter rig (slurry samples)

Table 5.4: List of apparatus used

Nr	Apparatus	Type/manufacturer/model
1	Glass flask	Schott Duran, 1000 ml, Germany
2	Glass measuring cylinder	Silber Brand Eterna, Germany
3	Filter	Larox, Pannevis
4	Filter cloth	DrM/Markert/Clear Edge/Septek
5	Filtration pump	KnF Neuberger Laboport, 0-1 bar
6	Vacuum guage	Wikai, 0-1 bar, pipe - Glaskeller, Italy
7	Filter	Sartorius Gmbh D-3400 Goettingen
8	Filter cloth	DrM/Markert/Clear Edge/Septek
9	Heater and temperature senser	IKA werke RCT basic, -50
10	Magnetic stirrer	IKA werke RCT basic, 0-1400 rpm
11	Glass beaker containing magnet	250 ml beaker, magnet - Prismeformet, length 25 mm
12	Millipore filter	Sartorium Stedium, Goettingen
13	Millipore filter paper	Sartorius Stedium Biotech, 0,65 µm
14	Buchner funnel	Haldenwanger
15	Filter paper	Whatman Schleicher & Schuell, 110 mm Ø
16	Viscometer	Cannon-Fenske, nr 50, Senott Gerate 513 03, mounted and stirred using apparatus 9, 10 and 11
17	Density Hydrometer	Widder, in glass cylinder

5.5. Analysis of Data

5.5.1. Laboratory experiments

Viscosity calculation

The viscosity of the filtrate is measured using the following relationship:

$$\mu_{t,1} = \mu_{t,H2O} \frac{T_{t,1}\delta_{t,1}}{T_{t,H2O}\delta_{t,H2O}}$$
[5.1]

Where:

$\mu_{t,H2O}$	Viscosity of distilled water at temperature t [cP]
$T_{t,1}$	Time recorded during viscosity test of sample at temperature t [mins]
$T_{t,H2O}$	Time recorded during viscosity test of distilled water at temperature t [mins]
δ_t	Specific weight of sample at temperature t [g/cm^3]
$\delta_{t,H2O}$	Specific weight of distilled water at temperature t [g/cm^3]

See appendix D1 for tables used to determine distilled water properties.

Determination of specific cake resistance (α) and medium resistance (R_m)

The relationship between filtrate volume and filtration time (as formulated in the literature review) can be represented as follows:

$$\frac{t}{V} = \frac{\alpha\mu c}{2A^2\Delta p}V + \frac{\mu R}{A\Delta p}$$
[5.2]

All data obtained was converted to S.I. units such that:

V	Set of volumes measured [m3]
t	Set of filtration times for each volume [sec]
μ	Viscosity of suspension [PaS]
A	Filter cake area [m^2]
Δp	Filtration pressure drop [bar]
c	Concentration of solids in suspension [kg/m^3]

Using the linear regression function in Excel, the slope (m) and y-intercept (C) was obtained from the range of filtrate volume and time data. The specific cake resistance (α) and medium resistance (R_m) was then calculated whereby:

$$\alpha = \text{m}\frac{2A^2\Delta p}{\mu c}$$
[5.3]

$$R_m = C\frac{A\Delta p}{\mu}$$
[5.4]

See appendix D2 for a sample calculation.

5.5.2. Filter Rig Operation

Viscosity calculation

The viscosity was calculated as shown in the laboratory section. It was then assumed that, given how close the measured viscosity was at 35 °C to that of distilled water, the viscosity followed the same shift in value with temperature as does distilled water. The appropriate viscosity was then extrapolated accordingly by the temperature of filtration (see appendix D3 for tables).

Pressure drop (Δp)

The inlet pressure on the filter is set. *(Δp)* is measured by the filter data system and is equal to the pressure at the inlet of the filter minus the pressure at the outlet of the filter.

Determination of specific cake resistance (α) and medium resistance (R$_m$)

As deduced in the literature review, the relationship for determination of α and R$_m$ from a starting point t$_s$, V$_s$ is given as:

$$\frac{t-t_s}{V-V_s} = \frac{\alpha\mu c}{2A^2 \Delta p}(V+V_s) + \frac{\mu R_m}{A\Delta p}$$ [5.6]

All data obtained was converted to S.I. units such that:

V	Set of accumulated volumes measured [m3]
t	Set of filtration times for each volume [sec]
μ	Viscosity of suspension [PaS]
A	Filter cake area [m^2]
Δp	Filtration pressure drop [bar]
c	Concentration of solids in suspension [kg/m^3]

A trend of the pressure drop over the filter as a function of time was plotted for each test in order to determine the period whereby the pressure is constant. The pressure drop appears to reach a reasonably constant level (figure 5.5), however upon enlargement of this (figure 5.6), the pressure drop actually fluctuates slightly around a narrow point as it attempts to remain constant. An average Δp was thus calculated for the values in this period. Because these fluctuations were so narrow, the pressure was mostly constant and constant pressure calculations were applied.

A plot of $\frac{t-t_s}{V-V_s}$ against V for the whole range of accumulated volume and corresponding time data, and incorporating t$_s$ and V$_s$ (which are the time and accumulated volume at the start of the 'constant' pressure drop period), was plotted (figure 5.7). Using the linear regression function in Excel, the slope (m) and y-intercept (C) was obtained from the range of filtrate volume and time data recorded after t$_s$ and V$_s$, i.e. in the period that corresponds to 'constant pressure' operation.

Multiplying out the terms in equation 5.6, the slope is thus represented as:

$$m = \frac{\alpha\mu c}{2A^2 \Delta p} \qquad\qquad [5.7]$$

while the intercept is represented as:

$$C = \frac{\alpha\mu c}{2A^2 \Delta p}V_s + \frac{\mu R_m}{A\Delta p} \qquad\qquad [5.8]$$

The specific cake resistance (α) and medium resistance (R_m) was then calculated whereby:

$$\alpha = m\frac{2A^2 \Delta p}{\mu c} \qquad\qquad [5.9]$$

$$R_m = (C - mV_s)(\frac{A\Delta p}{\mu}) \qquad\qquad [5.10]$$

Using the calculated slope and y-intercept, a range of y-data for the constant pressure period was calculated whereby:

$$y = mV + c \qquad\qquad [5.11]$$

This range of y-values was plotted against the corresponding range of x values as can be seen by the black straight line represented in figure 5.7. This essentially shows how well the range of experimental data points fits the given slope and y-intercept values calculated by using an averaged Δp. The quadratic value for the experimental points in the 'constant pressure' period was calculated using the quadratic function in Excel, and this also shows the reproducibility of the data.
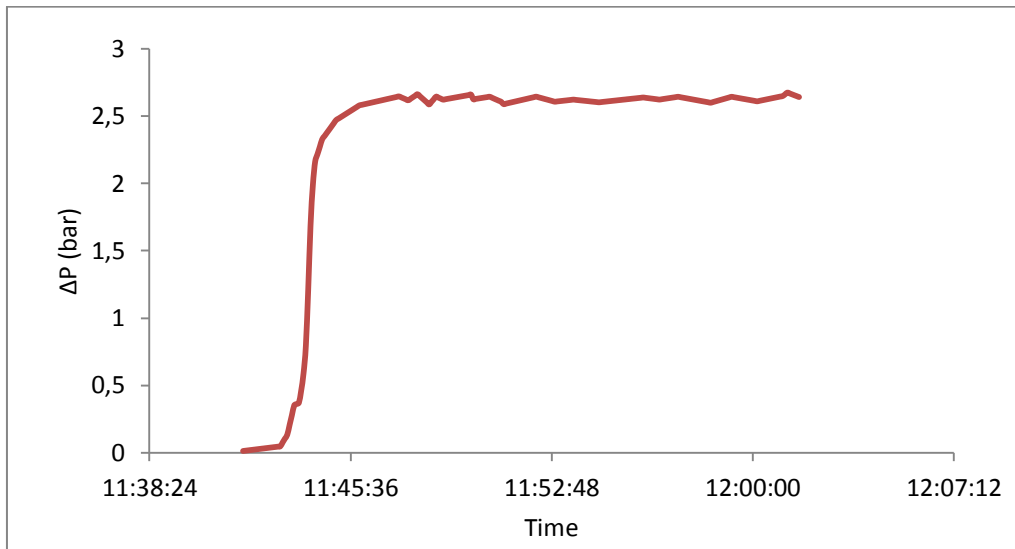
Figure 5.5: Plot of Δp as a function of time
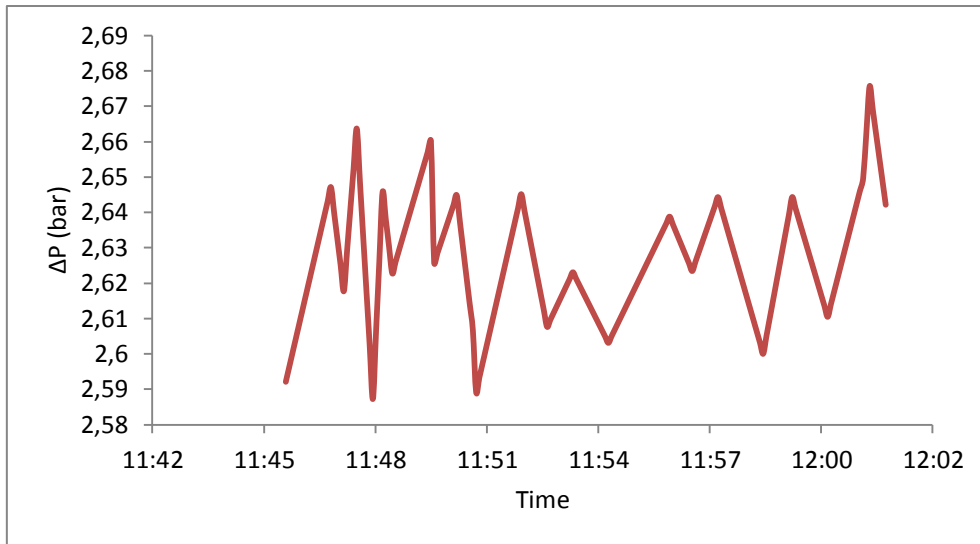
Figure 5.6: Enlarged portion of part of curve whereby Δp fluctuates around a narrow point
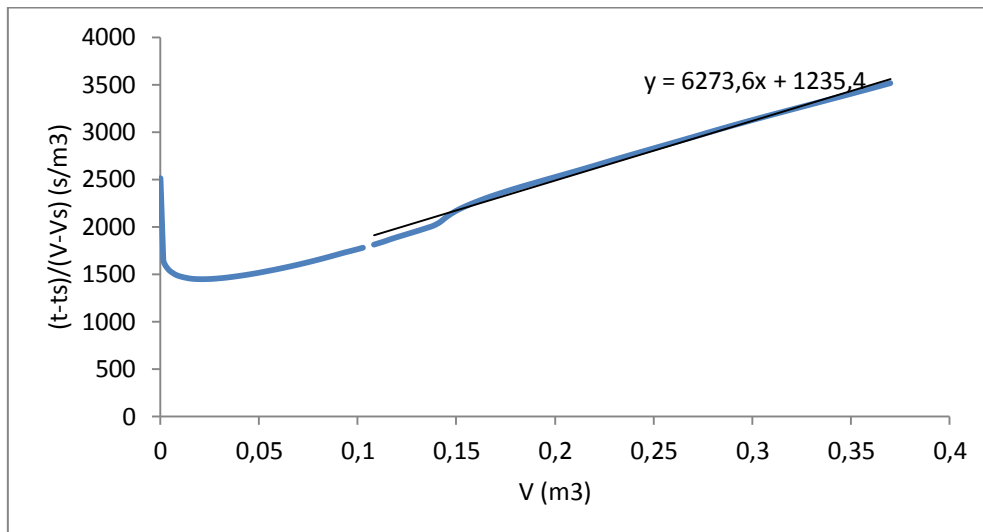
Figure 5.7: Plot of $\frac{t-t_s}{V-V_s}$ against V for the whole range of accumulated volume and corresponding time data

Proportion of pressure drop used up by filter medium

From equation 5.6, the term containing α was cancelled out and two points (t, V) were taken from the data, while the rest of the points, including the calculated R_m value were substituted into the following equation to solve for Δp_{Rm}. This value was therefore the Δp realised by the filter medium.

$$\Delta p_{Rm} = \frac{\mu R_m}{\left(\frac{t-t_s}{V-V_s}\right)A} \qquad\qquad [5.12]$$

61

There is a temperature sensor on the filter rig that records the temperature of the slurry every 5 seconds. An average temperature was calculated for the period of reasonably constant pressure.

pH

The pH monitor in the tank 1411B (which feeds slurry to the filter) records the pH continuously. An average pH was calculated for the period of reasonably constant pressure.

Accumulative volume of filtrate

The filter rig records the volumetric flowrate of filtrate out of the filter rig in 5 second intervals. The accumulative filtrate volume was thus calculated by multiplying each flowrate by 5 seconds and adding it to the previously calculated volume.

Mass of filter cake
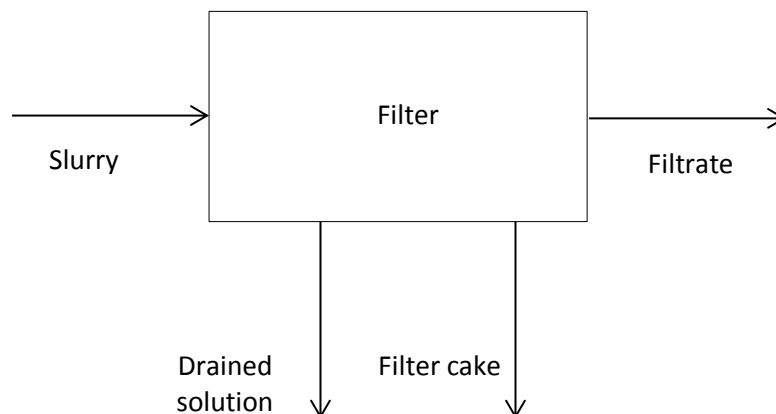
Figure 5.8: Representative mass and volume balance over the filter system

The diagram represents the volume/mass balance over the filter. The liquid volume balance is:

$$V_{l,slurry} = V_{l,drained\ solution} + V_{l,filter\ cake} + V_{l,filtrate} \qquad [5.13]$$

and the solid mass balance is:

$$m_{s,slurry} = m_{s,drained\ solution} + m_{s,filter\ cake} + m_{s,filtrate} \qquad [5.14]$$

The accumulated volume of slurry is known from multiplying the flowrate of slurry by the time passed and adding the accumulated totals. From laboratory measurements, the concentration of dry solids in the slurry is calculated which can then be converted to the total mass of solids in the slurry by multiplying by the total volume of slurry passed through the filter.

The accumulated volume of filtrate is known from multiplying the flowrate of filtrate by the time passed and adding the accumulated totals. The accumulated volume of filtrate passed through the filter after 5 minutes ($V_{l,filtrate(5min)}$) and at the end of the filtration period ($V_{l,filtrate(total)}$) was recorded. The concentration of dry solids in the filtrate was recorded immediately after the first drop of filtrate passed through ($c_{s,filtrate(0min)}$), and after 5 minutes of filtration ($c_{s,filtrate(5min)}$). These concentrations were extremely low for almost all tests runs. It was thus assumed that the concentration of solids passed through immediately was constant during the first 5 minutes, and that the concentration of solids passed after 5 minutes was constant until the end of the filtration period. The total dry mass of solids passed through the filter was then calculated whereby:

$$m_{s,filtrate} = c_{s,filtrate(0min)}V_{l,filtrate(5min)} + c_{s,filtrate(5min)}V_{l,filtrate(total)} \qquad [5.15]$$

The volume of solution that is drained after filtration and prior to cake release is unknown. The total mass of cake produced was therefore calculated by corresponding the solids concentration in the slurry to the total volume of filtrate produced.

$$m_{s,filter\ cake} = c_{s,slurry}V_{l,filtrate} - m_{s,filtrate} \qquad [5.16]$$

As this is the dry mass of filter cake produced, the wet mass was calculated given the moisture content of the cake:

$$m_{s,filter\ cake(wet)} = \frac{m_{s,filter\ cake(dry)}}{1-moisture\ content} \qquad [5.17]$$

6. Results

The results are presented with explanatory text accompanied *below* the tables and figures.

6.1. Initial Cloth Screening Tests

Table 6.1: Evaluation of various cloth types during laboratory tests

Nr.	Supplier	Cloth Type	Dry solids concentration in filtrate	Assigned value (30%)	Overall filtration rate	Assigned value (30%)	Cloth slip	Assigned value (40%)	Overall rating
			(g/l)		(ml/s)				
1	Clear Edge	25130 F	0,017	3	2,8	2	4	1	1,9
2	Markert	PPM 3508	0,030	3	2,4	1	4	1	1,6
3	Markert	PPD 3214	0,087	2	2,8	2	4	1	1,6
4	Markert	PPV 2737	0,022	3	3,0	2	3	3	2,7
5	Markert	PP 2436	0,027	3	2,9	2	4	1	1,9
6	Clear Edge	98080F	0,067	2	2,8	2	3	3	2,4
7	Markert	PPM 3502	0,52	1	3,0	2	4	1	1,3
8	Clear Edge	28560F	0,037	3	2,9	2	4	1	1,9
9	Markert	NST 648	0,033	3	3,0	2	3,5	2	2,3
10	DrM	G11 U 010	0,033	3	3,2	2	3	1	2,7
11	DrM	B11 MU 200	5,8	1	4,4	3	4	1	1,6
12	DrM	G11 M 025	0,23	1	2,9	2	4	1	1,3
13	DrM	B11 MU 100	5,1	1	4,2	3	4	1	1,6
14	Markert	PP 24901	0,032	3	2,4	1	3,5	2	2
15	Markert	PP 2448	0,020	3	2,4	1	3,5	2	2
16	Septek	PES 1950 MPX	0,028	3	3,3	2	3,5	2	2,3
17	Markert	PP 2402	0,031	3	3,2	2	3	3	2,7
18	Markert	PP 2433	0,051	2	3,3	2	3	3	2,4
19	Markert	PP 2455	0,14	1	3,1	2	3,5	2	1,7
20	Septek	PP 890X	0,033	3	2,8	2	4	1	1,9
21	Septek	PP CCCX Special	0,038	3	3,3	2	3,5	2	2,3
22	Septek	PP-555-X	0,55	1	2,7	2	4	1	1,3
23	Septek	PP-blue-Special	0,051	2	2,5	2	3,5	2	2
24	Septek	PP-LUMX-Special	0,033	3	3,2	2	4	1	1,9
25	Septek	Prop 3 SC	0,024	3	3,0	2	3	3	2,7
26	Septek	PP-677X	0,0080	3	2,8	2	3,5	2	2,3
27	Septek	Prop 2 NC	0,033	3	3,0	2	3,5	2	2,3
28	DrM	F11 U 020	0,017	3	3,1	2	3	2	2,7
29	DrM	N11 U 030	0,029	3	3,2	2	3	2	2,7

Table 6.2: Key for assigned values given in table 6.1

	Dry solids concentration in filtrate	Filtration rate	Cloth slip	Value assigned
	(g/l)	(ml/s)		
Good	0-0,05	>3,5	0-3	3
Medium	>0,05; <0,1	>2,5; <3,5	>3; <4	2
Poor	>0,1	0-2,5	4	1
Weighting	30 %	30 %	40 %	

Table 6.3: Element analysis of solution used for filtration tests

Element	Concentration in filtrate	Concentration in residue
	(mg/l)	(%)
Ni	0,37	39,01
Co	0,01	2,45
Cu	0,02	2,30
Fe	0,01	5,46

Table 6.1 shows the clarity of filtrate obtained, the filtration rate and cloth slip ratings from laboratory filtration tests on various cloths. Using the key in table 6.2, these ratings were then converted to an overall rating whereby the filtrate clarity had a weighting of 30 %, the filtration rate 30 % and the cloth slip 40 %. The issue with the effluent treatment plant residue is that it is so moist and slippery and can be released prematurely from the candles. A cloth that enabled good adhesion and thus little slip was thus desired. As cake release is critical for filtration cycle to be complete, the cloth slip weighting was highest.

Table 6.3 shows the concentration of metals in the filtrate and residue of the solution used for all filtration tests. The element analysis shows that the solution is representative of a typical solution fed to the effluent treatment plant filter presses.

The results show the following cloths to have the best overall filtration properties with a rating of 2,7 out of 3:

- DrM G 11 U 010
- DrM F 11 U 020
- DrM N 11 U 030
- Markert PPV 2737
- Markert PP 2402
- Septek Prop 3 SC

And with a rating of 2,4 out of 3:

- Clear Edge 98080F
- Markert PP 2433

Of these cloths, the following cloths were available from the various suppliers for testing on the pilot rig during the given test period:

- DrM G 11 U 010
- DrM F 11 U 020
- DrM N 11 U 030
- Markert PPV 2737
- Clear Edge 98080F

6.2. DrM Filter Rig Operation - Comparison of Cloths and Operating Parameters

The following results pertain to tests carried out on the filter rig. When operating using cloth Clear Edge 98080F, the cake stuck to the cloth and cake release did not occur. The cloth was operated on for three days with this problem occurring continually. The candles were eventually demounted in order to remove the cake manually. Results pertaining to this cloth were not obtained and are thus not represented. The aforementioned cloth names will be abbreviated to DrM G, DrM F, DrM N and Markert henceforth.

Note: *for the following sections (6.2 – 6.4), unless otherwise indicated, all data and measurements were obtained from tests run at identical set parameters.*

Table 6.4: Parameters set for filtration operation

Flowrate feed	*(m^3/hr)*	*5*
Inlet pressure	*(bar)*	*4*
Filtration time	*(mins)*	*20*

6.2.1. Clarity of filtrate obtained
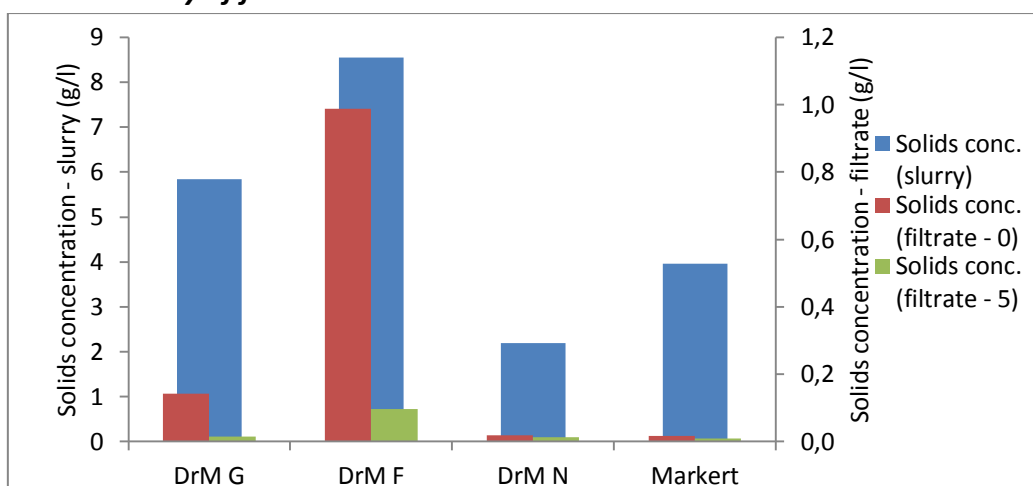
Figure 6.1: Average over all measured filtration tests for each cloth of the concentration of solids in the feed slurry, the concentration of the solids in the filtrate immediately after filtrate exits the filter (0) and the concentration of solids in the filtrate after filtration has occurred for 5 minutes (5)

The average concentration of solids in the feed slurry varied with DrM F experiencing the highest concentration (8,55 g/l) and DrM N experiencing the lowest concentration (2,19 g/l). Both DrM N and Markert achieved clean filtrate (0,02 g/l of solids in the filtrate) immediately while DrM G achieved such clarity only after 5 minutes of filtration. DrM F experienced the least clarity of filtrate whereby after 5 minutes, the filtrate contained 0,1 g/l solids.
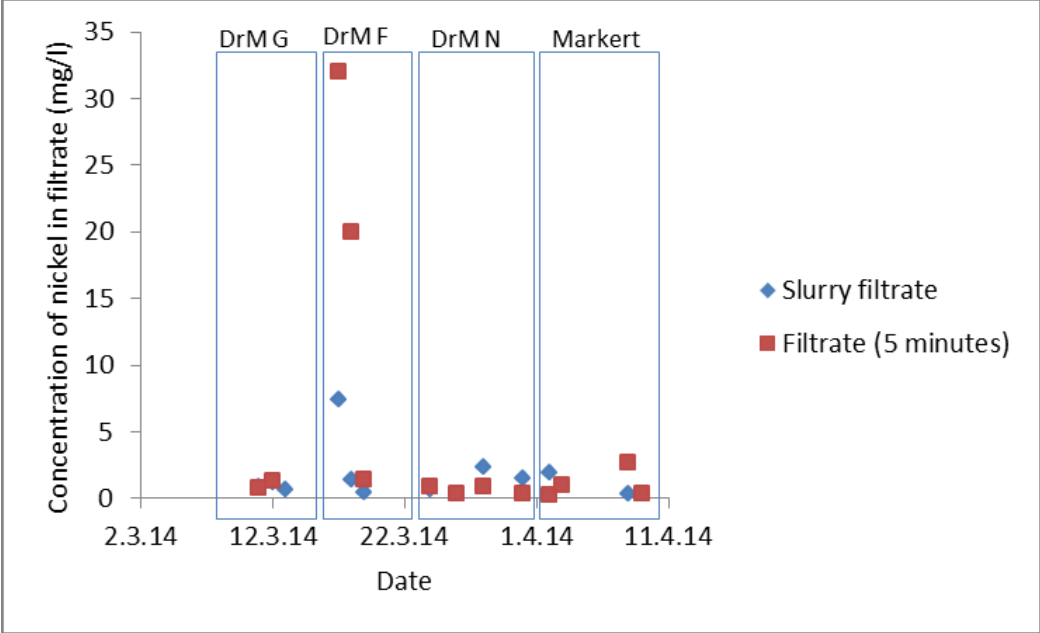
Figure 6.2: Comparison of the concentration nickel in the filtrate from obtained slurry sample to that in filtrate obtained from the filter rig after 5 minutes

Nickel is concentrated on as it constitutes the highest concentration of elements in the filtrate and is most pertinent for removal. The slurry sample obtained was fine-filtered in the laboratory using a buchner funnel. For optimal filtration, the filtrate collected from the filter rig should contain equally low values of nickel to that of the slurry filtrate. This is not achieved for cloth DrM F. Where the concentration of nickel in the filtrate from the slurry is slightly higher than that of the filtrate from the filter rig, some re-dissolution of metals may have occurred during filtration.
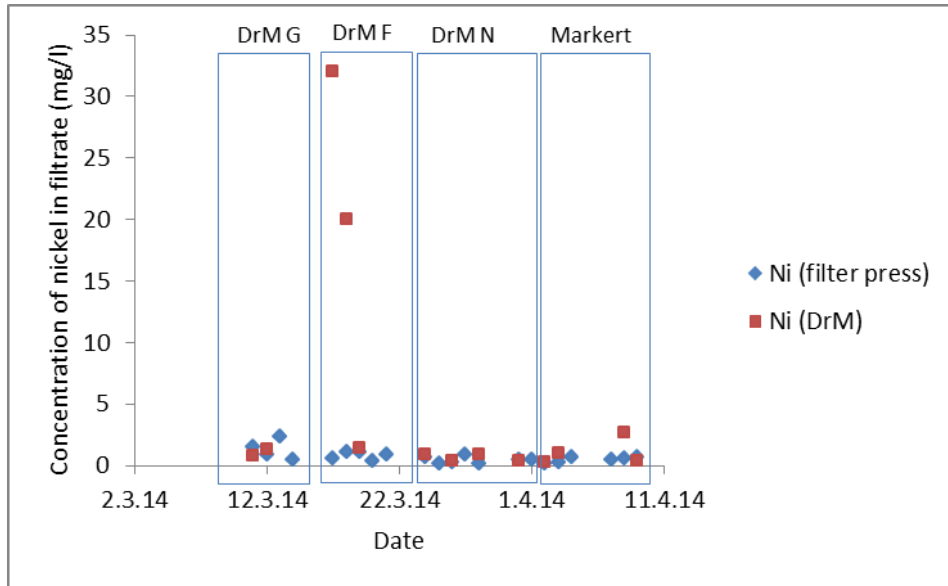
Figure 6.3: Comparison of the nickel concentration in the filtrate from the filter presses to that of the DrM filter rig
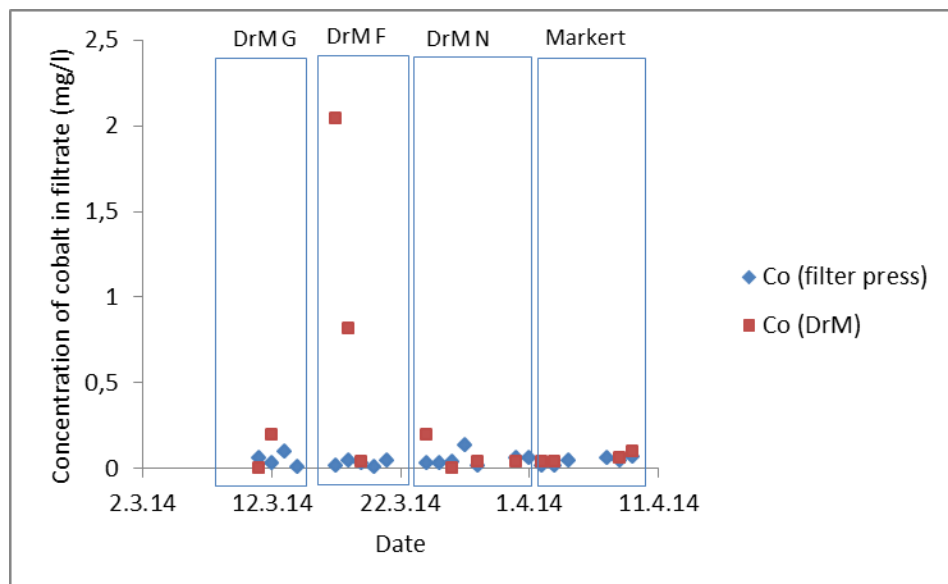
Figure 6.4: Comparison of the cobalt concentration in the filtrate from the filter presses to that of the DrM filter rig
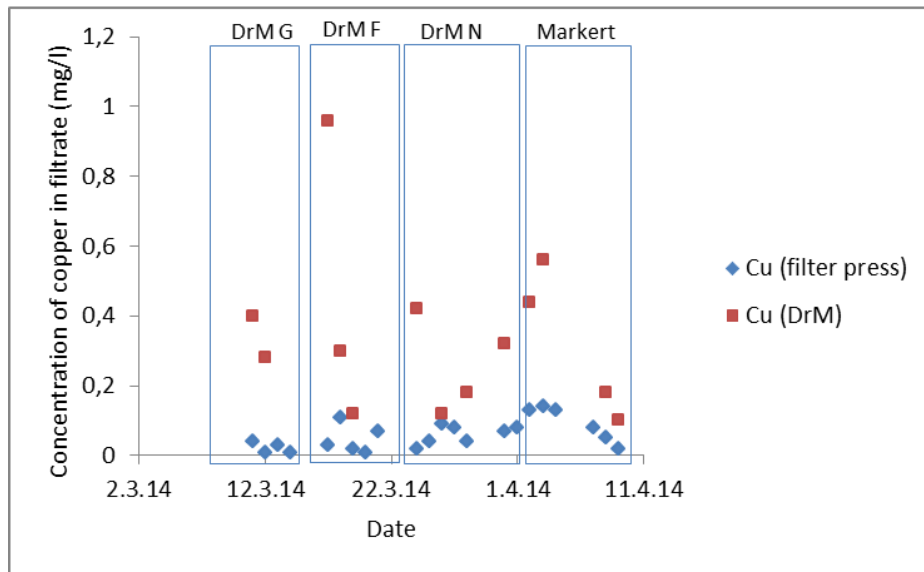
Figure 6.5: Comparison of the copper concentration in the filtrate from the filter presses to that of the DrM filter rig

Filtrate samples from the filter presses in the effluent treatment plant are taken daily and analysed for nickel, cobalt and copper (not iron). The sample is therefore not necessarily taken at the exact same time as the sample taken from the DrM filter rig, but enables an approximate comparison. In comparing the concentration of nickel and cobalt in the two different filtrate samples, equally low concentrations are achieved for all but cloth DrM F. The concentration of copper from the DrM filter rig sample is slightly than from the filter presses for all cloth types but given the very small scale, the difference is not significant.

6.2.2. Observation of cake release

There were no measurements made here, however the observations are important to mention. For cloths DrM G and DrM F, early discharge of cake occurred on many of the runs. That means that when pressure inside the filter chamber was released, cake fell immediately upon opening of the bottom valve. This occurred very seldom for cloths DrM N and Markert.

6.2.3. Evaluating optimal operating parameters for filtration
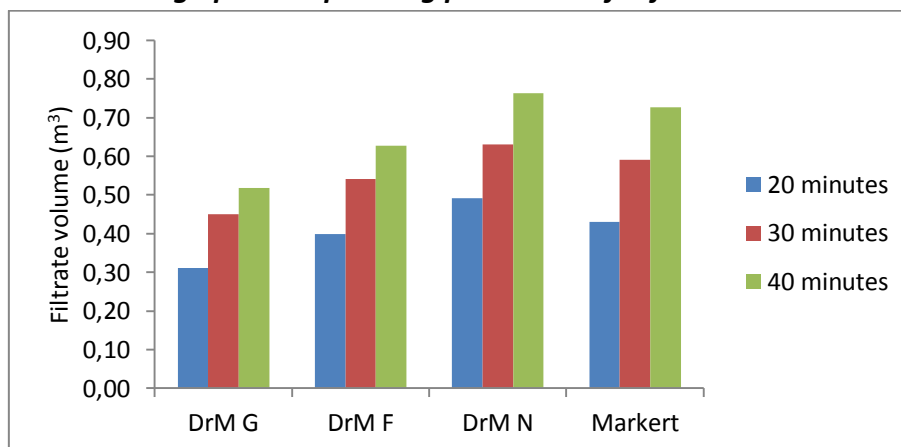
Figure 6.6: Comparison of accumulated filtrate volume obtained upon a filtration time of 20 minutes, 30 minutes and 40 minutes (values are averaged for 20, 30 and 40 minute runs)

69
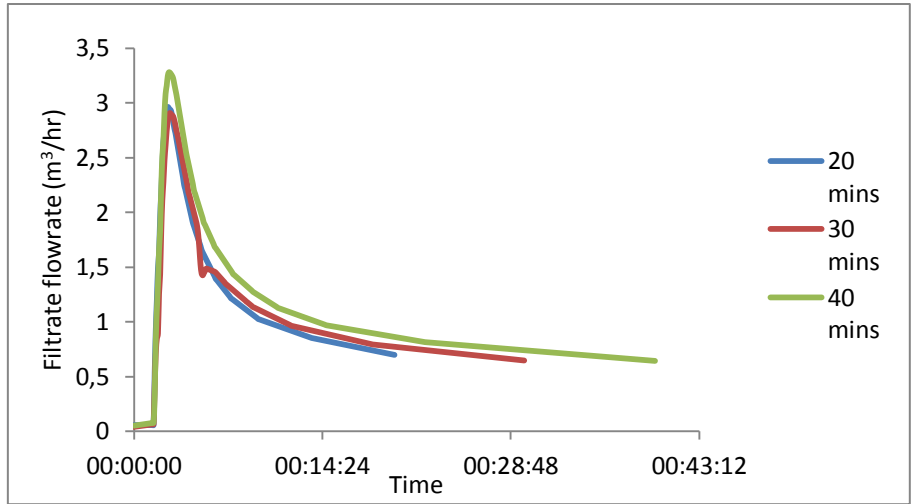
Figure 6.7: Example of the filtrate flowrate trends seen during 20 minutes, 30 minutes and 40 minutes filtration runs (taken from the first three runs on 08.04.14 using the Markert cloth)

For all cloths, an increase in filtration time resulted in an increase in accumulative filtrate volume. At this stage, for all runs, the cake width was below 3 cm and therefore below the threshold width. Data pertaining to the plot of figure 6.7 is available for every run in the electronic appendix. The data shows similar trends to that of figure 6.7, though the peak flowrate differs slightly for some data.

Table 6.5: Accumulated filtrate volume for 20, 30 and 40 minute runs (left column) after 20, 30 and 40 minutes (top row) correlating to figure 6.7

	Vol (20 mins) (m³)	Vol (30 mins) (m³)	Vol (40 mins) (m³)
20 minute run	0,37		
30 minute run	0,39	0,5	
40 minute run	0,44	0,57	0,681
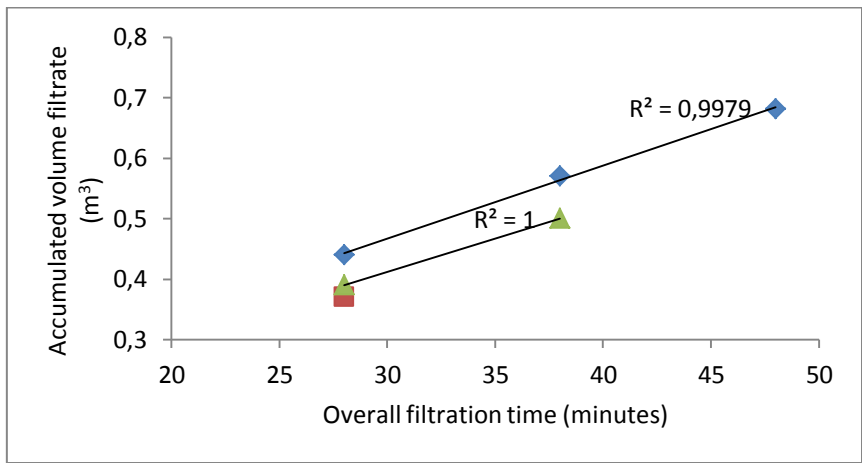
Figure 6.8: Accumulated volume of filtrate data from table 6,5 is plotted for the overall time of the filtration cycle resulting (i.e. for 28 minutes, 38 minutes and 48 minutes)

70

Figure 6.7 shows an example of how the filtration rate changes over a period of 20 minutes, 30 minutes and 40 minutes. The gradients of each trend are similar and only continue longer for longer filtration times. Table 6.5 shows the accumulated filtrate volume for this particle set of data after 20, 30 and 40 minutes. If the 40 minute run were to be stopped at 20 minutes, 30 minutes or 40 minutes, the overall cycle time (including downtime) would be 28 minutes, 38 minutes and 48 minutes respectively. Figure 6.8 therefore plots the accumulative volume of filtrate resulting from what the theoretical overall cycle time would be if the filtration part of the cycle were to be stopped after 20, 30 or 40 minutes.

Note: The coefficient of determination (R^2 value) shown in trends indicates how closely the data conforms to a linear relationship, whereby $R^2 = 1$ represents a perfect fit between the data and the line drawn through the data points.
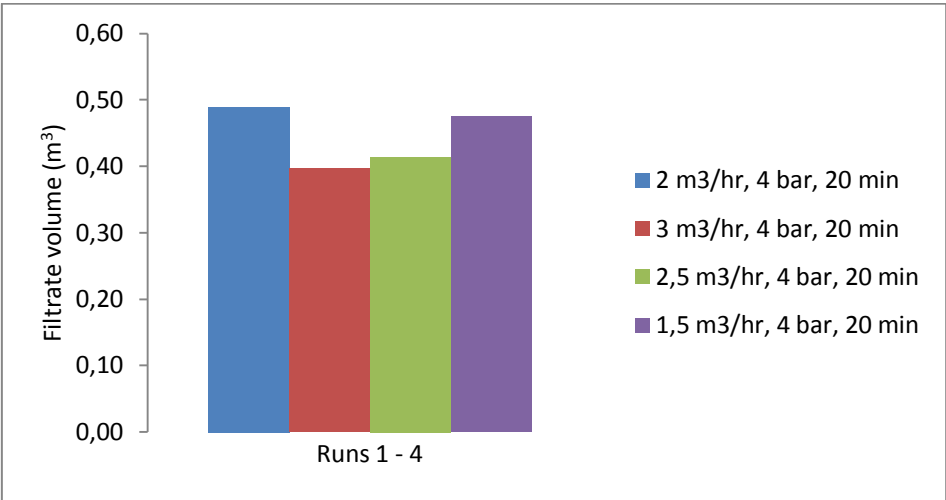
Figure 6.9: Accumulated filtrate volume obtained upon varied flowrates of feed solution for DrM G
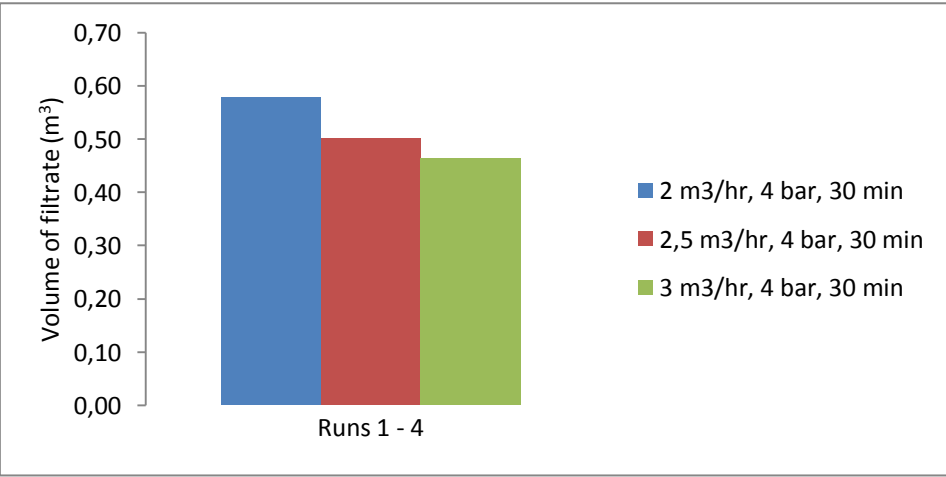
Figure 6.10: Accumulated filtrate volume obtained upon varied flowrates of feed solution for DrM F

71
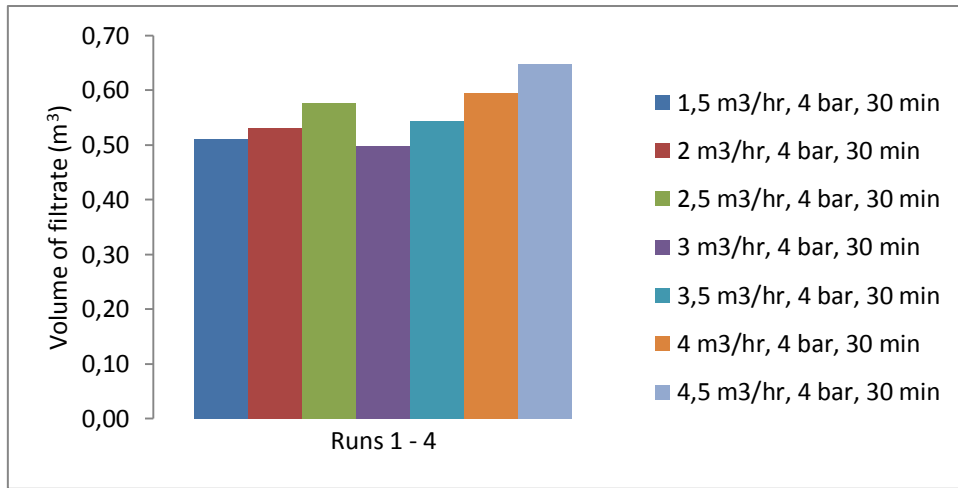
Figure 6.11: Accumulated filtrate volume obtained upon varied flowrates of feed solution for DrM N
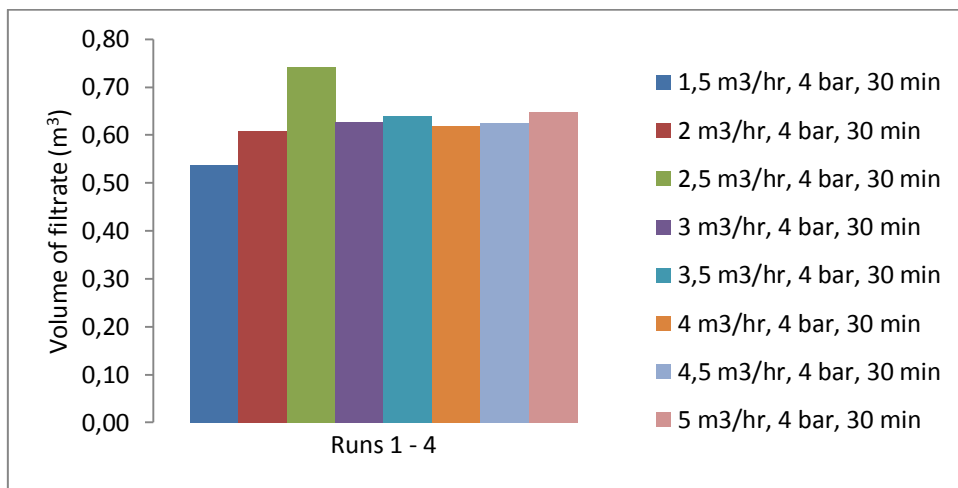
Figure 6.12: Accumulated filtrate volume obtained upon varied flowrates of feed solution for Markert
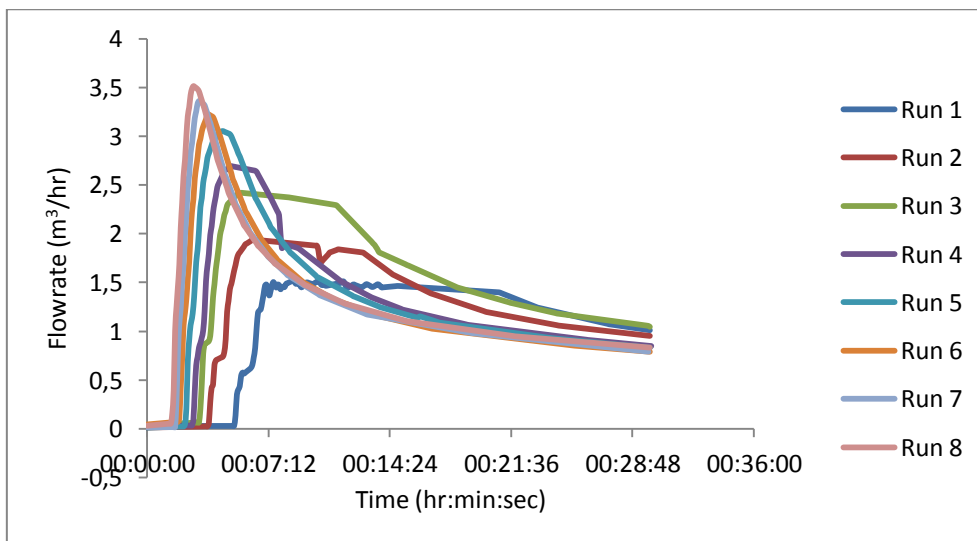
Figure 6.13: Flowrate trends of filtrate for various runs for Markert

72
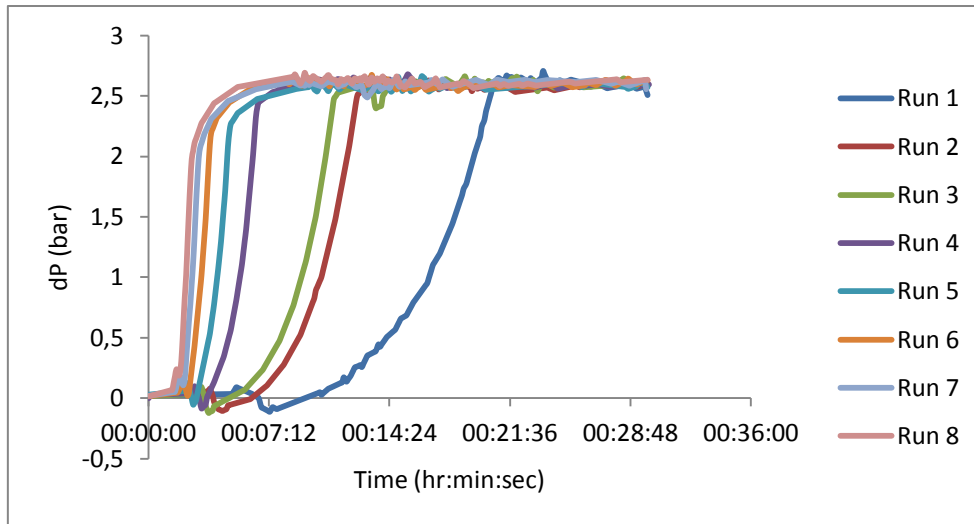
Figure 6.14: Pressure drop over filter trends for various runs for Markert

The legends for figures 6.9 to 6.12 indicate the inlet flowrate of slurry, the inlet applied pressure and the time set for the filtration part of the cycle. The figures illustrate the accumulative volume of filtrate that was obtained under tests whereby inlet flowrate of slurry was changed but the applied pressure and filtration time was constant. There is no clear trend amongst all cloth types between a low or high flowrate correlating to a low or high throughput of filtrate. Figures 6.13 and 6.14 illustrate the flow and pressure drop patterns experienced during the filtration part of the cycle (for similar graphs pertaining to DrM G, DrM F and DrM N see appendix E). A high inlet flowrate results in a filtrate flowrate that reaches a peak and then declines sharply. The constant pressure drop period is reached faster. A low inlet flowrate results in a filtrate flowrate whereby the peak continues for a longer period of time. The maximum pressure is reached after a longer time.

6.3. DrM Filter Rig Operation – Observing Trends in Filtration Performance

6.3.1. Specific cake resistance and medium resistance
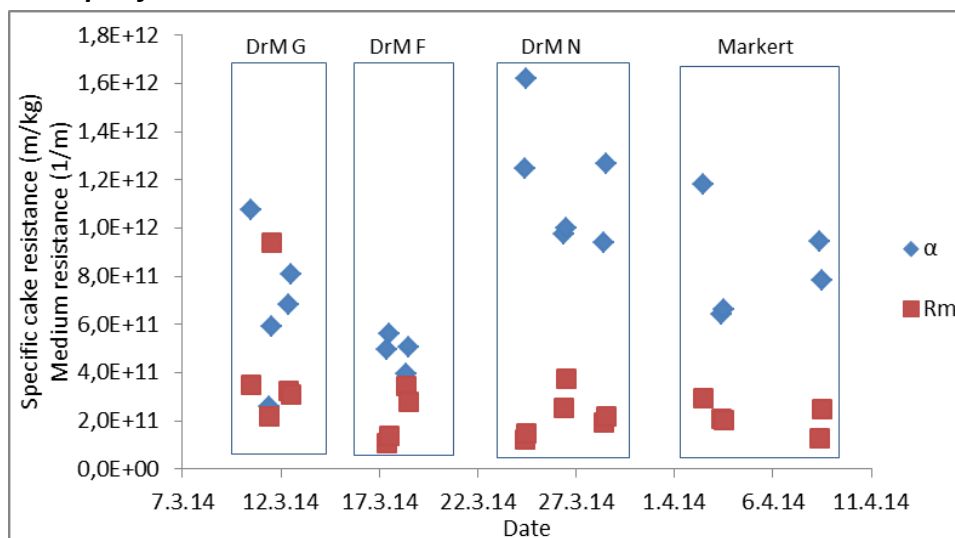
Figure 6.15: The specific cake resistance (α) and medium resistance (R_m) calculated for each filtration test

73
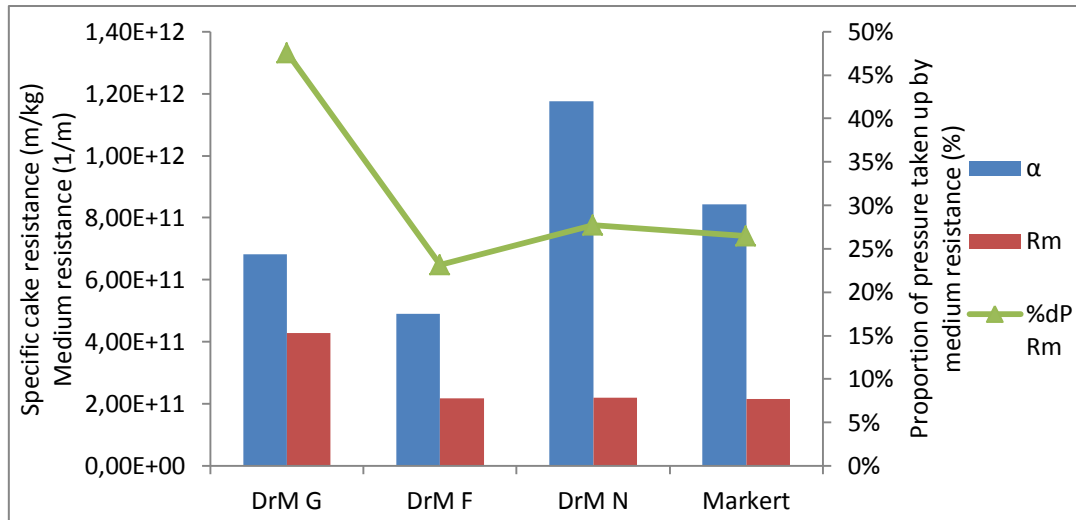
Figure 6.16: Average specific cake resistance (α) and medium resistance (R_m) for each cloth, showing the proportion of the pressure drop across the filter taken up by medium resistance (as opposed to specific cake resistance)

The cloth DrM G experienced the highest average medium resistance. The specific cake resistance was highest during the runs using cloths DrM N and Markert. For all cloths, the filter cloth resistance used up less of the applied pressure than the filter cake resistance, though for cloth DrM G these two values were almost equal (48 % used up by the filter cloth and 52 % used up by the filter cake).

Table 6.6: Comparison of the medium resistance measured in laboratory tests to the average medium resistance obtained for each cloth

	Laboratory - R_m	Pilot filter - R_m
Cloth	*(1/m)*	*(1/m)*
DrM G 11 U 010	2,78E+11	4,29E+11
DrM F11 U 020	2,48E+11	2,18E+11
DrM N 11 U 030	2,68E+11	2,19E+11
Markert PPV 2737	2,16E+11	2,16E+11

The medium resistance was calculated in the laboratory using the same solution as used for the initial cloth screening tests. For both laboratory test and pilot filter test values, the medium resistance increases in respective order for cloths Markert; DrM F; DrM N and DrM.

6.3.2. Effect of inlet feed conditions on filterability and on the filter cake
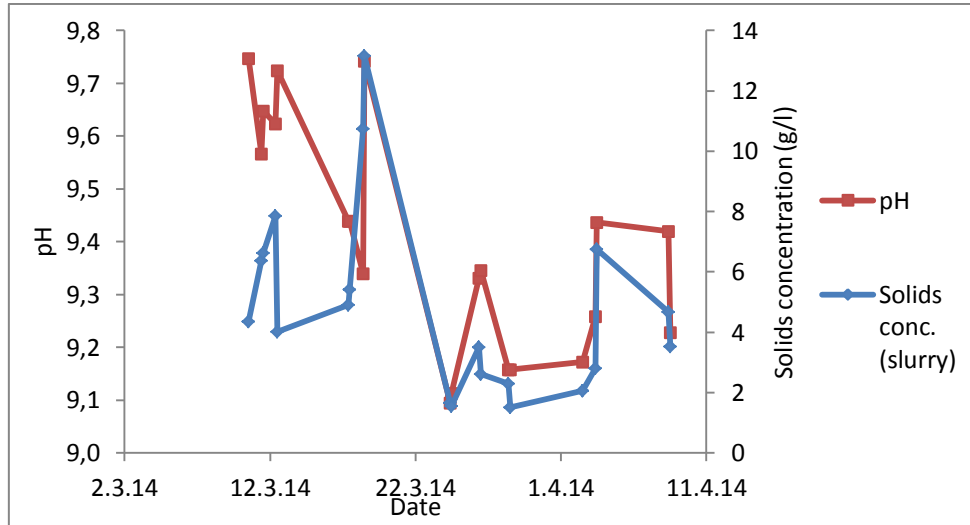
Figure 6.17: Change in solids concentration in the feed solution (right axis) and change in pH in T-1411B (left axis) over time
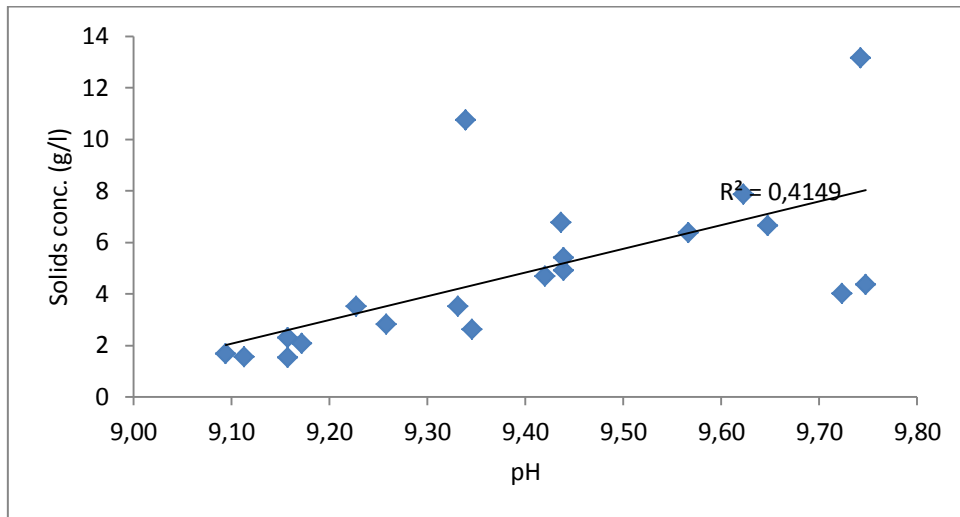
Figure 6.18: Change in solids concentration in the feed solution as a function of pH in T-1411B

Solution is fed directly from the final precipitation tank (T-1411B) to the filter and the pH recorded is that measured in the tank during filtration. Figure 6.16 shows how the pH varies over time and thus how the different cloths will have experienced filtration of solutions under differing pH values. The pH range shown is between 9,09 and 9,75. Apart from a number of outliers, particularly in the early period of testing, there is a trend showing an increase in pH in T-1411B resulting in an increase in solids concentration in the feed solution.
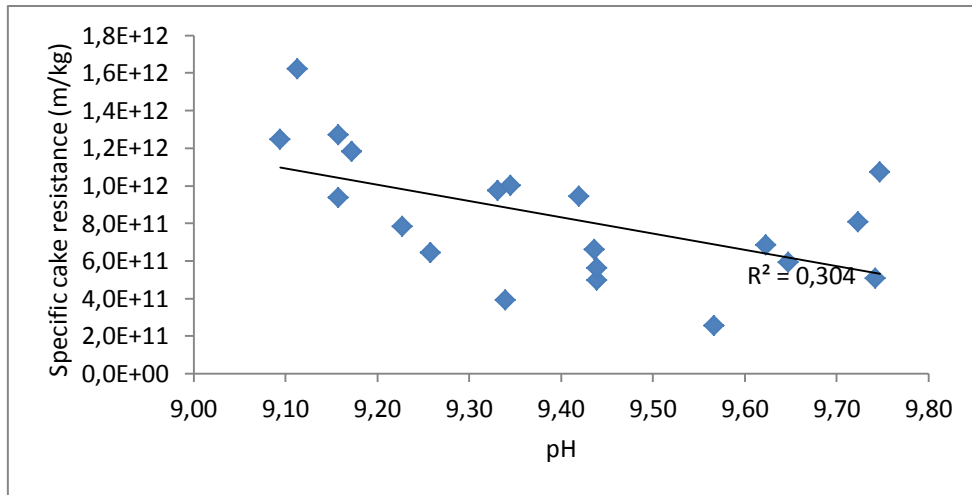
Figure 6.19: Specific cake resistance as a function of solution pH
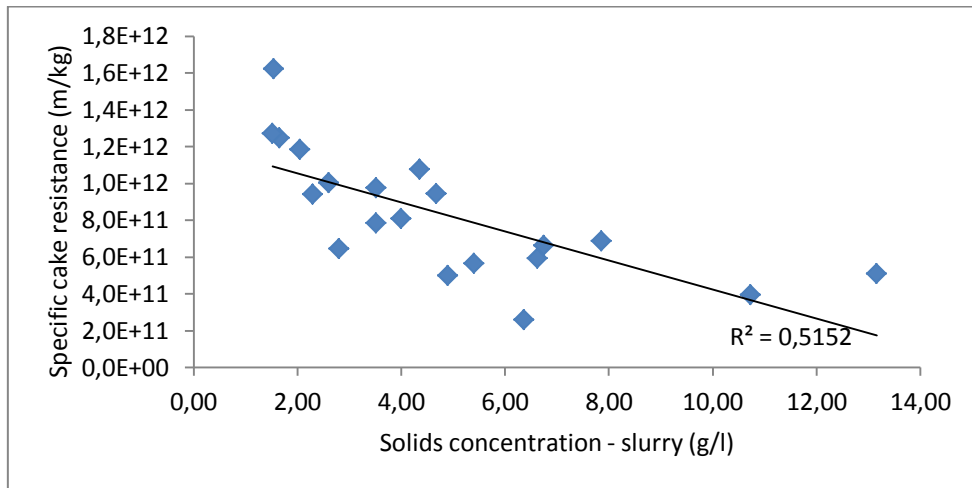
Figure 6.20: Specific cake resistance as a function of solids concentration in the slurry

The general trend in figures 6.19 and 6.20 shows that an increase in pH and consequently also in solids concentration both result in a decrease in the specific cake resistance.
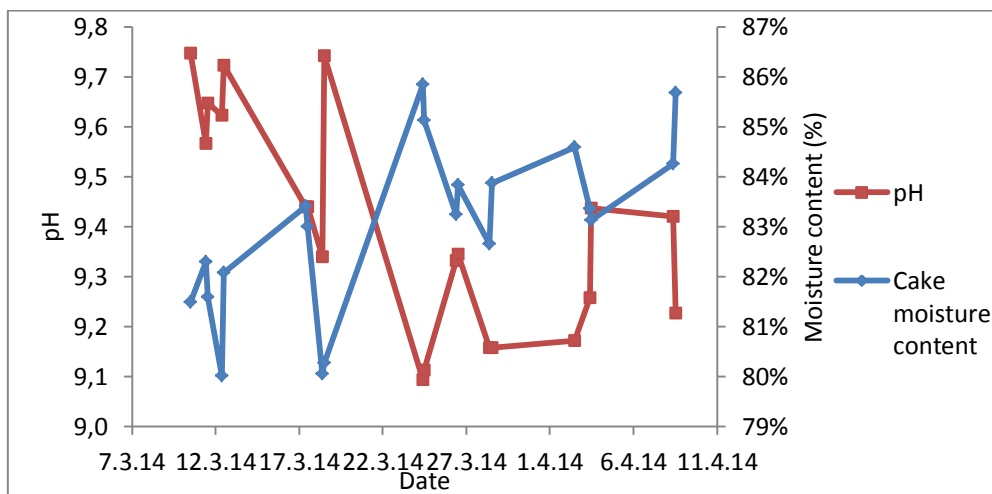
Figure 6.21: Variations in moisture content of the filter cake and solution pH over time

76
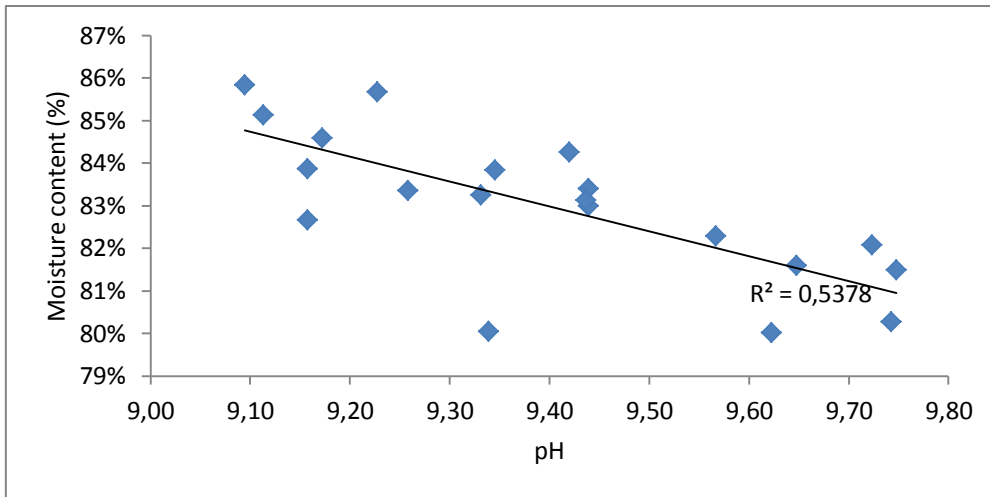
Figure 6.22: Variation in filter cake moisture content as a function of solution pH
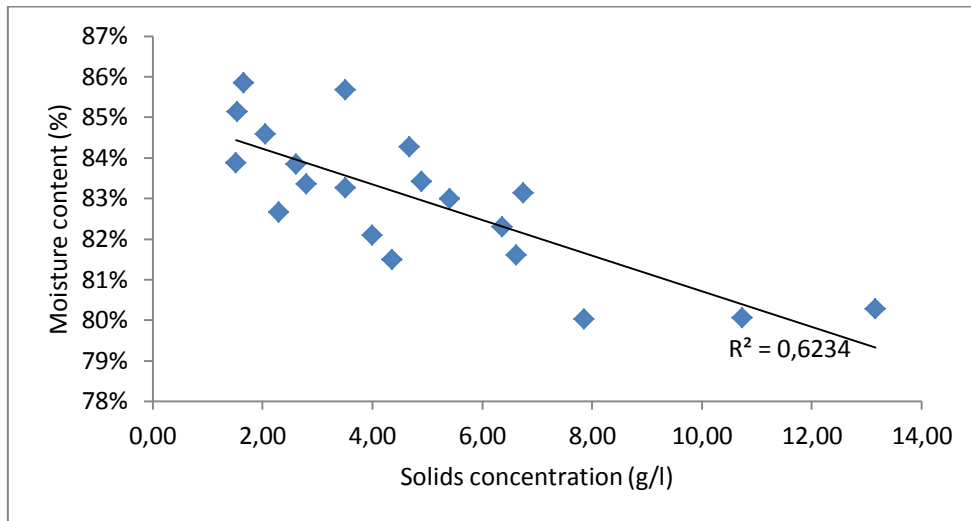
Figure 6.23: Variation in filter cake moisture content as a function of solids concentration in the slurry

Figure 6.21 shows that the moisture content of the filter cake obtained varied between 80 % and 86 %. The general trend in figures 6.22 and 6.23 shows that an increase in pH and thus also in solids concentration results in a decrease in the moisture content of the filter cake.

6.3.3. Filtration capacity
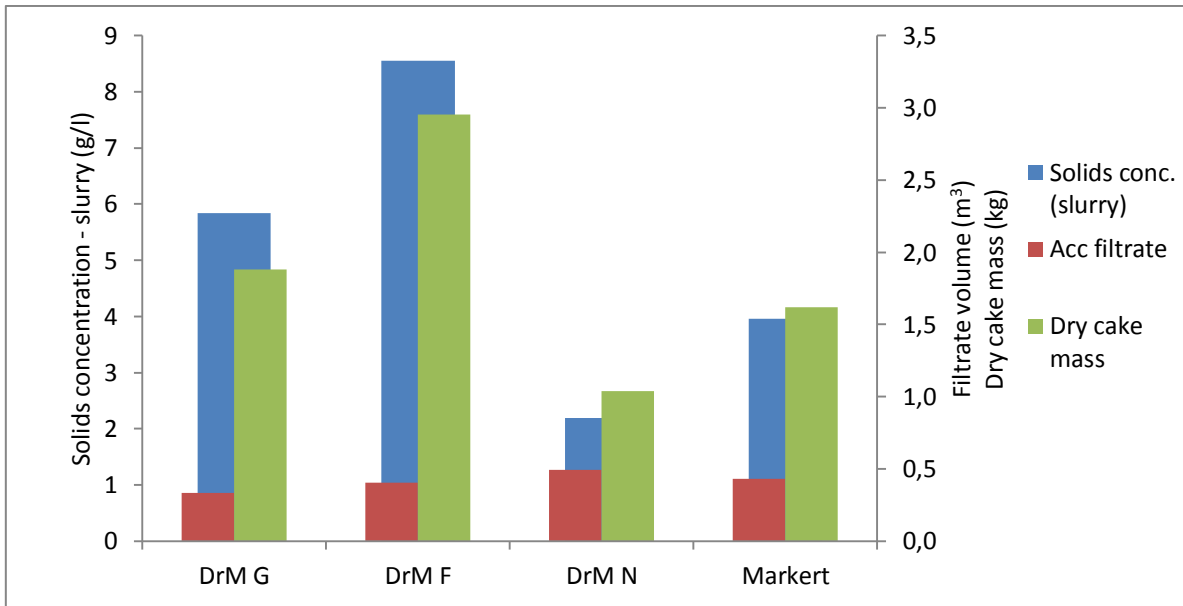
Figure 6.24: Accumulative volume of filtrate obtained in 20 minutes and the dry cake mass obtained at the end of the filtration cycle (both right axis) and showing the concentration of solids in the feed (left axis)
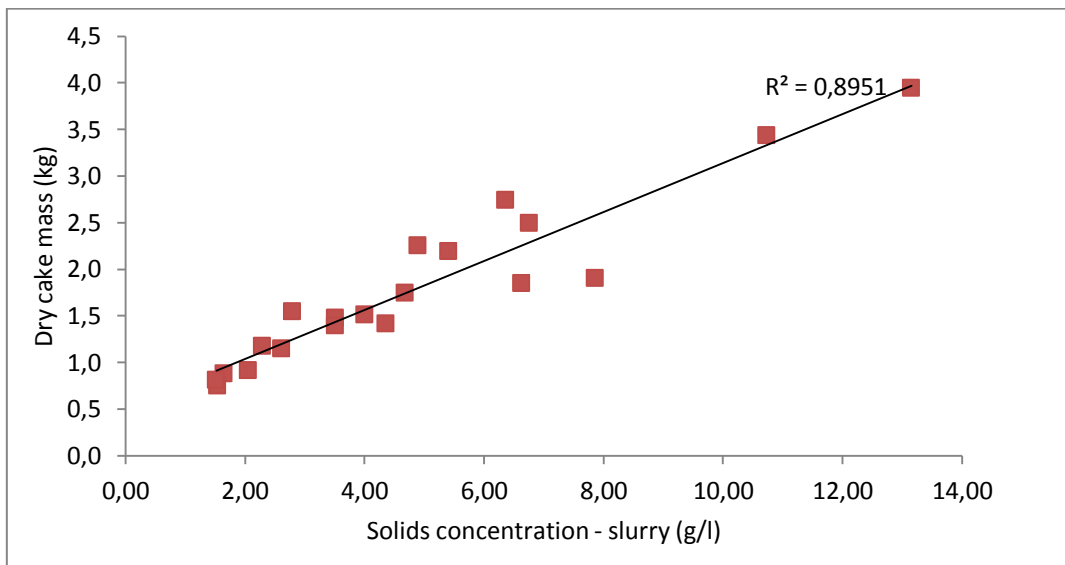
Figure 6.25: Dry cake mass produced as a function of solids concentration in the feed
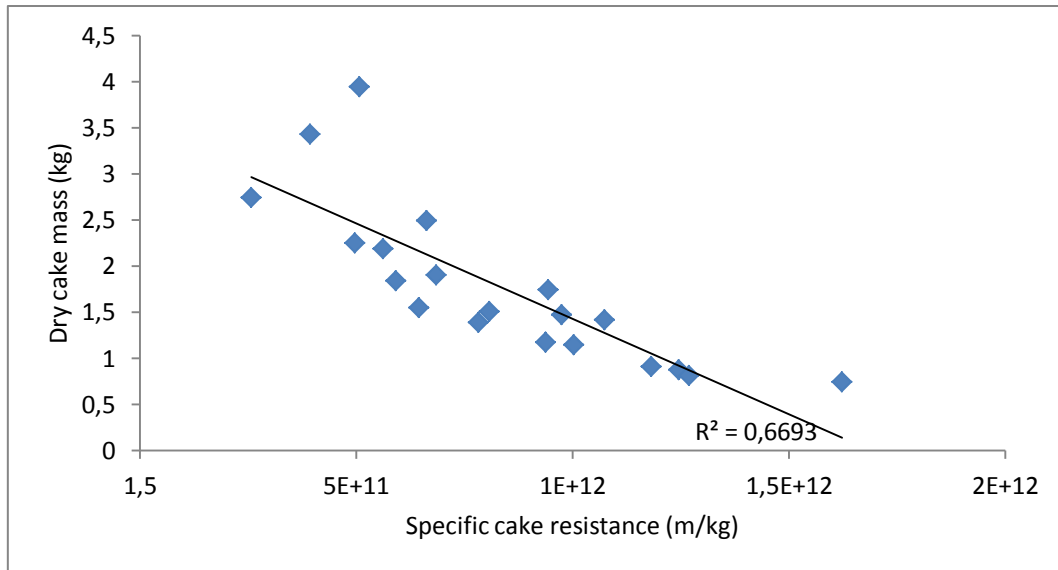
Figure 6.26: Dry cake mass produced as a function of specific cake resistance

There is a trend (figure 6.25) showing that an increase in the concentration of solids in the feed results in an increase in dry cake production. Figure 6.26 shows that an increase in specific cake resistance results in a decrease in dry cake production. Accordingly, DrM F resulted in the largest mass of dry filter cake produced while DrM N resulted in the largest volume of filtrate produced.

6.4. Particle Size Distribution Analysis, Element Analysis and Filtration Resistance

Four identical filtration tests were carried out during one day using the Markert cloth. The following parameters were set:

Table 6.7: Set parameters for samples sent for PSD and element analysis

Flowrate feed	*(m³/hr)*	2,5
Inlet pressure	*(bar)*	4
Filtration time	*(mins)*	20

Samples were taken for filtration performance analysis on three out of the four tests (one test was not sampled due to a sampling error). For all four tests, a filter cake sample was taken and sent for Malvern particle size distribution analysis at the Resitec laboratories and for element analysis in the analytical laboratory. Ultrasound was used during Malvern analysis in order to break agglomerates.

6.4.1. Particle size distributions

Table 6.8: The d(0,1), d(0,5) and d(0,9) of the four samples

	d(0,1) (µm)	d(0,5) (µm)	d(0,9) (µm)
1	2,45	7,84	18,26
2	6,52	17,99	37,55
3	3,07	11,09	23,83
4	3,12	10,34	21,95
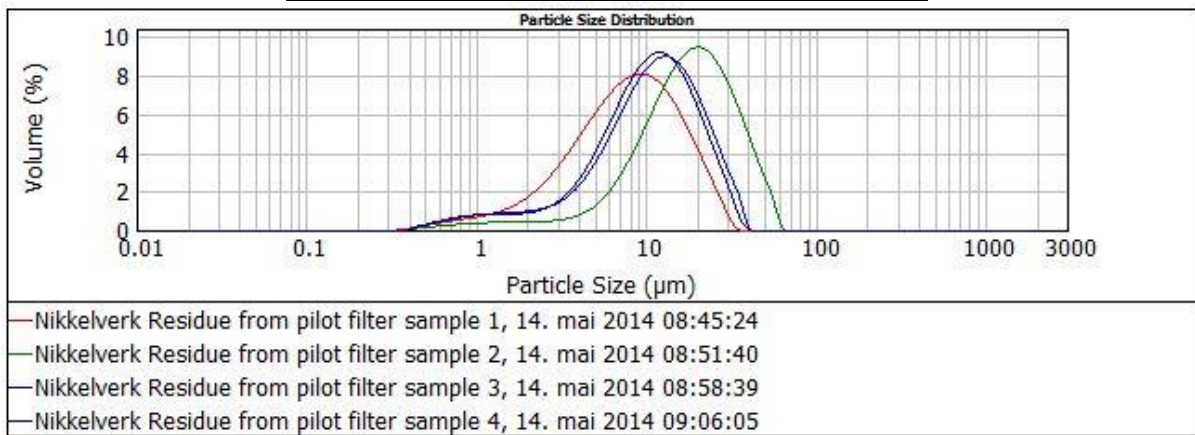
Figure 6.27: PSD of four samples

The d(0,1), d(0,5) and d(0,9) refer to the particle size at which 10 %, 50 % and 90 % of particles are smaller, respectively. Table 6.8 and figure 6.27 shows that the PSD of four filter cake samples taken on the same day varies very much. For individual plots for each sample, see appendix F.

6.4.2. Trends in PSD, element analyses and specific cake resistance
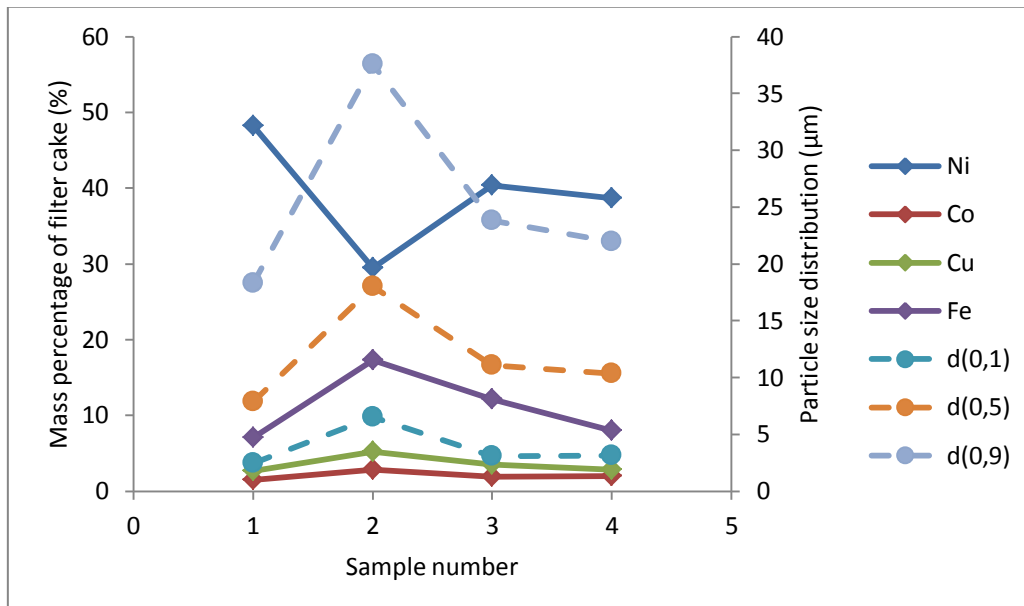
Figure 6.28: Elemental composition of filter cake (left axis) and PSD (right axis) for four samples.

80
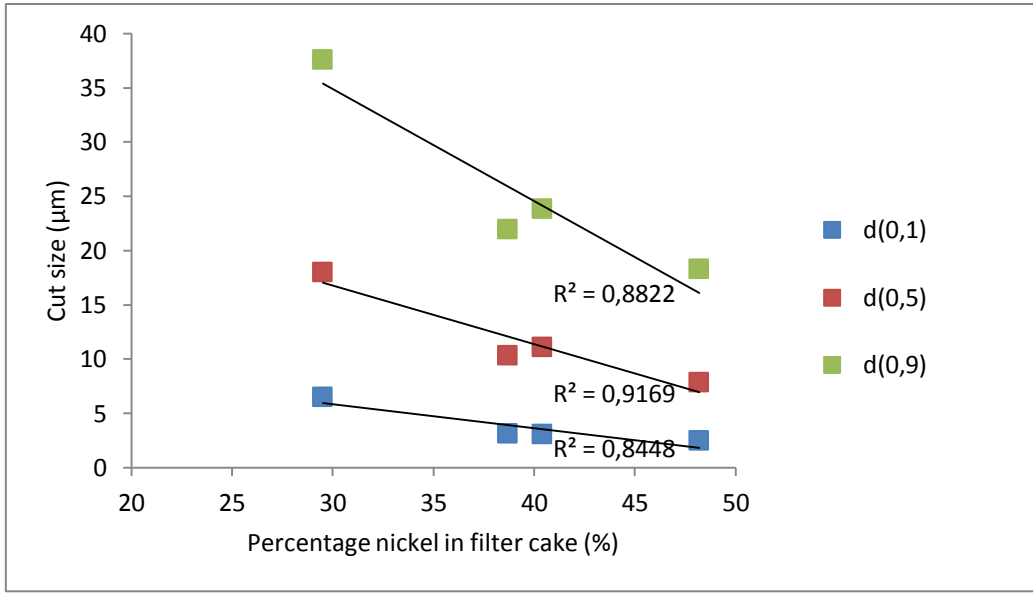
Figure 6.29: The d(0,1), d(0,5) and d(0,9) of four samples as a function of the percentage of nickel comprising the filter cake

Figure 6.29 shows that an increasing percentage of nickel in the filter cake results in a cake comprising of a higher percentage of smaller particles.
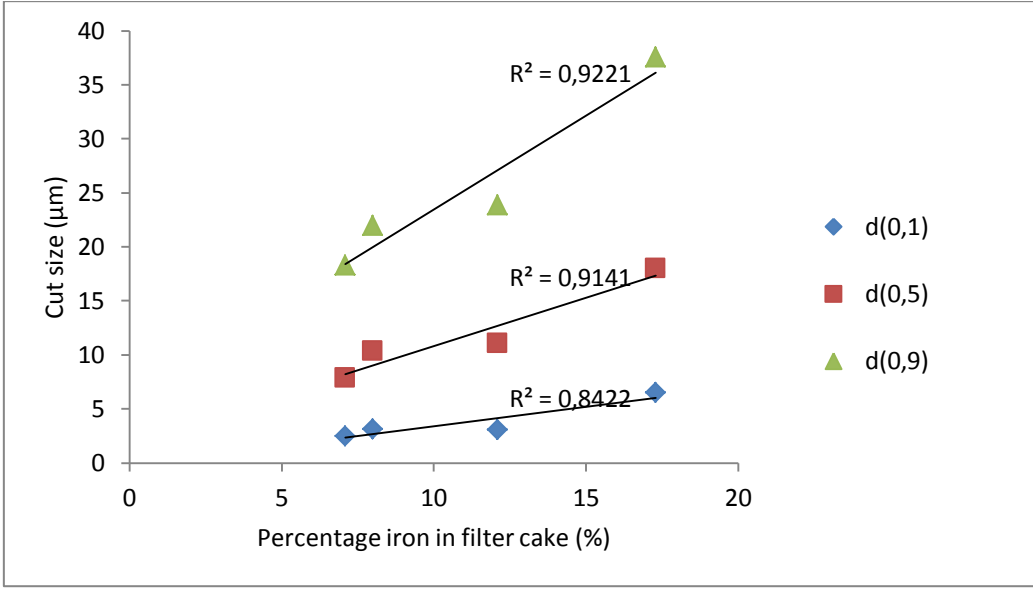
Figure 6.30: The d(0,1), d(0,5) and d(0,9) of four samples as a function of the percentage of iron comprising the filter cake

Figure 6.30 shows that an increasing percentage of iron in the filter cake results in a cake comprising of a higher percentage of larger particles.
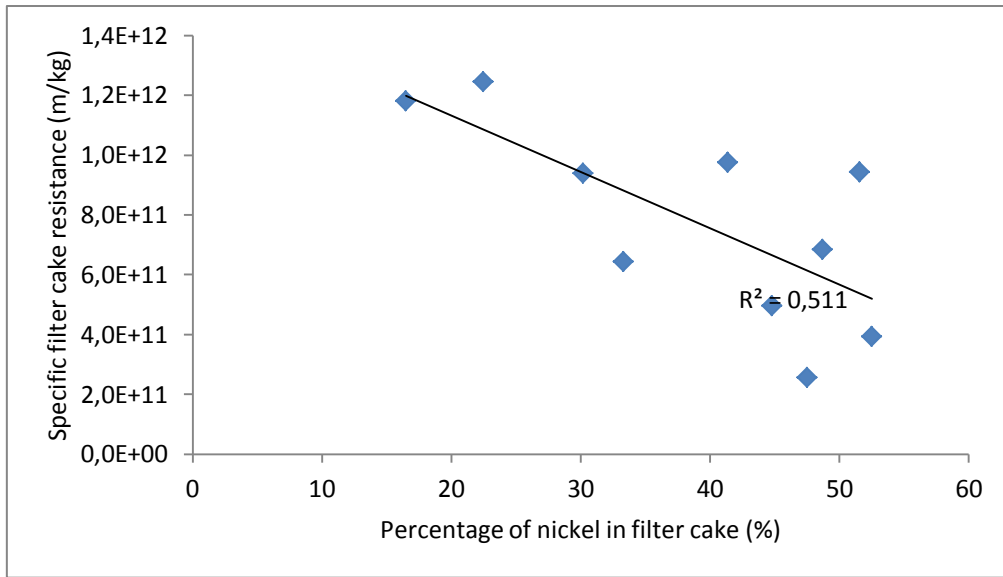
Figure 6.31: Specific cake resistance as a function of the filter cake composition with respect to nickel for samples taken over full duration of testing period
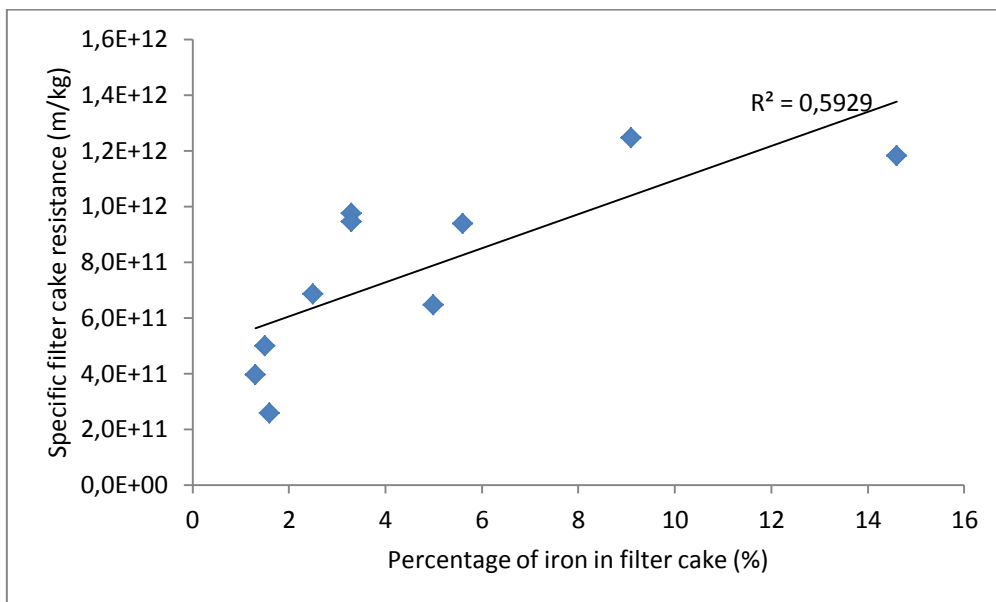
Figure 6.32: Specific cake resistance as a function of the filter cake composition with respect to iron for samples taken over full duration of testing period

During the testing period where different cloths were tested, a residue sample was taken daily at the same time samples were taken for filtration resistance analysis. This sample was analysed for elemental composition. There appears to be some trend showing a decreased specific cake resistance to be a result of an increase in the nickel concentration in the cake and a decrease in the iron concentration in the cake.

Three samples were also sent for SEM analysis. The magnification is not sufficient to gain an impression of the shape of the particles and they instead appear as amorphous agglomerates or flocculates, and possibly even small cake pieces. The SEM pictures are shown in appendix F.

7. Discussion

As the feed to the filter varies continually and cannot be controlled, the conditions under which filtration was experienced day to day and from cloth to cloth also varied continually. This therefore made reproduction of a trial impossible but also pointed to the importance of analysing how the feed changed and repeating tests as often as possible so as to incorporate all variations. Essentially the filtration investigation aims to conclude on three matters. Firstly, if the filter rig functions, the optimal filter cloth should be found. It should also be assessed how the rig should be operated for optimal performance. Lastly, an understanding of how filtration performance is affected by variations in the feed should be gained.

7.1. Evaluation of Filter Cloth Performance from Laboratory and Filter Rig Tests

7.1.1. Cake release

When evaluating whether the laboratory filtration tests are indicative of those on the pilot filter rig, it is important to note that all laboratory tests were performed under vacuum pressure as opposed to the applied pressure used on the filter rig. It was experienced that for all cloth types tested, the cake stuck more firmly onto the cloth on the filter rig than it did on the cloth under laboratory tests. For the Clear Edge cloth, which was observed to have the best cake-cloth adhesion in the laboratory, cake release on the filter rig was not even possible as the cake stuck too much. This may be because, under applied pressure, the layer of moisture in between the cake and cloth is removed more sufficiently, allowing better cake-cloth adhesion.

Initial tests showed that the cloth currently used on the filter presses was not suitable for operation on the pilot filter rig because cake release occurred prematurely upon release of chamber pressure, before the bottom valve was opened. It was therefore sought in the laboratory to find a cloth that gave very good cake adhesion. This is important, as in large-scale operation when there are many candles (up to 250 is possible), premature cake release from all candles would result in the bottom valve being blocked before opening. Equally important, however, is that all of the cake is actually released from the candle after blow-back pressure is applied. Observations therefore show that it can be expected that cloth-cake adhesion on the filter rig will be even better than on laboratory filtration tests, and a cloth giving very high amount of adhesion in the laboratory may give too much adhesion on the candle filter. This was the case of cloth Clear Edge.

Observation from filter rig operation showed that cloths DrM G and DrM F enforced too little cake-cloth adhesion which resulted in parts of the cake falling just as the bottom valve opened, before blow back was applied. The cake fall enabled from cloths DrM N and Markert are thus the preferred options on the matter of cake release.

7.1.2. Medium resistance

The medium resistance results for the laboratory tests are of the same order of magnitude to the results obtained for the cloth on the filter rig. The comparison in table 6.5 shows the

result for the pilot filter as an average of all measured runs. It is thus expected that these results will differ as the medium resistance of the cloth will change over time and the average reflects these changes. The laboratory test is, however, useful for giving an indication of which cloth will apply the most resistance to filtration on the filter rig and for getting an approximation of the resistance possible.

7.2. Comparisons of Filter Cloths – Clarity of Filtrate

There are no restrictions set specifically on the concentration of metals in the filtrate out of the filter presses. This filtrate is diluted with various other aqueous streams (the volumes of which vary) before the stream is analysed for metal concentrations. If the requirements are met, this diluted stream is then sent to the sea. Given that the filtrate eventually enters the sea, it is crucial that the filtrate is very clean. An apt measurement of whether the filter rig achieves satisfactory solids-liquid separation is to compare the metals concentration in the filtrate from the rig to that of the filter presses.

For cloths DrM G, DrM N and Market, the concentrations of nickel, copper and cobalt in the filtrate are similar to that of the filter press. The concentrations of all metals in the filtrate are higher for DrM F. These measurements show that, using the filter press filtrate as a bench mark for metal concentrations, the filter rig coupled with cloths DrM G, DrM N and Market enabled satisfactory solid-liquid separation.

Figure 6.1 shows that, of the above-mentioned cloths, DrM N and Markert were the preferred cloths in that they enabled production of a filtrate with very low solids concentration immediately after filtration began. The elemental analysis was done on filtrate obtained after 5 minutes of filtration. Once a layer of solid particles form on the filter, a filter cake begins to build which become the new filter medium. As seen for cloth DrM G, once this has occurred (measured after 5 minutes of filtration), clean filtrate then passes through. For DrM F, even after the cake has begun to build, particles continue to penetrate the cloth. It is optimal to have clean filtration immediately as it eliminates the need to introduce a recycle stream to the system.

7.3. Optimal Operating Parameters

7.3.1. Filtration time

It is necessary that the filtration part of the cycle is set so that it enables maximum capacity, but so that the filter cake does not grow beyond the threshold width. In this case the threshold width is 3,5 cm. Because the feed to the filter varies so much, enough leeway should be given to allow for periods where a very high concentration of solids may be fed, thus increasing the usual filter cake thickness. Though a long filtration time can result in a thicker cake and larger volume of filtrate, filtration rates can rapidly decrease towards the end of filtration. Once a cake begins to form, a larger amount of the pressure drop is taken up by the cake itself which is why the flowrate of filtrate gradually decreases. It can therefore be beneficial to stop filtration while the filtration rate is still reasonably high.

It is shown in figure 6.8 that for this particular data set, there is a linear increase in the accumulated volume of filtrate with an increase in overall cycle time. The assumption is that if the volume of filtrate increases, the mass of filter cake will also increase because more filtrate being processed would mean more cake is left on the surface. According to this data set and figure 6.6 that shows that for all cloths a higher capacity was achieved after a longer filtration time, it is beneficial to set the filtration time to 40 minutes. As well as this, the cake thickness did not reach its threshold for any runs, but did reach between 2,5 cm and 3 cm for the 40 minute runs. This means that further trials could involve increasing the filtration time slightly more to investigate if there is still an overall linear increase in filtration capacity without reaching the filter cake threshold.

7.3.2. Applied pressure

According to the relationship derived from Darcy's law which relates pressure drop to dry solids yield (equation 1.1 in the literature review), an increase in pressure drop should result in an increase in dry cake production. This is the case if the filter cake is not highly compressible such that the specific cake resistance increases with pressure drop (Svarovsky, 2000). It is also beneficial to gradually increase the pressure until a constant pressure is reached. This is because the solids are non-homogeneous and a high initial pressure drop can result in particles plugging the interstices of the cloth (Reynolds, et al., 2003). With the assumption that the cake was not highly compressible, the applied pressure was thus set to a maximum of 4 bars for all runs. It was also necessary to have the applied pressure as high as possible to enable maximum pressure drop over the filter. This is to ensure that the cake was held firmly onto the candles during filtration. Because of the length and set-up of the pipes from the pump, and because of the pump that sends the same feed solution to the filter presses, an applied pressure of slightly lower than 4 bar was achieved.

7.3.3. Flowrate of feed

There is no clear trend (figures 6.9 to 6.12) for the cloths relating an increase or decrease in the flowrate to a higher filtrate capacity. Though a lower inlet flowrate results in a lower peak filtrate flowrate, the filtrate flowrate is maintained for a longer period of time that for a high inlet flowrate. Thus the overall volumes filtered were similar for different inlet flowrates. Variations in the nature of the feed may also have had a stronger effect on filtration than variations in the flowrate of the feed.

7.4. Observing Trends in Filtration Performance

7.4.1. Specific cake resistance and medium resistance

The calculations made for the specific cake and medium resistance were based on derivations shown in Svarovsky (2000) for constant pressure operation preceded by a period of increasing pressure. Though in fact the pressure drop over the filter fluctuates as it attempts to remain constant, these fluctuations are so narrow that an averaged pressure over the fluctuating period enables an apt representation of constant pressure operation. The calculations were based on the assumption that the inlet feed concentration of solids

remained constant for each run, and that the viscosity of filtrate was constant throughout the testing period. Results thus represent an approximation.

The medium resistance for each cloth does not remain constant over total the trial period. There are two interacting phenomena that may change the medium itself. Fine solids can clog the cloth pores, and simultaneously the applied pressure can compress the fibres in the medium (Svarovsky, 2000). On average, the value of the specific cake resistance for cloth DrM G was highest while the values for the other cloths were similar. Of the pressure applied during filtration, when using cloth DrM G, almost 50 % was applied by medium/cloth resistance with the rest being applied by the cake resistance. For the other cloths, this proportion was closer to 25 % - 75 %. Given that the average specific cake resistance for DrM G was not comparatively high, this result is further indicative that much of the applied pressure would be used up against resistance of cloth DrM G if it were in operation. The specific cake resistance is affected by the concentration of feed to the filter and this cannot be controlled. This value was, on average, highest for cloths DrM N and Markert (figures 6.6 and 6.7). This is further discussed with reference to inlet feed conditions.

7.4.2. Effect of inlet feed conditions on filterability and on the filter cake

Two identified properties that measure filtration performance are the specific cake resistance and the moisture content of the filter cake. These are discussed with reference to how they are affected by the identified inlet feed properties (namely pH and solids concentration) of the solution.

The pH range from measurements in this study is between 9,09 and 9,75. The introductory study to this (Kuiper, 2013), as well as studies from literature Lewis (2010), show that for all the main metals in question, the insoluble metal concentrations will change between a pH of 9 and 10. It was shown experimentally that the concentration of precipitated nickel hydroxide would increase, more specifically, between a pH of 9,5 and 10. Theoretical studies predict such an increase between a pH of 9 and 10. Nickel constitutes the highest concentration of metals in solution, thus a change in the concentration of nickel precipitated has the largest effect on the total concentration of solids in solution.

The relationship in figure 6.18 shows a possible trend between an increase in pH in the precipitation tanks relating to an increase in solids concentration of the solution out of the final precipitation tank. This points to an overall higher precipitation efficiency obtained when increasing the pH of the solution. The possible reason for the outliers that do not follow the trend is that there is continually a different composition of elements in the feed to the precipitation tanks. For example, the comparatively high point in figure 6.18 (pH 9,74 corresponding to solids concentration 13,2 g/l) may result because there was a particularly high concentration of nickel (or other metals) in the feed to the precipitation tanks. This is unknown without analysis of the feed. The overall trend is, however, consistent with the solubility curves that predict an overall increase in the precipitated concentration of metal hydroxides with an increase in pH.

It is thus shown that pH has an effect on the concentration of solids in the solution as the soluble concentration of metal hydroxide differs even within the width of pH 9 to 10. In addition, the pH affects the overall charge of the solution. It is not known what the isoelectric point of the solution is, and this of course changes constantly as the concentration of elements in the solution changes. It is only known that the electrostatic forces experienced by the interacting particles will vary with the surface charge of the particles which vary with the solution environment. This is affected by pH (Iritani, 2003). When the zeta potential in the solution is low and thus inter-particle repulsion forces are low, lower specific cake resistance and a cake with higher moisture content can be expected (Wakeman, 2007). The pH thus affects this specific solution by changing the concentration of precipitated hydroxide metals, and also by affecting the zeta potential which affects the way the particles aggregate in solution.

Trends shown in figures 6.19 to 6.23 reflect that both an increase in pH and in solids concentration of the feed slurry result in a decrease in specific cake resistance and in the moisture content of the filter cake. The relationship for determining specific cake resistance is calculated with respect to the solids concentration, whereby it is expected that an increase in solids concentration will result in a decreased specific cake resistance and thus higher production capacity. Another possible phenomenon to mention is that of particle relaxation time. When a large number of particles approach the filter bed simultaneously, there is less time for them to orientate themselves in an ordered form before more particles fall and surround them. The particles therefore pack together loosely, forming a more porous filter cake. The filter cake is thus more permeable, offering less resistance to the flow of solution.

There is a minimum moisture content that cannot be removed by air displacement at any pressure (Svarovsky, 2000). Beyond this, when particles are orientated loosely, the voids that the moisture content fills are larger. Due to the more loosely packed, permeable cake, when air pressure for blowing and dewatering is applied, the moisture is released from the cake more easily than if it had been trapped within a tightly packed cake.

It is not certain whether the effect of an increased pH on decreased specific cake resistance and cake moisture content is due to the increase in solids concentration that it causes, or because of how it affects the zeta potential. It may be such that increasing the pH results in a decreased zeta potential such that the inter-particle repulsive forces are low. This could lead to the creation of porous flocs with a loose structure that make the cake more permeable. This would then decrease the specific cake resistance and make dewatering more efficient, leading to a filter cake with a lower moisture content. A measurement of the isoelectric point for each solution that was filtered is necessary in order to gain a better indication as to how the pH affects the inter-particle forces.

The only parameter than can be controlled in the precipitation process is the pH of the solution by addition of sodium hydroxide. It is generally a satisfactory goal to maintain a pH at approximately 9,5, though allowing variation between 9 and 10. These results show that

more care should be taken to maintain the pH in the range of 9,5 and 10 – both for improved precipitation and improved filtration.

7.4.3. Filtration capacity

Essentially the valuable product in this solid-liquid separation process is the filter cake. This contains the metals that are then reprocessed and refined. It is thus optimal to have as high cake throughput as possible. Figure 6.24 shows the highest throughput of filter cake achieved during operation with cloths DrM G and DrM F while the highest throughput of filtrate was achieved during operation with cloths DrM N and Markert. Further investigation, however, shows that this result is likely to be a consequence not only the filter cloth but also the inlet feed conditions experienced (namely the concentration of solids in the feed) as well as the specific cake resistance.

Results show that an increase in the concentration of solids in the feed results in an increase in dry cake production and that an increase in the specific cake resistance can result in a decrease in the dry cake production. Derivation of Darcy's law and neglecting filter medium resistance leads a relationship between the solids concentration and the dry cake production capacity (in kg/m^2/s) (Svarovsky):

$$Y = (\frac{2\Delta pfc}{\alpha\mu t_c})^{1/2}$$

The relationship the total dry cake produced and the solids concentration is very nearly accurate to the relationship described above. A four-fold increase in solids concentration results in approximately double the total production of dry solids for many of the data points. Deviation from linearity can be due to the effect of the filter medium resistance, which is neglected in the derivation of the relationship.

The trend is not quite as replicable for the specific cake resistance in that the ratio between an increase in specific cake resistance and decrease in dry cake mass changes. One of the reasons that an increase in specific cake resistance results in lower cake production on the candle filter may be because, as the resistance against flow increases, the residual layer of slurry on top of the cake increases. During drainage, this layer may be flushed from the filter without the particles having had a chance to form a cake. Because the feed varied continually, it is difficult to classify one cloth as enabling better throughput than another.

7.4.4. Particle size distribution, element analysis and filtration resistance

The particle size distributions for four cake samples produced on one day are indicative of the large variations in the type of cake produced. The results show that an increase in the concentration of nickel in the filter cake results in an increase in the percentage of smaller particles and fines. Concurrently, an increase in the concentration of iron in the filter cake results in the production of fewer fines and more larger particles. This may point to the fact that nickel particles are smaller than iron particles. For an accurate comparison, however, more samples and measurements are required from a longer period of sampling.

Important to note is that most of the iron that is sent to the effluent treatment plant comes from the storage caverns. This iron is present in the caverns as a ferrous iron residue. Sulphuric acid from the gas cleaning plant is also sent to the caverns which then oxidised the iron to produce a ferric iron leachate. This is then sent to the effluent treatment plant. Not all of the iron is oxidised, thus some iron is present as a precipitate while the rest is dissolved. The pH of this leachate is low (below 3). When it enters the first mixing tank where the pH is generally between 3 and 6,5, some precipitation of dissolved iron can occur. The main precipitation reactions then takes place in the following precipitation tank. It is possible that during the process of precipitation, agglomerates or flocs of iron hydroxide are formed. The precipitated particles that entered the treatment process from the caverns are understood to be very fine. It is therefore possible that there is a large particle size distribution within the iron hydroxide particles alone.

Over the total period of testing, the composition of elements in the slurry residue that forms the cake was measured daily. There is a trend showing that an increase in the concentration of nickel in the cake and a decrease in the concentration of iron in the cake can result in a decrease in the specific cake resistance. This refutes the PSD results that relate a lower concentration of nickel in the cake and a higher concentration of iron in the cake to a higher concentration of larger particles. Typically a cake formed of few fines and more larger particles experiences lower resistance to filtration as the large particles form a more porous cake. This may signify that four samples taken for the PSD measurements are an insufficient number to depict the variations in the types of iron particles. It could also signify that the inter-particle forces that change with a change in the concentration of metals have a greater result on filtration than the particle size distribution. However, if indeed the precipitation process in the iron caverns and then in effluent treatment plant results in a large size distribution of iron particles, there may be many fines as well as many agglomerates or flocculants. Small iron particles may settle in between the large particles, forming a more packed or ordered cake and thus increasing the specific cake resistance. To further conclude on the effect of the particles types on filterability, more information pertaining to the particle size distributions and elemental concentrations is required.

The particles sent for SEM were inconclusive with respect to particle morphology. It is possible that during the drying process, agglomerates are formed. It appears that very fine cake pieces are visible. For more information pertaining to the particle morphology, the samples need to be more finely crushed. Higher magnification may also be necessary.

7.5. Performance comparison
This study does not contain a comparison of candle filter performance to the existing filter press performance. Operation of the pilot rig differs to that of a full scale candle filter, whereby sectional filtration occurs. Specific design data pertaining to full scale operation would thus be necessary for such a comparison.

8. Conclusions and Recommendations

8.1. Conclusions

Referring to the objectives listed in the introduction, the following conclusions can be drawn:

i. The DrM candle filter operates effectively and through the use of either DrM N 11 U 030 or Markert PPV 2737 filter cloth qualities, good filter cake release and the production of filtrate of equal clarity to that of the filter presses is enabled. Laboratory tests enable a good approximation of filter cloth performance, however filter cake release found from laboratory equipment is higher than that of the filter rig. This is possibly because vacuum pressure is used during laboratory as opposed to the applied pressure used on the filter rig.

ii. For optimal operation, the filtration time should be set to at least 40 minutes and the applied pressure to 4 bar. This enables the highest throughput of filtrate without the cake being prematurely released from the candles.

iii. Care should be taken to maintain a higher pH in the range of 9 to 10 during the precipitation process as it is both beneficial for precipitation and for filtration. It results in a higher concentration of solids in the feed to the filter. A solution of higher pH experiences a lower specific cake resistance and results in the production of a less moist cake. This may be due to the inter-particle forces resulting from a change in pH as well as from the increased concentration of solid particles. An increase in the concentration of solid particles has a similar effect on the specific cake resistance and cake moisture content, possibly due to the particle orientation within the cake. Such increase in the concentration of solid particles in the feed also results in a larger production of filter cake mass. Further information on the particle size distribution in the solution is required in order to conclude on its effect on filtration. It appears that an increased concentration of nickel hydroxide precipitate and a decreased concentration of iron hydroxide precipitate in the feed result in a lower specific cake resistance, and are thus beneficial for filtration.

8.2. Recommendations and further studies

The following recommendations are made for continuation of the study:

- Operate the filter rig for a longer period of time using the DrM N and Markert cloths to test their durability and whether they handle all variations in feed before evaluating which cloth is preferable. More cloths can also be tested to increase the choice pool.
- Investigate whether it is beneficial to operate the filtration part of the cycle for longer than 40 minutes.
- Obtain design data to enable a theoretical comparison of full scale candle filter operation against the existing chamber filter press operation.

List of References

Armenante, P., u.d. *Coagulation and Flocculation.* [Internett]
Available at: http://cpe.njit.edu/dlnotes/che685/cls07-1.pdf
[Funnet 16 June 2014].

Baltpurvins, K. A., Burns, R. C. & Lawrence, G. A., 1996. Use of the Solubility Domain Approach for the Modeling of the Hydroxide Precipitation of Heavy Metals from Wastewater. *Environmental Science & Technology,* Issue 30, pp. 1493-1499.

Birdi red., 2009. Handbook of Surface and Colloid Chemistry. I: U.S.A.: CRC Press, p. 120.

CMC, C. M. C. (., 2014. *What is Zeta Potential?.* [Internett]
Available at: http://www.colloidmeasurements.com/zeta.html
[Funnet 05 May 2014].

Collins, R. & Pickering, T., 1997. Comparative Performance of Centrifugal and Pressure Filtration. *Fluid/Particle Separation Journal,* 10(3), pp. 275-282.

Djedidi, Z. et al., 2009. Comparative study of dewatering characteristics of meta precipitates generated during treatment of monometallic solutions. *Hydrometallurgy,* pp. 61-69.

DrM, 2014. *DrM.* [Internett]
Available at: http://www.drm.ch/
[Funnet 17 June 2014].

DrM, 2014. *DrM Fundabac.* [Internett]
Available at: http://www.drm.ch/products/filtration-systems/fundabac?lang=en
[Funnet 28 March 2014].

Eaton-Dikeman Company, 1960. *Handbook of Filtration.* 1 red. Mt. Holly Springs: The Eaton-Dikeman Company.

Encyclopædia-Britannica, 2013. *Refractive Index.* [Internett]
Available at: http://www.britannica.com/EBchecked/topic/495677/refractive-index
[Funnet 29 October 2013].

Guillard, D. & Lewis, A. E., 2001. Nickel Carbonate Precipitation ina Fluidized-Bed Reactor. *Industrial & Engineering Chemistry Research,* Issue 40, pp. 5564-5569.

Halberthal, J., u.d. *Candle Filters.* [Internett]
Available at: http://www.solidliquid-separation.com/pressurefilters/candle/candle.htm
[Funnet 07 May 2014].

Iritani, E., 2003. Properties of Filter Cake in Cake Filtration and Membrane Filtration. *Kona: Powder and Particle Journal,* Issue 21, pp. 19-32.

Kuiper, E. C., 2013. *Removal of Heavy Metals in the Effluent Treatment Plant at Nikkelverk,* Kristiansand: s.n.

Lewis, A. E., 2010. Review of metal sulphide precipitation. *Hydrometallurgy,* Issue 104, pp. 222-234.

Lide, D., 1980. *Handbook of Physics and Chemistry.* 61 red. s.l.:CRC Press.

Lu, P. J. & Weitz, D. A., 2013. Colloidal Particles: Crystals, Glasses and Gels. *Annual Review of Condensed Matter Physics,* Issue 4, pp. 217-233.

Malvern(a), 2013. *Malvern, What is Particle Size?.* [Internett]
Available at:
http://www.malvern.com/labeng/technology/laser_diffraction/what_is_particle_size.htm
[Funnet 29 October 2013].

Malvern(b), 2013. *Malvern - Laser diffraction particle sizing.* [Internett]
Available at:
http://www.malvern.com/labeng/technology/laser_diffraction/particle_sizing.htm
[Funnet 29 October 2013].

Malvern(c), 2013. *Malvern - Analyzing Light Scattering Data.* [Internett]
Available at:
http://www.malvern.com/labeng/technology/laser_diffraction/analyzing_light_scattering.htm
[Funnet 29 October 2013].

Marchioretto, M. M., Bruning, H. & Rulkens, W., 2005. Heavy Metals Precipitation in Sewage Sludge. *Separation Science and Technology,* Issue 40, pp. 3393-3405.

MarkertGruppe, 2014. *Company Presentation.* Neumunster: Markert Group Company.

MarkertGruppe, 2014. *Hose and Filter Technology.* [Internett]
Available at: http://www.markert.de/index.php/en/
[Funnet 17 June 2014].

Monhemius, A. J., 1977. Precipitation diagrams for metal hydroxides, sulphides, arsenates and phosphates. *Institution of Mining and Metallurgy,* pp. C202-C206.

Mullin, J. W., 2001. *Crystallization.* 4 red. Oxford: Butterworth Heinemann.

Pansu, M. & Gautheyrou, J., 2006. I: *Handbook of Soil Analysis - Mineralogical, Organic and Inorganic Methods.* Netherlands: Springer, pp. 646 - 647.

Patterson, J. W., Allen, H. E. & Scala, J. J., 1977. Carbonate Precipitation for Heavy Metal Pollutants. *Water Pollution Control Federation,* 49(12), pp. 2397-2410.

Perlmutter, B. A., u.d. *Continuous Pressure and Vacuum Filtration and Washing of Organic Cellulose and Biomass Products.* [Internett]
Available at:
www.chemicalprocessing.com/assets/wp_downloads/pdh/bhs_wpa_090914.pdf
[Funnet 20 April 2014].

Perry, R. H. & Green, D., 1984. *Perry's Chemical Engineers' Handbook.* 6 red. s.l.:McGraw-Hill Book Company.

Rajamath , M., Kamatha, V. & Sesh, R., 1999. Polymorphism in nickel hydroxide: role of interstratification. *Journal of materials chemistry.*

Ramesh, T. N. & Vishnu Kamath, P., 2005. Synthesis of nickel hydroxide: Effect of precipitation conditions on phase selectivity and structural disorder. *Journal of Power Sources,* Volum 156, pp. 655-661.

Reynolds, T. et al., 2003. Scale-Down of Continuous Filtration for Rapid Bioprocess Design: Recovery and Dewatering of Protein Precipitate Suspensions. *Biotechnology and Bioengineering,* 4(83), pp. 454-464.

Richardson, J. F., Harker, J. H. & Backhurst, J. R., 2002 . *Coulson and Richardson's Chemical Engineering Volume 2 - Particle Technology and Separation Processes.* 5 red. s.l.:Elsevier.

Seidel, A., red., 2007. Kirk-Othmer Encyclopedia of Chemical Technology. I: New Jersey: John Wiley & Sons, pp. 321-397.

Song, Q., Tang, Z., Guo, H. & Chan, S. L., 2002. Structural characteristics of nickel hydroxide synthesized by a chemical precipitation route under different pH values. *Hournal or Power Sources,* Volum 112, pp. 428-434.

Stamatakis, K. & Tien, C., 1991. Cake Formation and Growth in Cake Filtration. *Chemical Engineering Science,* 8(46), pp. 1917-1933.

Stensholt, E. O., Zachariasen, H. & Lund, J. H., 1985. Falconbridge chlorine leach process. *Extraction Metallurgy,* pp. 377-397.

Svarovsky, L., 2000. *Solid-Liquid Separation.* 4 red. Oxford: Butterworth-Heinemann.

Svarovsky, L., 2000. *Solid-Liquid Separation.* 4 red. Oxford: Butterworth-Heinemann.

Swapp, S., 2013. *Scanning Electron Microscopy (SEM).* [Internett]
Available at:
http://serc.carleton.edu/research_education/geochemsheets/techniques/SEM.html
[Funnet 29 October 2013].

Tewari, P. & Campbell, A., 1976. Temperature Dependence of Point Zero Charge of Cobalt and Nickel Oxides and Hydroxides. *Journal of Coilloid and Interface Science,* 3(55), pp. 531-539.

Tien, C., 2002. Cake filtration research - a personal view. *Powder Technology,* Issue 127, pp. 1-8.

Wakeman, R., 2007. The influence of particle properties on filtration. *Separation and Purification Technology,* Issue 58, pp. 234-241.

Wakeman, R., 2011. *Liquid-Solid Separation.* [Internett]
Available at: http://www.thermopedia.com/content/928/
[Funnet 14 February 2014].

0. Appendices

The appendices show figures and data *not shown* in the main report. All raw data from the filter rig is shown in the electronic appendix.

Appendix A – Effluent Treatment Plant Process Data
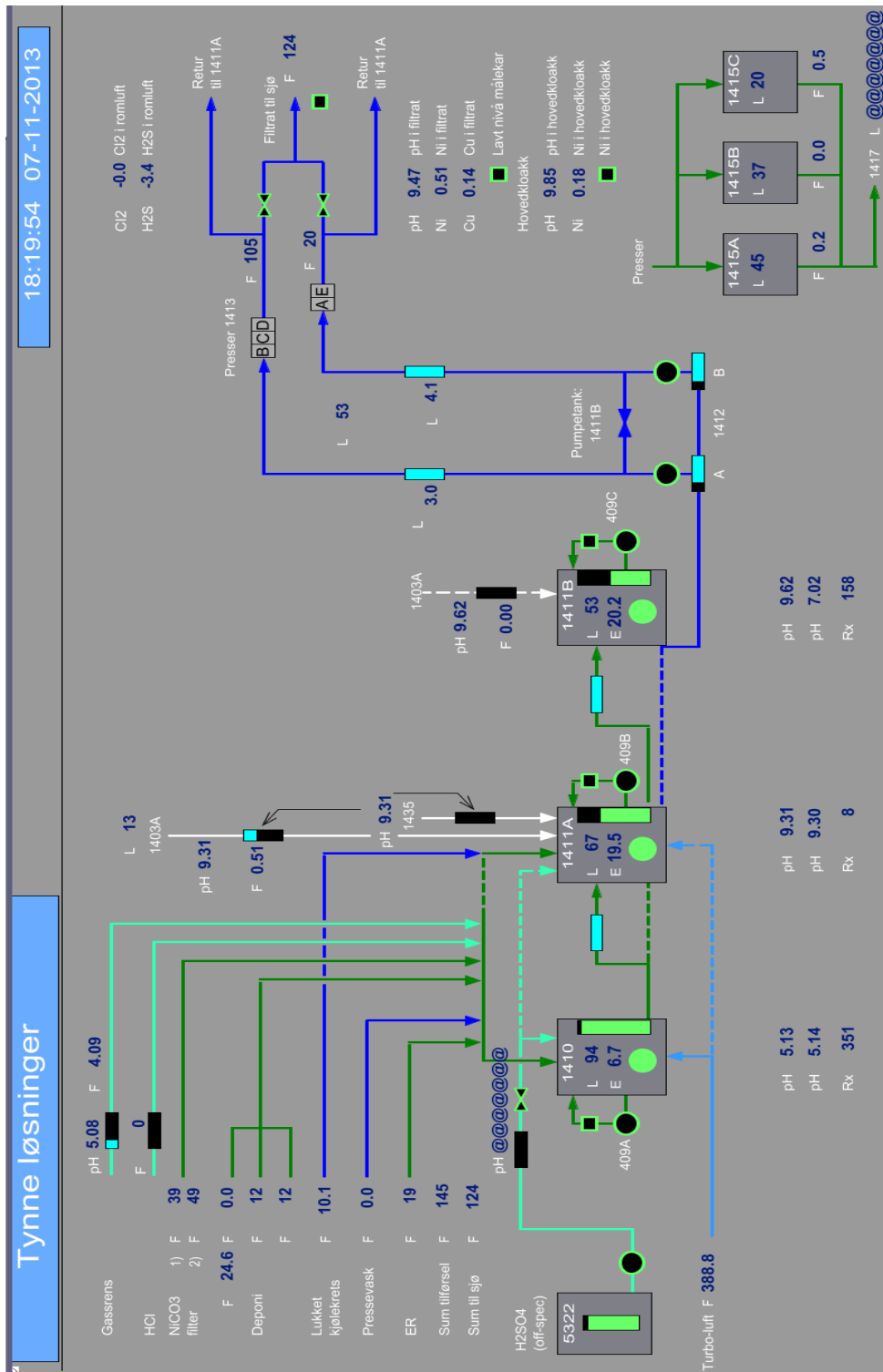
Figure 0.1: Detailed block diagram of the effluent treatment plant
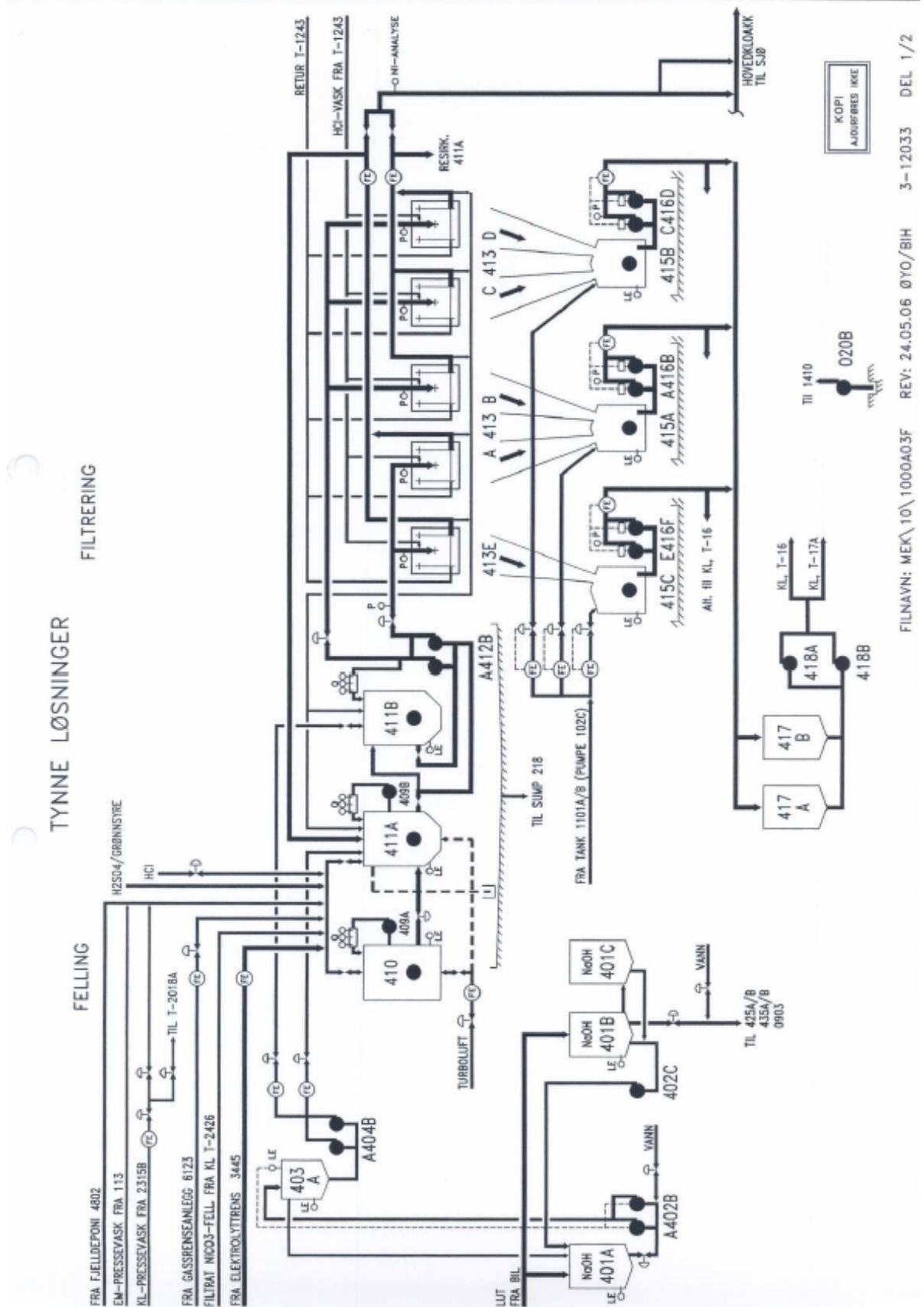
Figure 0.2: Detailed flow diagram of the effluent treatment plant

The streams come from various filtrate, leachate and wash water streams from the plant and caverns.

Table 0.1: The inlet streams to T-1410 and their typical approximate flowrates

Stream	Vol. Flowrate	Mass Flowrate Ni	Mass Flowrate Cu	Mass Flowrate Fe
	m^3/day	kg/day	kg/day	kg/day
Filtrate from $NiCO_3$ plant	1200	150	1	6
Leachate from residue deposit	35	25	4	1
Leachate from KL-plant deposit	30	50	3	3
Wash water from filter presses	30	10	2	1
Wash water from Ni-crone	15	10		
Wash water from Cu-cathode	15	5	6	1
Wash water from Cu starting plates	15	14	20	0
Wash water from filter presses – KL, ML	270	1000	150	
Scrubber solution – ML, KL, ER	10	0	0	0
Closed cooling circuit	300			

The typical flowrates of solution from the gas purification plant that can be treated are shown:

Stream	Acid Concentration	Acid Vol. Flowrate	Mass Flowrate Ni	Mass Flowrate Cu	Mass Flowrate Co
	g/l H_2SO_4	m^3/day	kg/day	kg/day	kg/day
Mountain cavern		450	90	90	15
Filtrate from T-6123	150	100	30	35	1

Chemical behaviour

CO_2 stripping tank – 1410:

Solution from the KL (chlorine leach) plant contains sodium bicarbonate ($NaHCO_3$) from nickel carbonate ($NiCO_3$) precipitation. This solution operates as a buffer – i.e. it is able to neutralise acid from the gas purification plant. Through mixing, the bicarbonate is converted to CO_2 gas which will be sparged off.

$$2NaHCO_3 + H_2SO_4 \leftrightarrow Na_2SO_4 + 2H_2O + 2CO_2 \qquad [3.1]$$
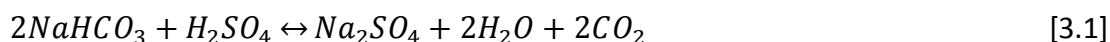
The more acid added, the lower the pH will be, resulting in higher conversion of bicarbonate to carbon dioxide. At pH 5.5 or lower, there will be insignificant amounts of bicarbonate left meaning that the buffer capacity is used up. Through natural de-gassing, the concentration of CO_2 in the solution can be below 1 g/litre. By increasing the pH in the precipitation reaction, CO_2 reacts with caustic soda (NaOH) to form bicarbonate again.

$$CO_2 + NaOH \leftrightarrow NaHCO_3 \qquad [3.2]$$

By blowing air through the solution in T-1410, before the pH is increased, most of the CO_2 in solution can be driven out. This means less NaOH will be used up for bicarbonate formation in the consequent precipitation tank and thus less NaOH is required. The sparging of air can also help to avoid fouling of tanks from magnesium and calcium. The redox potential is also measured in T-1410. If the redox is too low (<250 mV), it can mean that some copper is present as mono-valent copper. The risk here is that mono-valent copper can remain in solution without being precipitated out. Low redox can also cause the formation of SO_2 which further lowers the redox. If the redox is too high, there is a risk that chlorine gas ($Cl_{2(g)}$) will be released.

Air stripping prior to purification steps

It is possible to reduce the excess $NiCO_3$ that enters the effluent treatment as filtrate from the $NiCO_3$ production plant by air stripping through the $NiCO_3$ production tank. A reduction of $NiCO_3$ enables less NaOH to be used up during the precipitation stage of the treatment process. The following shows the stoichiometric chemical reactions that occur for the production of basic nickel carbonate:

Neutralisation of acid from Ni-anolyte:

$$2HCl + Na_2CO_3 \leftrightarrow 2NaCl + H_2CO_3 \qquad\qquad [3.7]$$

Nickel carbonate precipitation:

$$NiCl_2 + Na_2CO_3 \leftrightarrow NiCO_3 + 2NaCl \qquad\qquad [3.8]$$

Nickel hydroxide precipitation:

$$NiCl_2 + Na_2CO_3 + 2H_2O \leftrightarrow Ni(OH)_{2\,(s)} + H_2CO_3 + 2NaCl \qquad\qquad [3.9]$$
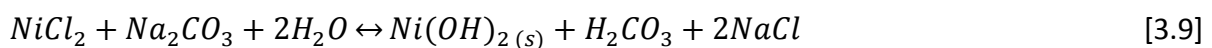
Dissociation of carbonic acid – CO_2 equilibrium, water-gas phase:

$$H_2CO_3 \leftrightarrow H_2O + CO_{2\,(aq)} \qquad\qquad [3.10]$$
$$CO_{2\,(aq)} \leftrightarrow CO_{2\,(g)} \qquad\qquad [3.11]$$

(Some carbonic acid will escape as CO_2 gas)

Dissolved carbonic acid will, at a pH of approximately 8, react with Na_2CO_3:

$$H_2CO_3 + Na_2CO_3 \leftrightarrow 2NaHCO_3 \qquad\qquad [3.12]$$

At neutral pH, a basic nickel carbonate is formed:

$$xNiCO_3 \cdot yNi(OH)_2 \cdot zH_2O \qquad\qquad [3.13]$$

98

x and y will be dependent on conditions.

There is also a mixture of NiCO$_3$ and Ni(OH)$_2$ that are described in the reaction mechanism:

Reaction 5 is reversible and can be reversed if the reaction product (CO$_2$) is removed effectively from the mixture.

$$2NaHCO_3 \leftrightarrow Na_2CO_3 + H_2CO_3 \leftrightarrow Na_2CO_3 + CO_{2\,(aq)} + H_2O \qquad\qquad [3.14]$$
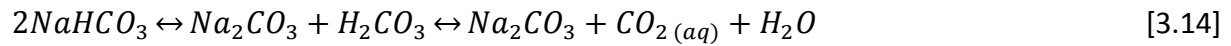
The only way to remove CO$_2$ is in its gaseous form. Air sparging is an effective way to strip CO$_2$ in the air whereby:

$$CO_{2\,(aq)} \leftrightarrow CO_{2\,(g)} \qquad\qquad [3.15]$$

A sodium carbonate molecule (which was used to bind CO$_2$) is hereby gained, which is produced by precipitation of Ni(OH)$_2$. The pH increases because sodium carbonate is more basic than bi-carbonate.

This sodium carbonate molecule can now be used to precipitate more NiCO$_3$:

$$NiCl_2 + Na_2CO_3 \leftrightarrow NiCO_3 + 2NaCl \qquad\qquad [3.16]$$

By adding more Ni-anolyte, or its equivalent, the addition of granulated soda (or dissolved soda) is reduced, and in this way, the pH is reduced.

Appendix B – Filter Cloth Specification Sheets and Images

Data is given pertaining to cloths used on the pilot filter rig.

FUNDABAC®Filter medien

FUNDABAC®Filter media

DrM

20140117

Typ Type	**G 11 U 010**
Lager Nr. Stock No.	**850027.11**
Kennfaden Mark	**Stock No.**
Kette material Warp material	**PP multifilament**
Schuss Material Weft material	**PP multifilament**
Gewicht g/m2 Weight g/m2	**330 - 380**
Max. Einsatz Temp. °C Max. Operating Temp. °C	**95**
Luftdurchlass Air permeability L/dm2 x min. (20 mm WS)	**5 - 15**
Porometer values — micron 10% >	
micron 50% >	**4.7**
micron 90% >	
Zusatzinformationen Additional information	

50-fold magnification (no scale)
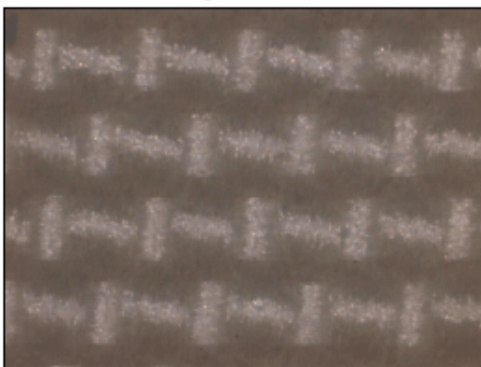
200-fold magnification (no scale)
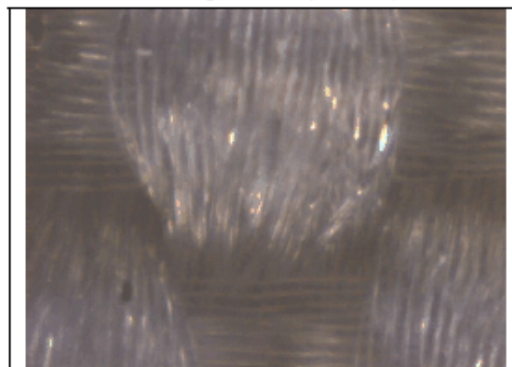
Bemerkung: Die Farbe der Filter Medien ist auf den Fotos teilweise verfälscht.
Note: Real colour of media may be different than on pictures.

Figure 0.3: Data sheet for cloth DrM G 11 U 010

FUNDABAC®Filter medien

FUNDABAC®Filter media

DrM

20140402

Typ Type	**F 11 U 020**
Lager Nr. Stock No.	850001.11
Kennfaden Mark	**none (white media)**
Kette material Warp material	**PP multifilament**
Schuss Material Weft material	**PP multifilament**
Gewicht g/m2 Weight g/m2	1010
Max. Einsatz Temp. °C Max. Operating Temp. °C	105
Luftdurchlass Air permeability L/dm2 x min. (20 mm WS)	15 - 30
Porometer values — micron 10% >	
Porometer values — micron 50% >	2.8
Porometer values — micron 90% >	
Zusatzinformationen Additional information	
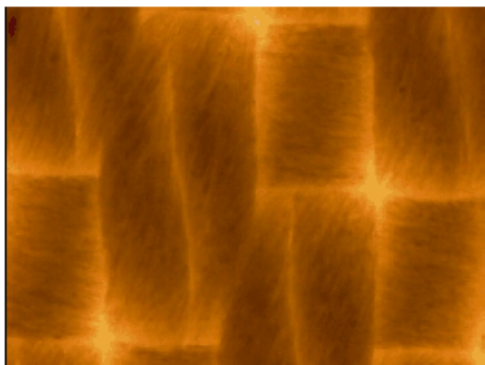
Bemerkung: Die Farbe der Filter Medien ist auf den Fotos teilweise verfälscht.
Note: Real colour of media may be different than on pictures.

Figure 0.4: Data sheet for cloth DrM F 11 U 020

FUNDABAC®Filter medien

FUNDABAC®Filter media

DrM

Typ Type	**N 11 U 030**
Lager Nr. Stock No.	850050.11
Kennfaden Mark	**none (whIte felt)**
Kette material Warp material	**PP felt**
Schuss Material Weft material	**PP felt**
Gewicht g/m2 Weight g/m2	439
Max. Einsatz Temp. °C Max. Operating Temp. °C	95
Luftdurchlass Air permeability L/dm2 x min. (20 mm WS)	30 - 60
Porometer values — micron 10% > micron 50% > micron 90% >	0
Zusatzinformationen Additional information	

Bemerkung: Die Farbe der Filter Medien ist auf den Fotos teilweise verfälscht.
Note: Real colour of media may be different than on pictures.

Figure 0.5: Data sheet for cloth DrM N 11 U 030

DATENBLATT
Data sheet / fiche technique / technische gegevens / ТЕХНИЧЕСКИЕ ДАННЫЕ

PPV 2737

MATERIAL
material / matière / Basis / МАТЕРИАЛ

: Polypropylen -Nadelfilz mit Stützgewebe
needle felt with supporting fabric / feutre aiguilleté avec toile de support / naaldvilt met steundoek / иглопробивная ткань с опорной тканью

AUSRÜSTUNG
finish / traitement / Afwerking / ОБРАБОТКА

: beidseitig geglättet
both sides smoothed / lissé des deux côtés / tweezijdig glad gemaakt / двухсторонний заглаженный

GEWICHT
weight / poids / Doekgewicht / ПОВЕРХНОСТНАЯ ПЛОТНОСТЬ

: ~ 600 g/m² (18,0 oz/sqyd)

DICKE
thickness / épaisseur / Dikte / ТОЛЩИНА

: ~ 1,7 mm

LUFTDURCHLÄSSIGKEIT bei 20 mm WS
air permeability / perméabilité à l'air / Luchtdoorlaatbaarheid / ВОЗДУХОПРОПУСКНАЯ СПОСОБНОСТЬ

: ~ 30 l / dm² min (6,2 cfm)

TEMPERATURBESTÄNDIGKEIT
temperature resistance / résistance à la température / Temperatuurbestendigheid / ТЕМПЕРАТУРА ПРИМЕНЕНИЯ

: 70° C Dauertemperatur
continuous temperature / température de travail / Bedrijfstemperatuur / продолжительная температура

: 95° C Spitzentemperatur
maximum temperature / brèves pointes / Piektemperatuur / максимальная температура

BESTÄNDIGKEIT
resistance / résistance / Bestendigheid / УСТОЙЧИВОСТЬ ПО ОТНОШЕНИЮ К:

SÄUREN acids / acides / Zuren / КИСЛОТАМ

: sehr gut very good / très bonne / zeer goed / очень хорошо

LAUGEN alcalics / alcalis / Basen / ЩЕЛОЧАМ

: sehr gut very good / très bonne / zeer goed / очень хорошо

OXYDATIONSMITTEL
oxydation solvents / solvants / Oxidatiemiddelen / ОКСИДАНТАМ

: beschränkt limited / limité / beperkt / ограниченная

REISSFESTIGKEIT
tensile strength / résistance à la rupture / Treksterkte / РАЗРЫВНАЯ НАГРУЗКА

KETTE warp / chaîne / Ketting / ОСНОВА
SCHUSS weft / trame / Inslag / УТОК

: 110 daN/5 cm
: 150 daN/5 cm

ABRIEBFESTIGKEIT
abrasive resistance / résistance à l'abrasion / Schuurweerstand / СТОЙКОСТЬ К ИСТИРАНИЮ

: mittel medium / moyenne / medium / средний

LICHTBESTÄNDIGKEIT
light stability / stabilité à la lumière / Lichtbestendigheid / СВЕТОУСТОЙЧИВОСТЬ

: gering poor / faible / gering / слабая

SPEZIFISCHES GEWICHT
specific weight / poids spécifique / Soortelijk gewicht / СПЕЦИФИЧЕСКИЙ ВЕС

: 0,91 g/cm³

edition: 08.10.2009

Figure 0.6: Data sheet for cloth Markert PPV 2737

Technical Data

Polynova™

98080F

PX513-45

CLEAR EDGE™ Filtration

Fibre	Threads - Warp
100% Polypropylene	(cm)
	15
Yarn Type - Warp	**Threads - Weft**
Staple Fibre	(cm)
	14
Yarn Type Weft	
Staple Fibre	**Thickness**
	(Micron)
Weight	1100
(g/m²)	
500	**Tensile Strength - Warp**
	(N/cm)
Weave Pattern	800
Plain	
	Tensile Strength - Weft
Air Permeability	(N/cm)
(l/dm²/min@20mmWG)	750
10	

Potential Industries

Titanium Dioxide

Fabric Properties

Retention Efficiency ●●●●○
Cake Discharge ●●○○○
Blinding Resistance ●●○○○
Mechanical Resistance ●●●○○
Stretch Resistance Warp ●●○○○
Stretch Resistance Weft ●●○○○
Bulk ●●●●○

Additional Guidance on Fibre - Polypropylene

- Good resistance to wear
- Very Good resistance to alkalis
- Very Good resistance to Hydrolysis

- Poor resistance to Oxidising Agents
- Very Good resistance to strong acids
- Maximum operating temp 95°C

Retention Efficiency Details Available Upon Request

IQNet CERTIFIED MANAGEMENT SYSTEM   DQS Quality Management ISO 9001

Figure 0.7: Data sheet for cloth Clear Edge 98080F
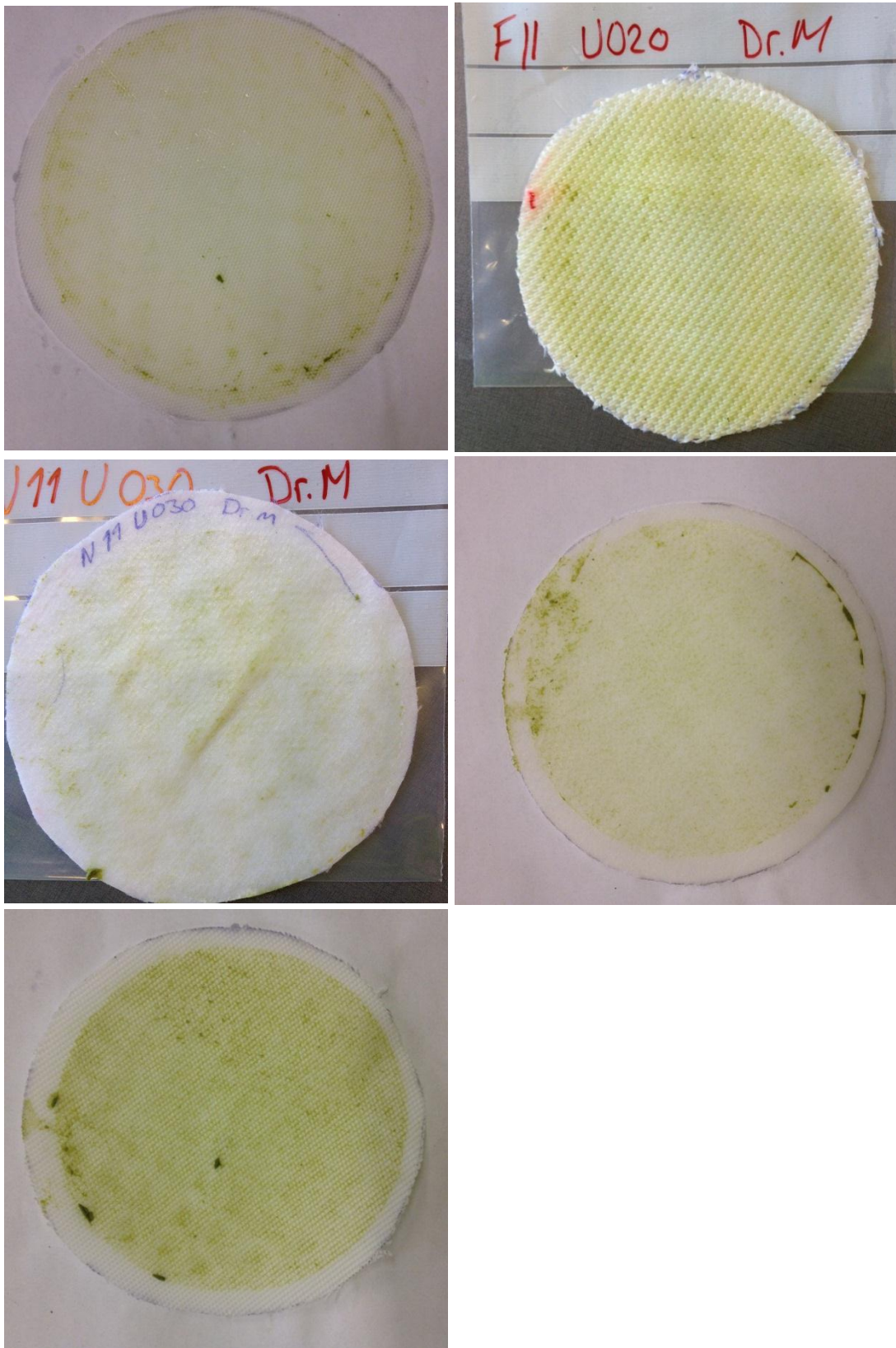
Figure 0.8: Images of the filter cloths after laboratory filtration experiments (from top left to right: DrM G 11 U 010, DrM F 11 U 020, DrM N 11 U 030, Markert PPV 2737 and Clear Edge 98080F)

Appendix C – Raw Data

Table 0.2: Screening filter cloth tests for cloths 1 to 29 showing the pressure recorded and time elapsed at certain volumetric intervals during filtration

Test:	1		Test:	2	
Type:	Clear Edge 25130F		Type:	Markert PMM 3508	
Date:	04.02.2014		Date:	04.02.2014	
Volume (ml)	*Pressure (bar)*	*Time (s)*	*Volume (ml)*	*Pressure (bar)*	*Time (s)*
50	-0,42	5,39	50	-0,4	9,75
100	-0,6	16,28	100	-0,6	20,66
150	-0,7	29,01	150	-0,75	35,09
200	-0,85	46,47	200	-0,87	53,29
250	-0,9	66,39	250	-0,9	75,45
300	-0,9	91,76	300	-0,9	101,66
350	-0,9	117,13	350	-0,9	132,29
390		136,99	390		159,98
Cloth grip:		4	Cloth grip:		4
Mass dry cake (g):		14,14	Mass dry cake (g):		14,53
Mass residue in filtrate, dry (g):		0,0066	Mass residue in filtrate, dry (g):		0,0118
Dry solids concentration in filtrate (g/l):	0,0169		Dry solids concentration in filtrate (g/l):	0,0303	
Test:	3		Test:	4	
Type:	Markert PPD 3214		Type:	Markert PPV 2737	
Date:	04.02.2014		Date:	04.02.2014	
Volume (ml)	*Pressure (bar)*	*Time (s)*	*Volume (ml)*	*Pressure (bar)*	*Time (s)*
50	-0,35	6,93	50	-3,2	6,56
100	-0,55	17,82	100	-5	16,15
150	-0,7	30,87	150	-6,5	27,01
200	-0,83	47,13	200	-8	42,45
250	-0,89	66,94	250	-8,9	60,68
300	-0,9	89,36	300	-9	83,72
350	-0,9	116,73	350	-9	108,86
390		141,64	387		129,86
Cloth grip:		4	Cloth grip:		3
Mass dry cake (g):		14,45	Mass dry cake (g):		14,39
Mass residue in filtrate, dry (g):		0,034	Mass residue in filtrate, dry (g):		0,0087
Dry solids concentration in filtrate (g/l):	0,0872		Dry solids concentration in filtrate (g/l):	0,0225	
Test:	5		Test:	6	
Type:	Markert PP 2436		Type:	Clear Edge 98080F	
Date:	04.02.2014		Date:	05.02.2014	
Volume (ml)	*Pressure (bar)*	*Time (s)*	*Volume (ml)*	*Pressure (bar)*	*Time (s)*
50	-0,3	6,75	50	-0,3	5,42
100	-0,5	16,65	100	-0,5	15,03
150	-0,72	28,67	150	-0,65	26,53
200	-0,82	45,18	200	-0,8	43,83
250	-0,89	64,65	250	-0,89	63,2
300	-0,9	87,24	300	-0,9	86,51
350	-0,9	115,79	350	-0,9	114,21
390		136,4	390		137,11
Cloth grip:		4	Cloth grip:		3
Mass dry cake (g):		15,21	Mass dry cake (g):		14,13
Mass residue in filtrate, dry (g):		0,0106	Mass residue in filtrate, dry (g):		0,026
Dry solids concentration in filtrate (g/l):	0,0272		Dry solids concentration in filtrate (g/l):	0,0667	

Test:	7		Test:	8	
Type:	Markert PPM 3502		Type:	Clear Edge 28560F	
Date:	05.02.2014		Date:	05.02.2014	
Volume (ml)	*Pressure (bar)*	*Time (s)*	*Volume (ml)*	*Pressure (bar)*	*Time (s)*
50	-0,32	6,6	50	-0,3	6,39
100	-0,55	17,17	100	-0,5	15,65
150	-0,7	28,64	150	-0,67	26,83
200	-0,82	43,92	200	-0,82	43,28
250	-0,88	61,18	250	-0,87	61,05
300	-0,9	83,47	300	-0,9	86,43
350	-0,9	107,71	350	-0,9	109,73
387		130,65	388		131,77
Cloth grip:		4	Cloth grip:		4
Mass dry cake (g):		13,98	Mass dry cake (g):		14,45
Mass residue in filtrate, dry (g):		0,2026	Mass residue in filtrate, dry (g):		0,0142
Dry solids concentration in filtrate (g/l):		0,5235	Dry solids concentration in filtrate (g/l):		0,0366

Test:	9		Test:	10	
Type:	Markert NST 648		Type:	DrM G11 U 010	
Date:	06.02.2014		Date:	06.02.2014	
Volume (ml)	*Pressure (bar)*	*Time (s)*	*Volume (ml)*	*Pressure (bar)*	*Time (s)*
50	-0,3	5,39	50	-0,31	6,33
100	-0,46	14,67	100	-0,5	15,39
150	-0,63	26,65	150	-0,65	26,16
200	-0,76	41,07	200	-0,8	40,75
250	-0,86	60,72	250	-0,88	58,16
300	-0,9	81,85	300	-0,9	78
350	-0,9	106,68	350	-0,9	102,96
388		127,87	392		122,32
Cloth grip:		3,5	Cloth grip:		3
Mass dry cake (g):		14,4	Mass dry cake (g):		14,41
Mass residue in filtrate, dry (g):		0,0128	Mass residue in filtrate, dry (g):		0,0129
Dry solids concentration in filtrate (g/l):		0,0330	Dry solids concentration in filtrate (g/l):		0,0329

Test:	11		Test:	12	
Type:	DrM B11 MU 200		Type:	DrM G11 M 025	
Date:	06.02.2014		Date:	06.02.2014	
Volume (ml)	*Pressure (bar)*	*Time (s)*	*Volume (ml)*	*Pressure (bar)*	*Time (s)*
50	Too fast	Too fast	50	-0,3	6,83
100	Too fast	3,42	100	-0,45	17,32
150	-0,36	9,21	150	-0,6	30,18
200	-0,53	19,01	200	-0,7	46,24
250	-0,7	31,25	250	-0,8	66,82
300	-0,83	46,89	300	-0,86	89,29
350	-0,88	66,57	350	-0,88	115,47
390		88,56	392		134,38
Cloth grip:		4	Cloth grip:		4
Mass dry cake (g):		11,79	Mass dry cake (g):		14,55
Mass residue in filtrate, dry (g):		2,252	Mass residue in filtrate, dry (g):		0,0903
Dry solids concentration in filtrate (g/l):		5,7744	Dry solids concentration in filtrate (g/l):		0,2304

Test:	13		Test:	14	
Type:	DrM B11 MU 100		Type:	Markert PP 24901	
Date:	06.02.2014		Date:	10.02.2014	
Volume (ml)	*Pressure (bar)*	*Time (s)*	*Volume (ml)*	*Pressure (bar)*	*Time (s)*
50	Too fast	1	50	-0,32	5,64
100	-0,2	2,9	100	-0,43	17,31
150	-0,34	9,84	150	-0,48	31,54
200	-0,5	20,92	200	-0,52	50,24
250	-0,66	34,58	250	-0,55	74,45
300	-0,75	50,34	300	-0,57	102,22
350	-0,81	69,77	350	-0,58	133,9
392		93,64	390		165,19
Cloth grip:		4	Cloth grip:		3,5
Mass dry cake (g):		12,1	Mass dry cake (g):		14,96
Mass residue in filtrate, dry (g):		1,9923	Mass residue in filtrate, dry (g):		0,0123
Dry solids concentration in filtrate (g/l):		5,0824	Dry solids concentration in filtrate (g/l):		0,0315
Test:	15		Test:	16	
Type:	Markert PP 2448		Type:	Septek PES 1950 MPX	
Date:	10.02.2014		Date:	10.02.2014	
Volume (ml)	*Pressure (bar)*	*Time (s)*	*Volume (ml)*	*Pressure (bar)*	*Time (s)*
50	-0,41	9,55	50	-0,3	4,35
100	-0,5	22,85	100	-0,41	12,63
150	-0,59	39,3	150	-0,47	22,72
200	-0,63	58,81	200	-0,56	36,8
250	-0,7	86,81	250	-0,61	34,28
300	-0,77	108,81	300	-0,68	75,28
350	-0,8	137,4	350	-0,74	98,78
386		159,04	390		116,89
Cloth grip:		3,5	Cloth grip:		3,5
Mass dry cake (g):		14,78	Mass dry cake (g):		
Mass residue in filtrate, dry (g):		0,0076	Mass residue in filtrate, dry (g):		0,0109
Dry solids concentration in filtrate (g/l):		0,0197	Dry solids concentration in filtrate (g/l):		0,0279
Test:	17		Test:	18	
Type:	Markert PP 2402		Type:	Markert PP 2433	
Date:	20.02.2014		Date:	20.02.2014	
Volume (ml)	*Pressure (bar)*	*Time (s)*	*Volume (ml)*	*Pressure (bar)*	*Time (s)*
50	-0,3	4,63	50	-0,3	4,73
100	-0,42	13,6	100	-0,42	13,59
150	-0,5	24,65	150	-0,5	24,96
200	-0,58	39,18	200	-0,58	39,47
250	-0,65	58,17	250	-0,65	58,22
300	-0,72	80,12	300	-0,74	79,95
350	-0,8	104,65	350	-0,79	104,11
377		116,78	376		114,05
Cloth grip:		3	Cloth grip:		3
Mass dry cake (g):		14,83	Mass dry cake (g):		14,62
Mass residue in filtrate, dry (g):		0,0115	Mass residue in filtrate, dry (g):		0,019
Dry solids concentration in filtrate (g/l):		0,0305	Dry solids concentration in filtrate (g/l):		0,0505

Test:	19		Test:	20	
Type:	Markert PP 2455		Type:	Septek PP890X	
Date:	20.02.2014		Date:	24.02.2014	
Volume (ml)	Pressure (bar)	Time (s)	Volume (ml)	Pressure (bar)	Time (s)
50	-0,3	5,17	50	-0,34	7,75
100	-0,41	13,35	100	-0,45	18,54
150	-0,5	24,81	150	-0,55	32,51
200	-0,6	40,61	200	-0,62	50,99
250	-0,65	60,08	250	-0,7	72,65
300	-0,74	81,37	300	-0,76	96,05
350	-0,79	106,53	350	-0,82	122,65
380		120,91	377		135,79
Cloth grip:		3,5	Cloth grip:		4
Mass dry cake (g):		14,44	Mass dry cake (g):		15,07
Mass residue in filtrate, dry (g):		0,0543	Mass residue in filtrate, dry (g):		0,0124
Dry solids concentration in filtrate (g/l):		0,1429	Dry solids concentration in filtrate (g/l):		0,0329
Test:	21		Test:	22	
Type:	Septek PPCCCX special		Type:	Septek PP-555X	
Date:	24.02.2014		Date:	24.02.2014	
Volume (ml)	Pressure (bar)	Time (s)	Volume (ml)	Pressure (bar)	Time (s)
50	-0,3	4,96	50	-0,3	7,34
100	-0,41	13,07	100	-0,37	18,47
150	-0,51	23,85	150	-0,38	34,3
200	-0,58	38,19	200	-0,43	55,33
250	-0,66	57,31	250	-0,57	76,59
300	-0,73	78,04	300	-0,67	101,32
350	-0,79	101,32	350	-0,75	128,77
380		113,74	372		138,28
Cloth grip:		3,5	Cloth grip:		4
Mass dry cake (g):		14,99	Mass dry cake (g):		14,81
Mass residue in filtrate, dry (g):		0,0144	Mass residue in filtrate, dry (g):		0,2042
Dry solids concentration in filtrate (g/l):		0,0379	Dry solids concentration in filtrate (g/l):		0,5489
Test:	23		Test:	24	
Type:	Septek PP-Blue-Special		Type:	Septek PP-Blue-Special	
Date:	24.02.2014		Date:	24.02.2014	
Volume (ml)	Pressure (bar)	Time (s)	Volume (ml)	Pressure (bar)	Time (s)
50	-0,34	7,6	50	-0,35	6,63
100	-0,44	18,54	100	-0,45	16,34
150	-0,5	33,54	150	-0,54	28,36
200	-0,52	51,76	200	-0,61	43,33
250	-0,52	75,69	250	-0,68	62,58
300	-0,52	104,13	300	-0,75	83,3
350	-0,52	134,94	350	-0,8	107,98
380		154,99	384		120,4
Cloth grip:		3,75	Cloth grip:		4
Mass dry cake (g):		15,11	Mass dry cake (g):		14,84
Mass residue in filtrate, dry (g):		0,0195	Mass residue in filtrate, dry (g):		0,0127
Dry solids concentration in filtrate (g/l):		0,0513	Dry solids concentration in filtrate (g/l):		0,0331

Test:	25		Test:	26	
Type:	Septek Prop 3 5C		Type:	Septek PP-677X	
Date:	24.02.2014		Date:	24.02.2014	
Volume (ml)	*Pressure (bar)*	*Time (s)*	*Volume (ml)*	*Pressure (bar)*	*Time (s)*
50	-0,35	5,94	50	-0,44	8,22
100	-0,45	14,72	100	-0,54	21,19
150	-0,55	27,22	150	-0,6	35,18
200	-0,62	41,82	200	-0,66	52,43
250	-0,7	62,09	250	-0,72	73,07
300	-0,75	83,18	300	-0,78	95,58
350	-0,81	108,19	350	-0,82	120,34
377		124,72	388		137,25
Cloth grip:		3	Cloth grip:		3,2
Mass dry cake (g):		15	Mass dry cake (g):		14,82
Mass residue in filtrate, dry (g):		0,0092	Mass residue in filtrate, dry (g):		0,0031
Dry solids concentration in filtrate (g/l):		0,0244	Dry solids concentration in filtrate (g/l):		0,0080
Test:	27		Test:	28	
Type:	Septek Prop 2 NC		Type:	DrM F11 U 020	
Date:	24.02.2014		Date:	03.03.2014	
Volume (ml)	*Pressure (bar)*	*Time (s)*	*Volume (ml)*	*Pressure (bar)*	*Time (s)*
50	-0,31	5,41	50	-0,3	5,83
100	-0,42	13,94	100	-0,41	14,84
150	-0,53	25,5	150	-0,5	25,83
200	-0,61	42,65	200	-0,59	41,2
250	-0,68	61,33	250	-0,65	58,9
300	-0,75	82,95	300	-0,72	81,18
350	-0,8	107,6	350	-0,79	104,99
373		123,89	380		120,76
Cloth grip:		3,5	Cloth grip:		3
Mass dry cake (g):			Mass dry cake (g):		14,91
Mass residue in filtrate, dry (g):		0,0124	Mass residue in filtrate, dry (g):		0,0065
Dry solids concentration in filtrate (g/l):		0,0332	Dry solids concentration in filtrate (g/l):		0,0171

Test:	29	
Type:	DrM N11 U 030	
Date:	03.03.2014	
Volume (ml)	*Pressure (bar)*	*Time (s)*
50	-0,3	5,54
100	-0,4	14,28
150	-0,5	25,98
200	-0,59	41,81
250	-0,65	59,12
300	-0,72	80,99
350	-0,78	104,79
380		118,45
Cloth grip:		3
Mass dry cake (g):		14,61
Mass residue in filtrate, dry (g):		0,0112
Dry solids concentration in filtrate (g/l):		0,0295

Table 0.3: Viscosity measurements for specific cake resistance and medium resistance tests during initial filter cloth screening trials

Temp	°C	35,00
μH2O	cp	0,72
T.H2O	min	2,82
δH2O	g/cm3	0,99
Tx,1	min	2,85
Tx,2	min	2,87
Tx,3	min	2,87
T.x,av	min	2,86
δx	g/cm3	1,03
μx	cp	0,76

Table 0.4: Time and corresponding volume measurements for filtrate points during calculation of specific cake resistance and medium resistance

Cloth	DrM G 11 U 010	DrM N 11 U 030	Markert PPV 2737	Septek Prop 3SC	Clear Edge 98080F	DrM F11 U 020
	Time (min)	Time (min)	Time (min)	Time (min)	Time (min)	Time (min)
1	0,04	0,03	0,05	0,03	0,03	0,04
2	0,10	0,07	0,10	0,08	0,09	0,07
3	0,16	0,15	0,18	0,14	0,16	0,11
4	0,25	0,22	0,26	0,21	0,24	0,17
5	0,37	0,32	0,37	0,31	0,33	0,24
6	0,49	0,42	0,49	0,42	0,46	0,32
7	0,64	0,55	0,62	0,54	0,58	0,41
	Volume (ml)	Volume (ml)	Volume (ml)	Volume (ml)	Volume (ml)	Volume (ml)
1	10	10	10	10	10	10
2	20	20	20	20	20	20
3	30	30	30	30	30	30
4	40	40	40	40	40	40
5	50	50	50	50	50	50
6	60	60	60	60	60	60
7	70	70	70	70	70	70

Table 0.5: Measurements of constants used in the specific cake resistance and medium resistance calculations

Cloth		DrM G 11 U 010	DrM N 11 U 030	Markert PPV 2737	Septek Prop 3SC	Clear Edge 98080F	DrM F11 U 020
Filter area	cm2	12,56	12,56	12,56	12,56	12,56	12,56
Conc. solids in suspension	g dry/l filtrate	6,801	6,801	6,801	6,801	6,801	6,801
Viscosity	cp	0,758	0,758	0,758	0,758	0,758	0,758
Pressure drop	bar	0,85	0,85	0,85	0,85	0,85	0,85
Moisture in cake	%	84,13	85,64	86,23	84,92	84,96	86,21
Temperature	°C	31	31	31	31	31	31
Volume filtrate	ml	76	76	76	76,5	76	76
Mass dry solids	g	0,493	0,517	0,525	0,514	0,486	0,443

Table 0.6: Data obtained for each filtration test on the filter rig

	Date	Time	Filt. time	Acc. slurry	Acc. filtrate volume (5 mins)	Acc. Filtrate volume (total)	pH	dP	Temp.
			(mins)	(m3)	(m3)	(m3)		(bar)	(°C)
DrM G	10.03.2014	09:43:40	20	0,34	0,057	0,19	9,75	2,91	32,4
	10.03.2014	10:13:20	30	0,39	0,087	0,31	9,67	2,64	34,9
	10.03.2014	10:50:05	40	0,63	0,091	0,50	9,74	2,32	36,2
	10.03.2014	12:09:25	20	0,41	0,12	0,33	9,75	2,37	34,3
	10.03.2014	12:35:35	30	0,56	0,14	0,46	9,75	2,03	33,7
	10.03.2014	13:11:45	40	0,73	0,18	0,60	9,74	2,11	33,1
	11.03.2014	09:29:30	20	0,60	0,11	0,43	9,57	1,63	37,0
	11.03.2014	09:56:05	30	0,71	0,18	0,61	9,57	2,01	37,2
	11.03.2014	10:35:20	40	0,71	0,12	0,57	9,57	2,38	36,8
	11.03.2014	12:48:55	20	0,38	0,10	0,28	9,65	2,48	35,1
	11.03.2014	13:15:45	30	0,49	0,13	0,42	9,65	1,59	35,8
	11.03.2014	13:58:20	40	0,64	0,10	0,51	9,65	1,63	35,5
	12.03.2014	09:18:15	20	0,41	0,076	0,26	9,62	1,81	33,5
	12.03.2014	09:44:00	30	0,46	0,11	0,38	9,56	2,42	35,3
	12.03.2014	10:19:20	40	0,51	0,11	0,42	9,59	1,62	35,8
	12.03.2014	11:59:05	20	0,47	0,14	0,38	9,72	2,28	34,0
	12.03.2014	12:25:10	30	0,66	0,11	0,52	9,65	1,55	35,3
	12.03.2014	13:01:00	40	0,65	0,10	0,51	9,57	1,46	36,0
	13.03.2014	09:24:50	40	1,08	0,011	0,94	9,49	2,17	37,3
	13.03.2014	10:32:10	20	0,64	0,015	0,49	9,49		
	13.03.2014	12:17:35	20	0,54	0,078	0,40	9,44	2,20	38,5
	13.03.2014	12:46:40	20	0,50	0,13	0,41	9,49	2,31	38,8
	13.03.2014	13:16:50	20	0,54	0,13	0,47	9,49	2,33	38,8
DrM F	17.03.2014	09:19:20	20	0,60	0,22	0,51	9,44	2,27	37,1
	17.03.2014	09:45:10	30	0,74	0,23	0,69	9,44	2,43	37,6
	17.03.2014	10:20:30	40	0,81	0,20	0,75	9,44	2,08	38,0
	17.03.2014	11:51:30	20	0,54	0,18	0,44	9,44	2,17	38,2
	17.03.2014	12:20:25	30	0,65	0,17	0,55	9,44	2,27	38,4
	17.03.2014	13:00:10	40	0,74	0,17	0,64	9,51	2,39	38,2
	18.03.2014	09:24:40	20	0,47	0,13	0,36	9,34	2,30	38,2
	18.03.2014	09:53:45	30	0,52	0,14	0,45	9,26	2,43	39,4
	18.03.2014	10:33:40	40	0,53	0,13	0,49	9,41	2,39	39,6
	18.03.2014	11:35:55	20	0,39	0,12	0,31	9,74	2,56	37,0
	18.03.2014	12:06:35	30	0,54	0,15	0,48	9,48	2,56	36,1
	18.03.2014	13:03:30	20	0,44	0,17	0,37	9,42	2,64	32,5
	19.03.2014	09:31:45	20	0,54	0,013	0,39	9,50	2,24	35,9
	19.03.2014	10:07:05	30	0,70	0,020	0,58	9,42	2,06	36,7

	19.03.2014	10:46:50	30	0,62	0,054	0,50	9,42	2,10	37,5
	19.03.2014	11:45:10	30	0,59	0,083	0,46	9,42	2,18	37,2
	19.03.2014	12:33:55	30	0,73	0,002	0,61	9,42	2,19	36,3
	19.03.2014	13:28:10	25	0,60	0,12	0,47	9,42	2,21	35,3
DrM N	24.03.2014	09:31:35	20	0,70	0,18	0,54	9,09	2,66	33,4
	24.03.2014	10:01:15	30	0,81	0,18	0,67	9,03	2,72	33,1
	24.03.2014	10:39:45	40	0,96	0,19	0,85	8,97	2,64	33,1
	24.03.2014	11:37:50	20	0,61	0,16	0,49	9,11	2,65	32,2
	24.03.2014	12:07:15	30	0,71	0,16	0,59	9,18	2,66	32,2
	24.03.2014	12:47:15	40	0,81	0,16	0,71	9,34	2,65	32,3
	26.03.2014	09:19:10	20	0,56	0,14	0,42	9,33	2,66	36,4
	26.03.2014	09:48:55	30	0,65	0,15	0,54	9,34	2,66	37,0
	26.03.2014	10:28:30	40	0,81	0,16	0,70	9,34	2,65	36,7
	26.03.2014	11:39:05	20	0,58	0,15	0,44	9,35	2,70	36,4
	26.03.2014	12:08:20	30	0,65	0,15	0,53	9,42	2,65	36,1
	26.03.2014	12:47:20	40	0,74	0,15	0,63	9,42	2,65	35,7
	28.03.2014	09:22:05	20	0,68	0,15	0,51	9,16	2,73	33,8
	28.03.2014	09:51:25	30	0,76	0,18	0,64	9,16	2,76	34,0
	28.03.2014	10:31:00	40	0,86	0,17	0,75	9,16	2,67	34,2
	28.03.2014	12:35:55	20	0,68	0,17	0,54	9,16	2,70	35,3
	28.03.2014	13:06:30	30	0,91	0,21	0,81	9,16	2,70	35,5
	28.03.2014	13:48:00	40	1,04	0,20	0,93	9,31	2,75	35,6
	31.03.2014	09:18:35	30	0,63	0,049	0,51	9,24	2,64	34,4
	31.03.2014	09:58:05	30	0,65	0,023	0,53	9,20	2,64	35,0
	31.03.2014	10:37:00	30	0,69	0,060	0,58	9,21	2,64	35,1
	31.03.2014	11:54:30	30	0,62	0,087	0,50	9,28	2,65	34,4
	31.03.2014	12:35:30	30	0,67	0,11	0,54	9,28	2,62	34,8
	31.03.2014	13:14:20	30	0,72	0,14	0,59	9,28	2,60	34,6
	31.03.2014	13:53:00	30	0,76	0,17	0,65	9,28	2,63	34,1
Markert	02.04.2014	11:49:45	20	0,59	0,15	0,45	9,17	2,51	34,1
	02.04.2014	12:18:20	30	0,73	0,16	0,60	9,21	2,63	33,9
	02.04.2014	12:57:35	40	0,84	0,16	0,72	9,14	2,62	33,7
	02.04.2014	13:46:10	40	0,82	0,15	0,70	9,13		
	03.04.2014	09:26:05	20	0,70	0,17	0,56	9,26	2,67	35,2
	03.04.2014	09:55:10	30	0,91	0,198	0,79	9,23	2,68	36,6
	03.04.2014	10:34:15	40	0,98	0,19	0,87	9,31	2,68	37,3
	03.04.2014	11:41:45	20	0,51	0,12	0,37	9,44	2,63	33,9
	03.04.2014	12:11:05	30	0,63	0,14	0,51	9,54	2,65	32,7
	03.04.2014	12:51:05	40	0,77	0,14	0,65	9,54	2,48	31,5
	08.04.2014	09:16:10	20	0,50	0,13	0,37	9,42	2,65	29,9
	08.04.2014	09:45:30	30	0,64	0,13	0,50	9,42	2,60	28,3
	08.04.2014	10:24:10	40	0,79	0,15	0,68	9,42	2,60	26,6
	08.04.2014	12:27:15	20	0,54	0,12	0,40	9,23	2,58	25,8

	08.04.2014	12:56:55	30	0,68	0,15	0,55	9,23	2,59	25,8
	09.04.2014	09:30:35	30	0,67	0,002	0,54	9,23	2,61	34,1
	09.04.2014	10:09:25	30	0,75	0,020	0,61	9,23	2,58	34,4
	09.04.2014	10:48:40	30	0,87	0,051	0,74	9,23	2,60	34,9
	09.04.2014	11:39:10	30	0,77	0,073	0,63	9,17	2,60	35,1
	09.04.2014	12:18:00	30	0,77	0,11	0,64	9,15	2,58	35,2
	09.04.2014	12:57:20	30	0,74	0,13	0,62	9,15	2,59	35,4
	09.04.2014	13:37:50	30	0,76	0,15	0,62	9,15	2,61	35,7
	09.04.2014	14:16:40	30	0,77	0,16	0,65	9,15	2,61	35,7
Markert	30.04.2014	09:46:10	40	0,84	0,043	0,71	9,22	2,67	33,5
	30.04.2014	12:07:10	40	0,76	0,047	0,65	9,27		
	30.04.2014	12:57:40	40	0,85	0,042	0,72	9,13	2,43	31,0
	30.04.2014	14:08:40	40	0,79	0,038	0,66	9,07	2,80	35,7

Table 0.7: Average values for each cloth in its filtration time categorie

Cloth	Filtration time	Acc slurry	Acc. filtrate volume (5 mins)	Acc. Filtrate volume (total)	pH	dP	Temperature
	(mins)	(m3)	(m3)	(m3)		(bar)	(°C)
DrM G	20	0,44	0,10	0,31	9,68	2,25	34,38
DrM F	20	0,49	0,16	0,40	9,48	2,32	37,62
DrM N	20	0,63	0,16	0,49	9,20	2,68	34,57
Markert	20	0,57	0,14	0,43	9,30	2,61	31,79
DrM G	30	0,54	0,13	0,45	9,64	2,04	35,34
DrM F	30	0,61	0,17	0,54	9,41	2,43	37,88
DrM N	30	0,75	0,17	0,63	9,21	2,69	34,66
Markert	30	0,72	0,15	0,59	9,33	2,63	31,46
DrM G	40	0,65	0,11	0,52	9,64	1,92	35,60
DrM F	40	0,69	0,17	0,63	9,45	2,29	38,61
DrM N	40	0,87	0,17	0,76	9,26	2,67	34,60
Markert	40	0,84	0,16	0,73	9,31	2,60	32,25

Table 0.8: Standard deviation associated with calculating the average values above

Cloth	Filtration time	Acc slurry	Acc. filtrate volume (5 mins)	Acc. Filtrate volume (total)	pH	dP	Temperature
	(mins)	(m3)	(m3)	(m3)		(bar)	(°C)
DrM G	20	0,08	0,03	0,08	0,07	0,43	1,43
DrM F	20	0,07	0,03	0,07	0,14	0,14	0,60
DrM N	20	0,05	0,01	0,05	0,10	0,03	1,57

Markert	20	0,08	0,02	0,07	0,11	0,06	3,49
DrM G	30	0,11	0,03	0,10	0,06	0,40	1,05
DrM F	30	0,09	0,04	0,09	0,09	0,10	1,22
DrM N	30	0,09	0,02	0,10	0,13	0,04	1,69
Markert	30	0,10	0,02	0,10	0,13	0,03	3,89
DrM G	40	0,07	0,03	0,06	0,07	0,36	1,17
DrM F	40	0,12	0,03	0,10	0,04	0,14	0,73
DrM N	40	0,10	0,02	0,10	0,15	0,04	1,54
Markert	40	0,07	0,02	0,08	0,16	0,07	3,85

Table 0.9: Data used in the calculation of specific cake resistance and medium resistance (part 1)

Cloth	Date	Operation time	Filtration time	ts	Vs	dP	Temp.	Slope	y-int	
			(mins)	(s)	(m3)	(Pa)	(°C)	a	b+aVs	b
	10.03.2014	10:13:20	30	110	0,023	263960	34,9	12728	1902	1608
	10.03.2014	10:50:00	40	280	0,083	232396	36,2	6544	1955	1926
	10.03.2014	12:09:25	20	125	0,037	236745	34,3	7226	1358	1088
	10.03.2014	12:35:35	30	85	0,018	203235	33,7	6386	981	867
	10.03.2014	13:11:45	40	135	0,068	210552	33,1	4330	823	530
	11.03.2014	09:29:25	20	340	0,138	162527	37,0	3484	1411	929
	11.03.2014	09:56:05	30	125	0,052	200714	37,2	3674	690	500
	11.03.2014	10:35:20	40	330	0,135	237876	36,8	5290	1741	1029
	11.03.2014	12:48:55	20	360	0,113	247585	35,1	5683	3366	2722
	11.03.2014	13:15:45	30	455	0,177	158574	35,8	5023	3463	2575
DrM G	11.03.2014	13:58:20	40	240	0,069	163429	35,5	7723	1426	891
	12.03.2014	09:18:10	20	210	0,042	180556	33,5	11079	1812	1345
	12.03.2014	09:44:00	30	225	0,084	242414	35,3	9195	1909	1135
	12.03.2014	10:19:20	40	515	0,156	161570	35,8	7956	3686	2446
	12.03.2014	11:59:05	20	105	0,030	228382	34,0	5205	1145	990
	12.03.2014	12:25:10	30	360	0,147	155256	35,3	4945	1286	559
	12.03.2014	13:01:00	40	310	0,101	146353	36,0	7206	1513	788
	13.03.2014	09:24:50	40	1140	0,456	217423	37,3	1141	1478	957
	13.03.2014	12:17:35	20	320	0,093	220076	38,5	5111	821	348
	13.03.2014	12:46:40	20	360	0,162	230567	38,8	3874	1665	1038
	13.03.2014	13:16:50	20	410	0,189	233099	38,8	2699	1413	902
	17.03.2014	09:19:15	20	245	0,191	227189	37,1	3705	1043	334
DrM F	17.03.2014	09:45:10	30	375	0,274	242982	37,6	3218	1192	311
	17.03.2014	10:20:30	40	235	0,162	208279	38,0	3767	947	335
	17.03.2014	11:51:30	20	230	0,138	216534	38,2	4747	1082	427

	17.03.2014	12:20:25	30	190	0,108	227278	38,4	5140	873	319
	17.03.2014	10:20:30	40	195	0,110	238635	38,2	4928	1030	486
	18.03.2014	09:24:35	20	245	0,111	229664	38,2	6227	1700	1009
	18.03.2014	09:53:45	30	165	0,071	243481	39,4	7139	1193	685
	18.03.2014	10:33:40	40	125	0,047	238911	39,6	8042	1333	955
	18.03.2014	11:35:55	20	135	0,050	255910	37,0	9054	1219	762
	18.03.2014	12:06:35	30	200	0,105	256321	36,1	6400	1256	585
	19.03.2014	09:31:40	20	675	0,198	223624	35,9	3219	1418	782
	19.03.2014	10:07:05	30	735	0,246	206091	36,7	3737	1036	118
	19.03.2014	10:46:50	30	880	0,309	210120	37,5	4464	2480	1102
	19.03.2014	11:45:10	30	365	0,122	218096	37,2	6651	1060	247
	19.03.2014	12:33:55	30	365	0,009	219329	36,3	3300	1782	1751
	19.03.2014	13:28:10	25	285	0,108	221184	35,3	5664	689	78
	24.03.2014	09:31:30	20	420	0,249	265561	33,4	2893	1060	339
	24.03.2014	10:01:15	30	565	0,321	272252	33,1	2950	1489	541
	24.03.2014	10:39:45	40	430	0,268	264344	33,1	2416	1325	678
	24.03.2014	11:37:50	20	360	0,200	264796	32,2	3615	1149	428
	24.03.2014	12:07:15	30	325	0,174	266100	32,2	3768	1304	648
	24.03.2014	12:47:15	40	295	0,159	264796	32,3	3721	1232	641
	26.03.2014	09:19:10	20	305	0,146	265551	36,4	4514	1325	664
	26.03.2014	09:48:55	30	270	0,131	265870	37,0	5051	1109	447
	26.03.2014	10:28:30	40	330	0,176	264518	36,7	3843	1360	685
	26.03.2014	11:39:05	20	270	0,135	269660	36,4	3404	1441	980
	26.03.2014	12:08:20	30	305	0,148	264618	36,1	5285	1206	425
	26.03.2014	12:47:20	40	290	0,141	264781	35,7	4797	1369	693
DrM N	28.03.2014	09:22:00	20	515	0,273	273461	33,8	2908	1324	528
	28.03.2014	09:51:25	30	635	0,335	276461	34,0	3324	1633	518
	28.03.2014	10:31:00	40	395	0,226	267290	34,2	3362	1313	554
	28.03.2014	12:35:55	20	490	0,275	270300	35,3	2552	1289	586
	28.03.2014	13:06:30	30	515	0,346	270414	35,5	1961	1194	516
	28.03.2014	13:48:00	40	590	0,379	275021	35,6	2111	1288	489
	31.03.2014	09:22:00	30	785	0,239	264271	34,4	4267	1580	558
	31.03.2014	09:58:05	30	630	0,191	264077	35,0	4036	1307	537
	31.03.2014	10:37:00	30	485	0,173	264473	35,1	3804	1081	422
	31.03.2014	11:54:30	30	355	0,120	264831	34,4	5305	1185	548
	31.03.2014	12:35:30	30	425	0,183	262371	34,8	4579	1343	506
	31.03.2014	13:14:20	30	390	0,196	259659	34,6	4005	1179	393
	31.03.2014	13:53:00	30	430	0,241	263345	34,1	3307	1253	456
	02.04.2014	11:49:45	20	595	0,279	251076	34,1	3549	1845	856
Markert	02.04.2014	12:18:20	30	340	0,180	262781	33,9	3834	1155	466
	02.04.2014	12:57:35	40	335	0,177	261701	33,7	3789	1155	483
	03.04.2014	09:26:05	20	520	0,299	267080	35,2	2422	1279	555

	03.04.2014	09:55:10	30	450	0,302	267719	36,6	2225	1036	364
	03.04.2014	10:34:15	40	490	0,313	268118	37,3	2651	1116	286
	03.04.2014	11:41:45	20	265	0,106	262663	33,9	6274	1235	573
	03.04.2014	12:11:05	30	270	0,119	264950	32,7	5436	1189	540
	03.04.2014	12:51:05	40	300	0,142	248050	31,5	4248	1399	795
	08.04.2014	09:16:10	20	250	0,105	265191	29,9	6657	1086	384
	08.04.2014	09:45:30	30	265	0,110	259867	28,3	5033	1442	886
	08.04.2014	10:24:10	40	325	0,160	260439	26,6	3804	1449	839
	08.04.2014	12:27:15	20	415	0,174	258452	25,8	4653	1650	843
	08.04.2014	12:56:55	30	350	0,173	259483	25,8	4765	1283	460
	09.04.2014	09:30:30	30	1240	0,356	260918	34,1	2901	1513	480
	09.04.2014	10:09:25	30	760	0,257	257570	34,4	2745	1270	565
	09.04.2014	10:48:40	30	860	0,401	260223	34,9	2093	1184	345
	09.04.2014	11:39:10	30	475	0,196	259607	35,1	2905	1236	667
	09.04.2014	12:18:00	30	485	0,231	257758	35,2	3111	1221	501
	09.04.2014	12:57:20	30	420	0,207	259412	35,4	3419	1247	540
	09.04.2014	13:37:50	30	440	0,225	260508	35,7	3166	1415	703
	09.04.2014	14:16:40	30	420	0,229	261476	35,7	2983	1366	683
	30.04.2014	09:46:10	40	615	0,229	266727	33,5	3494	1231	430
Markert	30.04.2014	12:57:40	40	310	0,048	242717	31,0	2661	1149	1022
	30.04.2014	14:08:40	40	1145	0,392	279565	35,7	3901	2171	640

Table 0.10: Data used in the calculation of specific cake resistance and medium resistance (part 2)

Cloth	Viscosity	Filt. Area	Solids Conc.	α	Rm	Regression coefficient
	(PaS)	(m2)	(kg/m3)	(m/kg)	(1/m)	
	0,00072	1	9,58	9,7E+11	5,9E+11	1,00
	0,00070	1	9,58	4,5E+11	6,4E+11	0,99
	0,00073	1	4,36	1,1E+12	3,5E+11	1,00
	0,00074	1	4,36	8,0E+11	2,4E+11	1,00
	0,00075	1	4,36	5,6E+11	1,5E+11	1,00
	0,00069	1	6,36	2,6E+11	2,2E+11	1,00
	0,00069	1	6,36	3,4E+11	1,5E+11	1,00
DrM G	0,00069	1	6,36	5,7E+11	3,5E+11	1,00
	0,00072	1	6,63	5,9E+11	9,4E+11	0,99
	0,00071	1	6,63	3,4E+11	5,8E+11	0,98
	0,00071	1	6,63	5,3E+11	2,0E+11	1,00
	0,00074	1	7,86	6,8E+11	3,3E+11	0,99
	0,00072	1	7,86	7,9E+11	3,8E+11	0,99
	0,00071	1	7,86	4,6E+11	5,6E+11	1,00

	0,00073	1	4,00	8,1E+11	3,1E+11	0,99
	0,00072	1	4,00	5,4E+11	1,2E+11	1,00
	0,00071	1	4,00	7,5E+11	1,6E+11	1,00
	0,00069	1	5,56	1,3E+11	3,0E+11	0,99
	0,00067	1	5,56	6,0E+11	1,1E+11	1,00
	0,00067	1	5,56	4,8E+11	3,6E+11	1,00
	0,00067	1	5,56	3,4E+11	3,1E+11	1,00
	0,00069	1	4,90	5,0E+11	1,1E+11	0,94
	0,00068	1	4,90	4,7E+11	1,1E+11	1,00
	0,00068	1	4,90	4,7E+11	1,0E+11	0,99
	0,00068	1	5,41	5,6E+11	1,4E+11	0,99
	0,00067	1	5,41	6,4E+11	1,1E+11	1,00
	0,00068	1	5,41	6,4E+11	1,7E+11	1,00
	0,00068	1	10,74	3,9E+11	3,4E+11	0,96
	0,00066	1	10,74	4,9E+11	2,5E+11	1,00
DrM F	0,00066	1	10,74	5,4E+11	3,5E+11	0,99
	0,00069	1	13,16	5,1E+11	2,8E+11	1,00
	0,00070	1	13,16	3,5E+11	2,1E+11	1,00
	0,00071	1	11,34	1,8E+11	2,5E+11	0,99
	0,00070	1	11,34	2,0E+11	3,5E+10	1,00
	0,00069	1	11,34	2,4E+11	3,4E+11	0,99
	0,00069	1	11,34	3,7E+11	7,8E+10	1,00
	0,00070	1	11,34	1,8E+11	5,5E+11	0,99
	0,00072	1	11,34	3,1E+11	2,4E+10	0,99
	0,00075	1	1,65	1,2E+12	1,2E+11	1,00
	0,00075	1	1,65	1,3E+12	2,0E+11	1,00
	0,00075	1	1,65	1,0E+12	2,4E+11	1,00
	0,00076	1	1,55	1,6E+12	1,5E+11	1,00
	0,00076	1	1,55	1,7E+12	2,3E+11	1,00
	0,00076	1	1,55	1,7E+12	2,2E+11	0,99
	0,00070	1	3,51	9,7E+11	2,5E+11	1,00
	0,00069	1	3,51	1,1E+12	1,7E+11	1,00
DrM N	0,00070	1	3,51	8,3E+11	2,6E+11	0,99
	0,00070	1	2,61	1,0E+12	3,8E+11	0,95
	0,00070	1	2,61	1,5E+12	1,6E+11	1,00
	0,00071	1	2,61	1,4E+12	2,6E+11	0,99
	0,00074	1	2,30	9,4E+11	2,0E+11	1,00
	0,00073	1	2,30	1,1E+12	1,9E+11	1,00
	0,00073	1	2,30	1,1E+12	2,0E+11	1,00
	0,00072	1	1,52	1,3E+12	2,2E+11	1,00
	0,00071	1	1,52	9,8E+11	2,0E+11	1,00

	0,00071	1	1,52	1,1E+12	1,9E+11	1,00
	0,00073	1	3,36	9,2E+11	2,0E+11	1,00
	0,00072	1	3,36	8,8E+11	2,0E+11	1,00
	0,00072	1	3,36	8,3E+11	1,6E+11	1,00
	0,00073	1	3,36	1,1E+12	2,0E+11	1,00
	0,00072	1	3,36	9,9E+11	1,8E+11	1,00
	0,00073	1	3,36	8,5E+11	1,4E+11	1,00
	0,00073	1	3,36	7,1E+11	1,6E+11	1,00
	0,00073	1	2,06	1,2E+12	2,9E+11	1,00
	0,00074	1	2,06	1,3E+12	1,7E+11	1,00
	0,00074	1	2,06	1,3E+12	1,7E+11	1,00
	0,00072	1	2,80	6,4E+11	2,1E+11	1,00
	0,00070	1	2,80	6,1E+11	1,4E+11	1,00
	0,00069	1	2,80	7,4E+11	1,1E+11	1,00
	0,00074	1	6,76	6,6E+11	2,0E+11	0,99
	0,00076	1	6,76	5,6E+11	1,9E+11	1,00
	0,00077	1	6,76	4,0E+11	2,5E+11	0,98
	0,00080	1	4,68	9,4E+11	1,3E+11	1,00
Markert	0,00083	1	4,68	6,7E+11	2,8E+11	0,99
	0,00086	1	4,68	4,9E+11	2,5E+11	0,99
	0,00087	1	3,51	7,8E+11	2,5E+11	1,00
	0,00087	1	3,51	8,0E+11	1,4E+11	1,00
	0,00073	1	2,68	7,7E+11	1,7E+11	1,00
	0,00073	1	2,68	7,2E+11	2,0E+11	1,00
	0,00072	1	2,68	5,6E+11	1,2E+11	1,00
	0,00072	1	2,68	7,8E+11	2,4E+11	1,00
	0,00072	1	2,06	1,1E+12	1,8E+11	1,00
	0,00071	1	2,06	1,2E+12	2,0E+11	1,00
	0,00071	1	2,06	1,1E+12	2,6E+11	1,00
	0,00071	1	2,06	1,1E+12	2,5E+11	1,00
	0,00074	1	4,29	5,9E+11	1,5E+11	1,00
Markert	0,00078	1	5,05	3,3E+11	3,2E+11	0,98
	0,00071	1	4,69	6,6E+11	2,5E+11	1,00

Note: *Measured values obtained for tests done on 20 minutes filtration runs was assumed for 30 and 40 minutes in order to estimate specific cake and medium resistances. Therefore only values for 20 minutes runs are shown in the report (as the remaining values are only estimates). See the following two tables for the measured data isolated.*

Table 0.11: Data from tests were samples were taken and analysed (part 1)

Cloth	Date	Time	dP	Temp.	pH	Solids conc. (slurry)	Acc. filtrate	Solids conc. (filtrate - 0)	Solids conc. (filtrate - 5)
			(bar)	(°C)		(g/l)	(m3)	(g/l)	(g/l)
DrM G	10.03.2014	12:09:25	2,37	34,3	9,75	4,36	0,33	0,031	0,016
	11.03.2014	09:29:30	1,63	37,0	9,57	6,36	0,43	0,019	0,017
	11.03.2014	12:48:55	2,48	35,1	9,65	6,63	0,28	0,019	0,016
	12.03.2014	09:18:15	1,81	33,5	9,62	7,86	0,26	0,621	0,017
	12.03.2014	11:59:05	2,28	34,0	9,72	4,00	0,38	0,022	0,013
DrM F	17.03.2014	09:19:20	2,27	37,1	9,44	4,90	0,51	0,696	0,149
	17.03.2014	11:51:30	2,17	38,2	9,44	5,41	0,44	0,710	0,106
	18.03.2014	09:24:40	2,30	38,2	9,34	10,74	0,36	1,621	0,088
	18.03.2014	11:35:55	2,56	37,0	9,74	13,16	0,31	0,926	0,044
DrM N	24.03.2014	09:31:35	2,66	33,4	9,09	1,65	0,54	0,044	0,019
	24.03.2014	11:37:50	2,65	32,2	9,11	1,55	0,49	0,015	0,008
	26.03.2014	09:19:10	2,66	36,4	9,33	3,51	0,42	0,015	0,013
	26.03.2014	11:39:05	2,70	36,4	9,35	2,61	0,44	0,016	0,011
	28.03.2014	09:22:05	2,73	33,8	9,16	2,30	0,51	0,018	0,010
	28.03.2014	12:35:55	2,70	35,3	9,16	1,52	0,54	0,007	0,014
Markert	02.04.2014	11:49:45	2,511	34,1	9,17	2,06	0,45	0,045	0,013
	03.04.2014	09:26:05	2,671	35,2	9,26	2,80	0,56	0,019	0,012
	03.04.2014	11:41:45	2,627	33,9	9,44	6,76	0,37	0,013	0,012
	08.04.2014	09:16:10	2,652	29,9	9,42	4,68	0,37	0,005	0,006
	08.04.2014	12:27:15	2,585	25,8	9,23	3,51	0,40	0,001	0,004

Table 0.12: Data from tests were samples were taken and analysed (part 2)

Cloth	Dry cake mass	Cake moisture content	α	Rm	Regression coefficient (R)	%dP alpha	%dp R
	(kg)	(%)	(m/kg)	(1/m)		(%)	(%)
DrM G	1,4	81,49	1,07E+12	3,52E+11	1,00	58,19	41,81
	2,7	82,29	2,57E+11	2,18E+11	1,00	56,24	43,76
	1,8	81,60	5,92E+11	9,39E+11	0,99	34,76	65,24
	1,9	80,01	6,85E+11	3,27E+11	0,99	57,96	42,04
	1,5	82,08	8,08E+11	3,08E+11	0,99	54,97	45,03
DrM F	2,3	83,41	4,97E+11	1,10E+11	0,94	84,59	15,41
	2,2	82,99	5,62E+11	1,37E+11	0,99	81,07	18,93
	3,4	80,05	3,93E+11	3,42E+11	0,96	65,08	34,92
	3,9	80,27	5,08E+11	2,81E+11	1,00	76,72	23,28
DrM N	0,9	85,85	1,25E+12	1,21E+11	1,00	81,92	18,08

	0,7	85,13	1,62E+12	1,49E+11	1,00	79,44	20,56
	1,5	83,25	9,75E+11	2,52E+11	1,00	71,45	28,55
	1,1	83,83	1,00E+12	3,77E+11	0,95	56,09	43,91
	1,2	82,66	9,38E+11	1,96E+11	1,00	74,48	25,52
	0,8	83,87	1,27E+12	2,21E+11	1,00	70,39	29,61
Markert	0,9	84,59	1,18E+12	2,93E+11	1,00	67,99	32,01
	1,5	83,36	6,45E+11	2,07E+11	1,00	71,58	28,42
	2,5	83,13	6,63E+11	2,05E+11	0,99	76,51	23,49
	1,7	84,26	9,44E+11	1,27E+11	1,00	84,12	15,88
	1,4	85,67	7,82E+11	2,49E+11	1,00	67,28	32,72

Table 0.13: Average values for the above data (part 1)

Cloth	dP	Temp.	pH	Solids conc. (slurry)	Acc. filtrate	Solids conc. (filtrate - 0)	Solids conc. (filtrate - 5)
	(bar)	(°C)		(g/l)	(m3)	(g/l)	(g/l)
DrM G	2,25	34,38	9,68	6,47	0,31	0,14	0,02
DrM F	2,32	37,62	9,49	8,55	0,41	0,99	0,10
DrM N	2,68	34,57	9,20	2,19	0,49	0,02	0,01
Markert	2,61	31,79	9,30	3,96	0,43	0,02	0,01

Table 0.14: Average values for the above data (part 2)

Cloth	Dry cake mass	Cake moisture content	α	Rm
	(kg)	(%)	(m/kg)	(1/m)
DrM G	1,87	0,81	7,91E+11	5,25E+11
DrM F	2,95	0,82	4,90E+11	2,18E+11
DrM N	1,04	0,84	1,18E+12	2,19E+11
Markert	1,62	0,84	8,43E+11	2,16E+11

Table 0.15: Standard deviation associated in calculating the averages in table 0.13

Cloth	dP	Temp.	pH	Solids conc. (slurry)	Acc. filtrate	Solids conc. (filtrate - 0)	Solids conc. (filtrate - 5)
	(bar)	(°C)		(g/l)	(m3)	(g/l)	(g/l)
DrM G	0,43	1,43	0,07	1,92	0,08	0,22	0,001
DrM F	0,14	0,60	0,15	3,51	0,08	0,38	0,038
DrM N	0,03	1,57	0,10	0,72	0,05	0,01	0,004
Markert	0,06	3,49	0,11	1,64	0,07	0,02	0,004

Table 0.16: Standard deviation associated in calculating the averages in table 0.14

Cloth	Dry cake mass	Cake moisture content	α	Rm
	(kg)	(%)	(m/kg)	(1/m)
DrM G	0,43	0,0074	3,43E+11	3,19E+11
DrM F	0,76	0,0153	6,11E+10	9,72E+10
DrM N	0,25	0,0108	2,38E+11	8,29E+10
Markert	0,52	0,0091	2,00E+11	5,50E+10

Appendix D – Data Analysis

D1. Viscosity Measurement
Calculation of Viscosity

Viscosity is measured through the following relationship

$$\mu_{t,1} = \mu_{t,H2O} \frac{T_{t,1}\delta_{t,1}}{T_{t,H2O}\delta_{t,H2O}}$$

If calculating the viscosity of filtrate at 35 °C, where the average time to move between two points in the viscometer ($T_{32,1}$) recorded is 2,86 minutes and the specific weight ($\delta_{t,1}$) is measured as 1,03 g/cm³, the following measurements can be used (the determined values are from the laboratory cloth tests):

Table 0.17: Viscosity and specific weight of distilled water at different temperatures (Lide, 1980)

Tabell 1. Viskositet av destillert vann i området 15 til 100 °C. Fra Handbook of Chemistry and Physics, 61. utgave, 1980.

Temp. °C	Viskositet cP	Temp. °C	Viskositet cP	Temp. °C	Viskositet cP
15	1,139	45	0,5960	75	0,3781
20	1,002	50	0,5468	80	0,3547
25	0,8904	55	0,5040	85	0,3337
30	0,7975	60	0,4665	90	0,3147
35	0,7194	65	0,4335	95	0,2975
40	0,6529	70	0,4042	100	0,2818

Tabell 2. Tetthet av rent vann fritt for luft ved varierende temperaturer. Fra Handbook of Chemistry and Physics, 61. utgave, 1980.

Temp. °C	Tetthet g/cm³	Temp. °C	Tetthet g/cm³	Temp. °C	Tetthet g/cm³
15	0,99913	45	0,99025	75	0,97489
20	0,99823	50	0,98807	80	0,97183
25	0,99707	55	0,98573	85	0,96865
30	0,99567	60	0,98324	90	0,96534
35	0,99406	65	0,98059	95	0,96192
40	0,99224	70	0,97781	100	0,95838

Obtaining values from tables above:

The viscosity of distilled water at 35 °C ($\mu_{35,H2O}$) is 0,7194 cP. The specific weight of distilled water at 35 °C ($\delta_{35,H2O}$) is 0,99406.
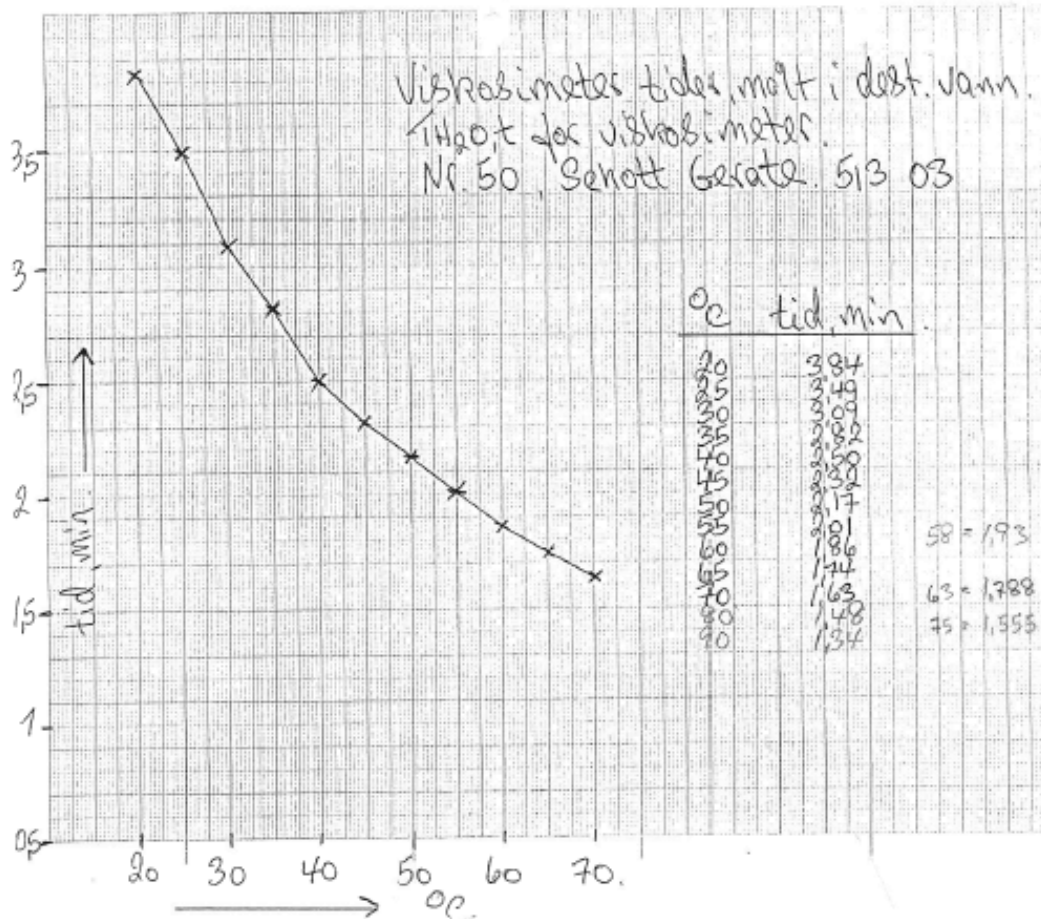
Figure 0.9: The relationship between time and temperature for the sized 50 Senott Gerate viscometer (calibrated at Nikkelverk)

The viscometer time for distilled water at 35 °C ($T_{35,H2O}$) seen from the trend above is 2,82 minutes. The calculated viscosity is therefore:

$$\mu_{32,1} = (0{,}7194)\frac{(2{,}86)(1{,}03)}{(2{,}82)(0{,}99406)}$$

$$= 0{,}7560 \; cP$$

The relationship between viscosity and temperature for distilled water given by Lide (1980) was used to extrapolate viscosity values for the slurry filtrate on the filtration rig.

Calculated using the above method, the viscosity for the slurry filtrate (μ_{35}) was 0,7194 PaS. If the operating temperature during a filtration experiment was, for example, 32,4 °C, the viscosity was interpolated between 30 °C and 35 °C.

$$\mu_{32,4} = \mu_{30,H2O} - (30°C - 32°C)\frac{\mu_{30,H2O} - \mu_{35,H2O}}{30°C - 35°C}$$

$$= 0{,}7975 - (30 - 32{,}4)\frac{0{,}7975 - 0{,}7194}{30 - 35}$$

$$= 0{,}76 \; cP$$

124

D2. Specific Cake Resistance (α) and Material Resistance (R) Calculations – cloth screening laboratory tests

The following relationship is developed in the literature review:

$$\frac{t}{V} = \frac{\alpha\mu c}{2A^2 \Delta p}V + \frac{\mu R}{A\Delta p}$$

Table 0.18: Time and filtrate volume data from experiment 1 (cloth DrM G 11 U 010)

Time (min)	Volume (ml)
0,04	10
0,10	20
0,16	30
0,25	40
0,37	50
0,49	60
0,64	70

Converting minutes to seconds and ml to m^3, a slope can be made:
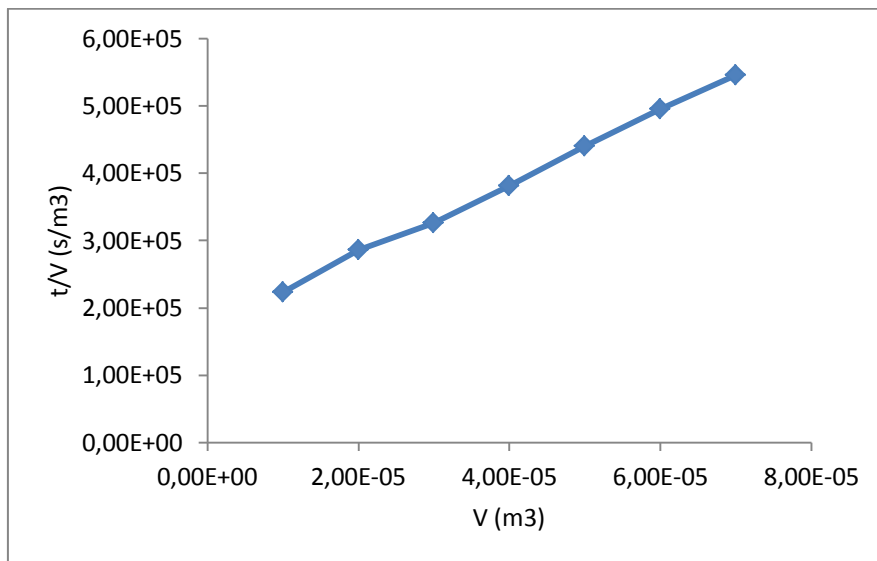
Figure 0.10: V vs t/V for cloth DrM G 11 U 010

Excel uses linear regression to calculate the slope (function: STIGNINGSTALL) and y-intercept (function: SKÆRINGSPUNKT).

The slope value from this data is given as:

$$m = 5,35 \times 10^9$$

and the y-intercept is given as:

$$c = 1,71 \times 10^5$$

Table 0.19: Constant values calculated for experiment

Filter area	m2	0,001256
Conc. dry solids in susp.	kg/m3	6,801
Viscosity	PaS	0,00075775
Pressure drop	Pa	85000
Temp. suspension	°C	32

Given the slope value, α can be calculated:

$$\alpha = \text{m} \frac{2A^2 \Delta p}{\mu c}$$

$$= (5,35 \text{ x } 10^9) \frac{(2*0,001256^2)(85000)}{(0,00075775)(6,801)}$$

$$= 2,78 \text{ x } 10^{11} \text{ m/kg}$$

And *R* can be calculated where:

$$R = C \frac{A \Delta p}{\mu}$$

$$= (1,71 \text{ x } 10^5) \frac{0,001256 * 85000}{0,00075775}$$

$$= 2,41 \text{ x } 10^{10} \text{ m}^{-1}$$

D3. Specific Cake Resistance (α) and Material Resistance (R) Calculations – filter rig operation

A worked example is shown from calculation using cloth Markert PPV 2737.

The following relationship is developed in the literature whereby the applied constant pressure period is preceded with a period whereby the pressure drop is gradually increased from a low value (Svarovsky, 2000).

$$\frac{t - t_s}{V - V_s} = \frac{\alpha \mu c}{2A^2 \Delta p} (V + V_s) + \frac{\mu R}{A \Delta p}$$

The pressure drop is plotted as a function of time:
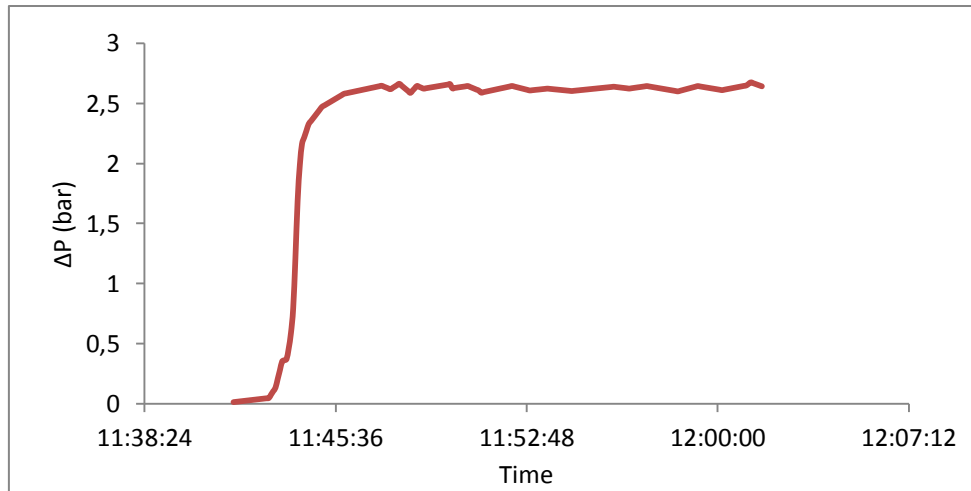
Figure 0.11: The change in pressure drop during filtration

The period whereby the pressure drop attempts to remain constant is enlarged:
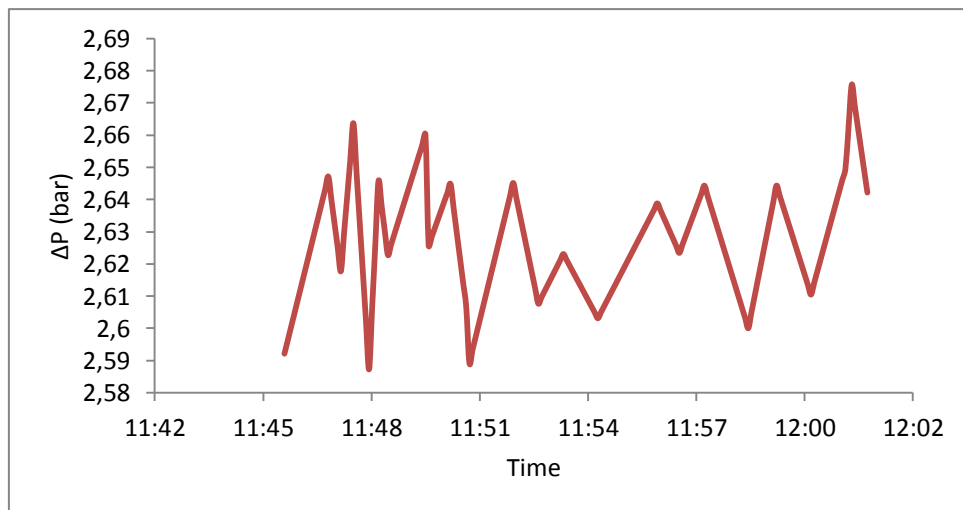
Figure 0.12: Fluctuation of pressure drop within a range of 0,1 bar

The volume of filtrate attained at the start of this period (V_s), and the time taken to reach this period (t_s) are noted:

$$V_s = 0,10551261 \ m^3$$

$$t_s = 265 \ seconds$$

For the range of time (t) and volume data points (V) (see the electronic appendix), a new set of data is calculated and plotted: $\left(\frac{t-t_s}{V-V_s}\right)$ is calculated and plotted against the volume data points:

127
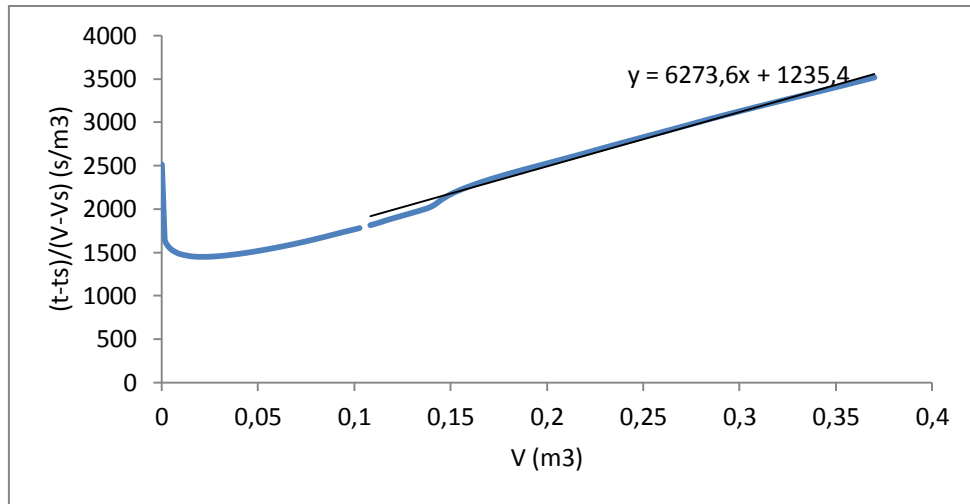
Figure 0.13 : $(\frac{t-t_s}{V-V_s})$ is calculated and plotted against the volume data points

Excel uses linear regression to calculate the slope (function: STIGNINGSTALL) and y-intercept (function: SKÆRINGSPUNKT) of the data points *after* V_s and t_s (i.e. in the period where the pressure drop is reasonably constant).

Multiplying out the terms, the slope is thus represented as:

$$m = \frac{\alpha \mu c}{2A^2 \Delta p}$$

$$= 6273,59$$

while the intercept is represented as:

$$C = \frac{\alpha \mu c}{2A^2 \Delta p} V_s + \frac{\mu R}{A \Delta p}$$

$$= 1235,43$$

The filter area of the filter rig is constant and known. The concentration of dry solids in suspension is determined from filtration and drying (as mentioned in the experimental section). The temperature and pressure drop is taken as the average of the data in the reasonably constant pressure period. The viscosity is extrapolated according to this temperature. The data is given below.

Table 0.20: Constant values used to calculate specific cake resistance and medium resistance

Filter area	m2	1
Conc. dry solids in susp.	kg/m3	6,76
Viscosity	PaS	0,00074
Pressure drop	Pa	262663,5
Temp. suspension	°C	33,9

The specific cake resistance (α) and medium resistance (R_m) was then calculated whereby:

128

$$\alpha = m \frac{2A^2 \Delta p}{\mu c}$$

$$= 6273,59 \frac{(2*1^2)(262663,5)}{(0,00074)(6,76)}$$

$$= 6,59 \times 10^{11} \, \text{m/kg}$$

$$R_m = (C - mV_s)\left(\frac{A\Delta p}{\mu}\right)$$

$$= (1235,43 - 6273,59 * 0,10551261)\left(\frac{1*262663,5}{0,00074}\right)$$

$$= 2,04 \times 10^{11} \, \text{m}^{-1}$$
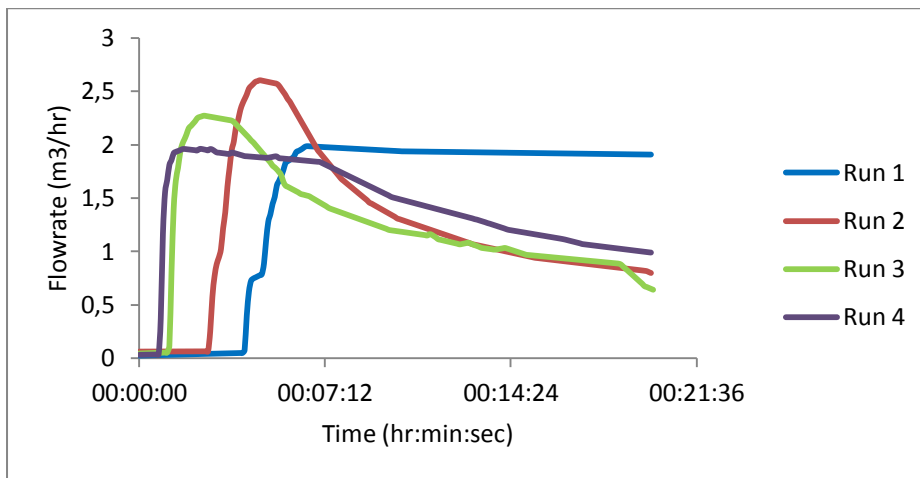
Flowrate trends of filtrate for various runs for DrM G
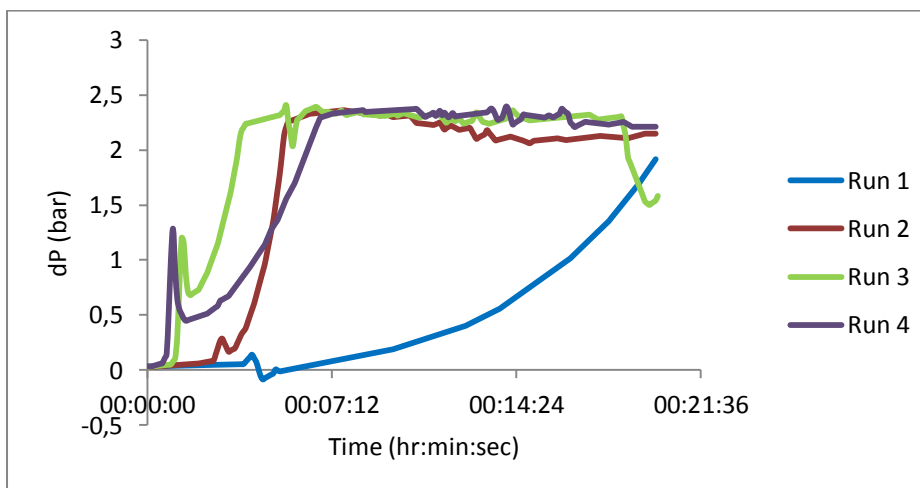
Pressure drop over filter trends for various runs for DrM G
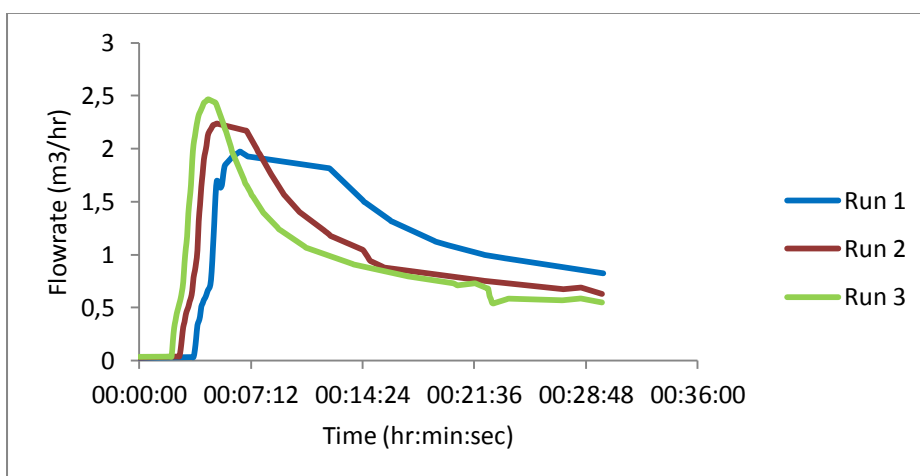
Flowrate trends of filtrate for various runs for DrM F
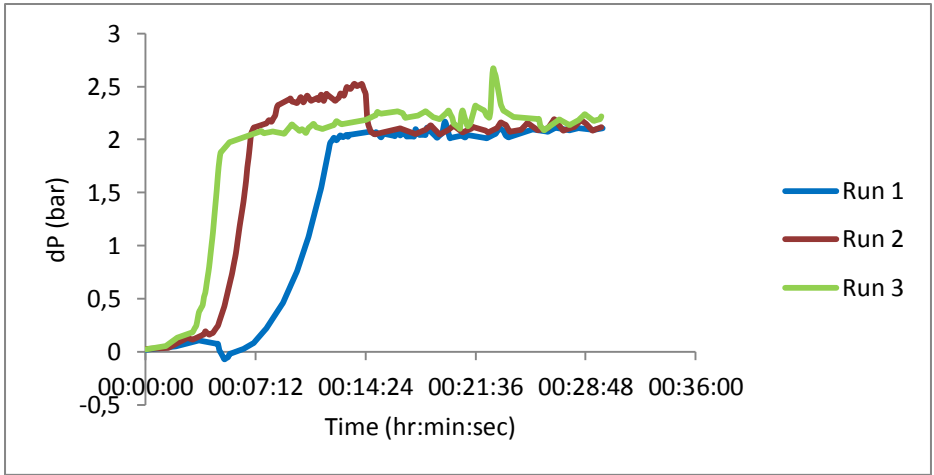
Pressure drop over filter trends for various runs for DrM F
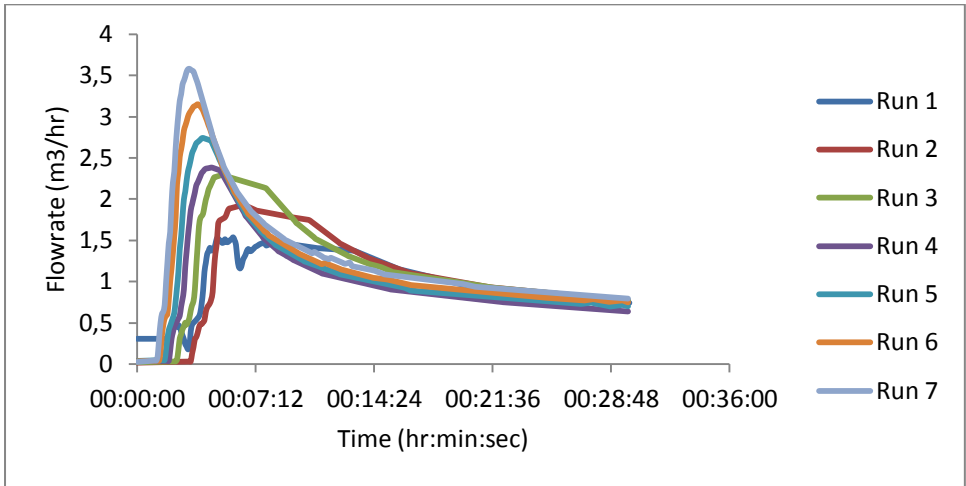
Flowrate trends of filtrate for various runs for DrM N
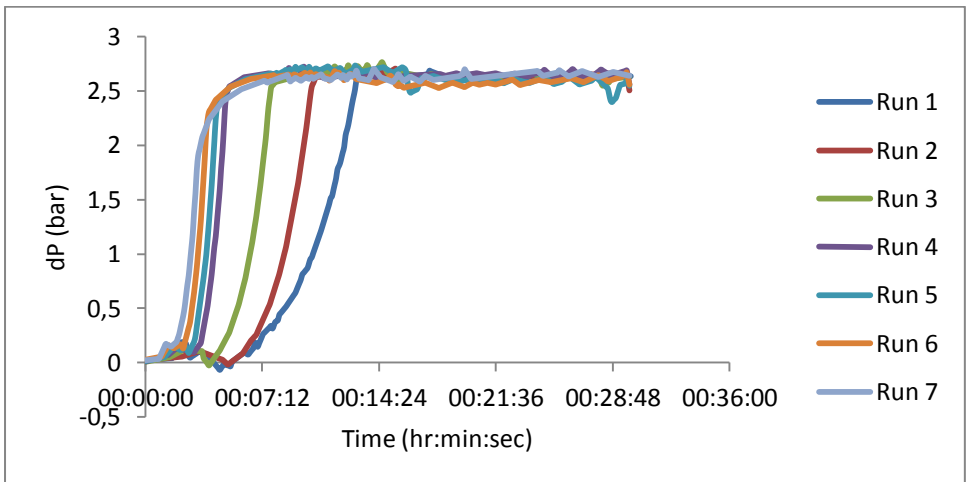
Pressure drop over filter trends for various runs for DrM N

Appendix F – Malvern Particle Size Analyses and SEM pictures
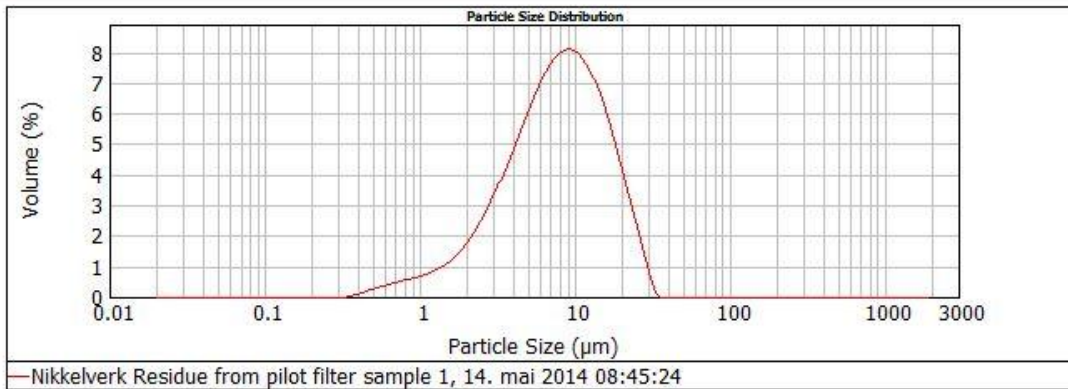
Figure 0.14: PSD of sample 1
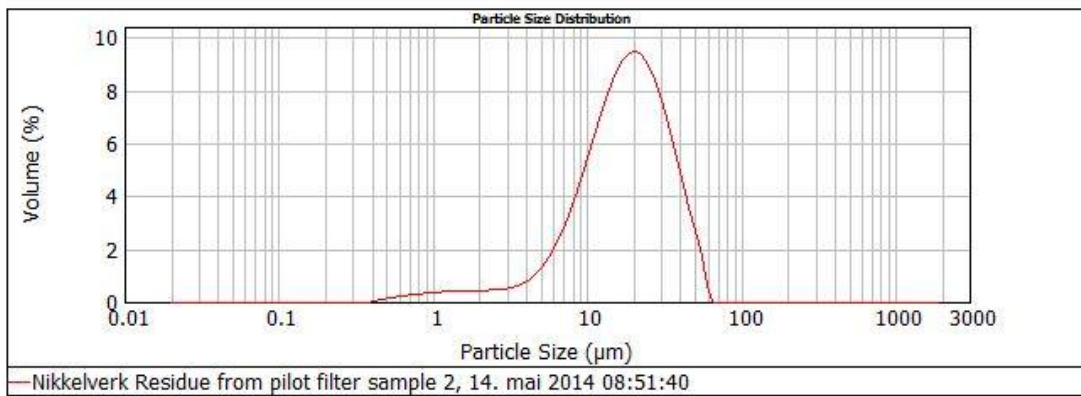
Figure 0.15: PSD of sample 2
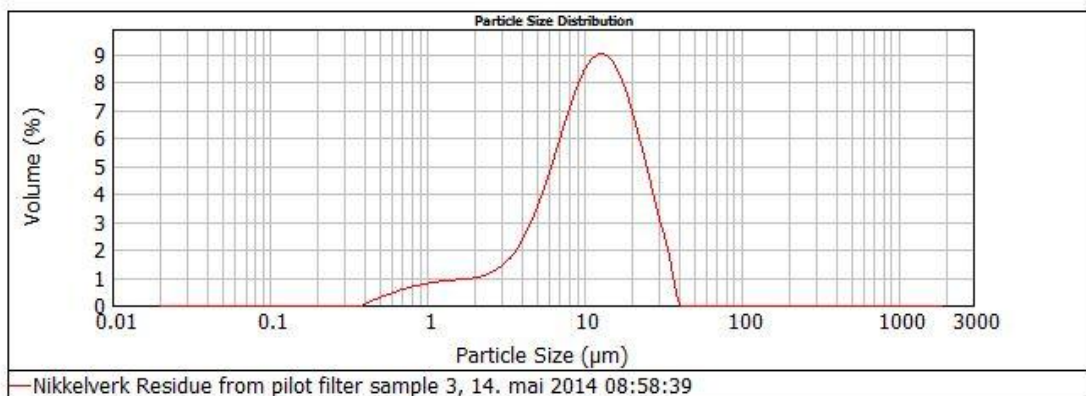
Figure 0.16: PSD of sample 3

d(0.1): 3.117 um   d(0.5): 10.338 um   d(0.9): 21.945 um
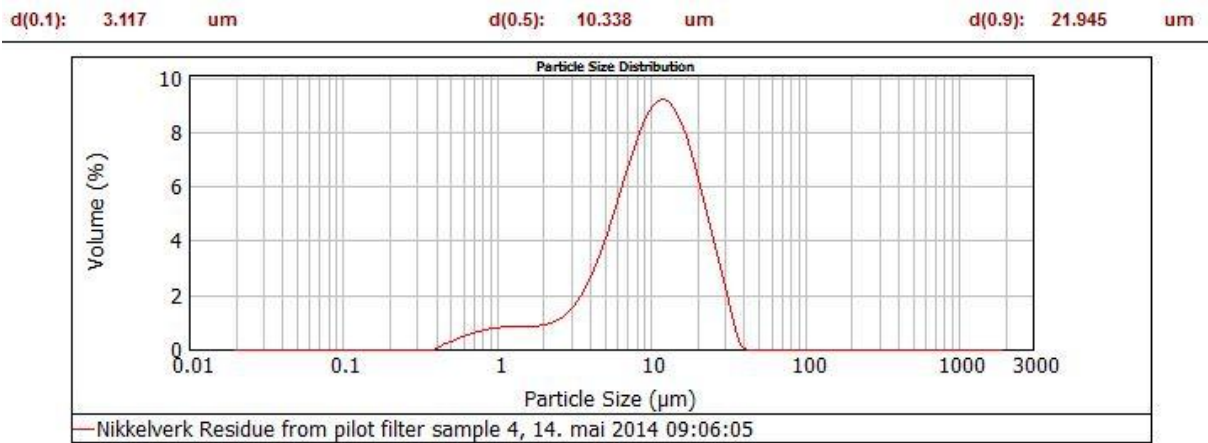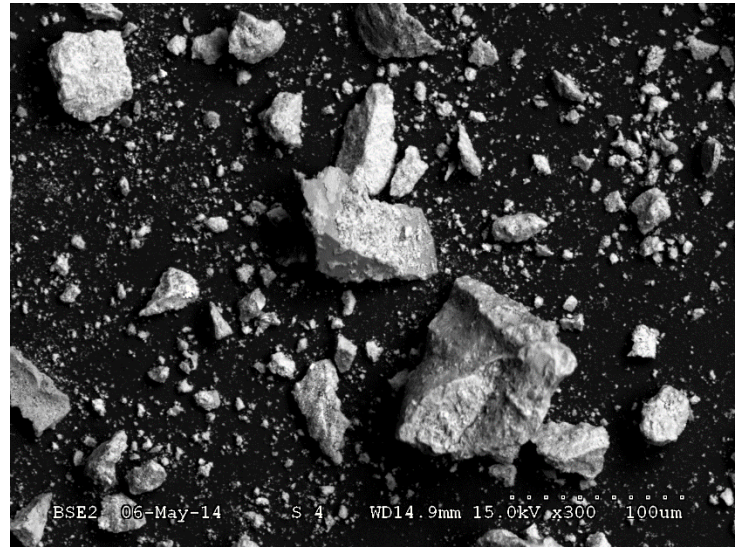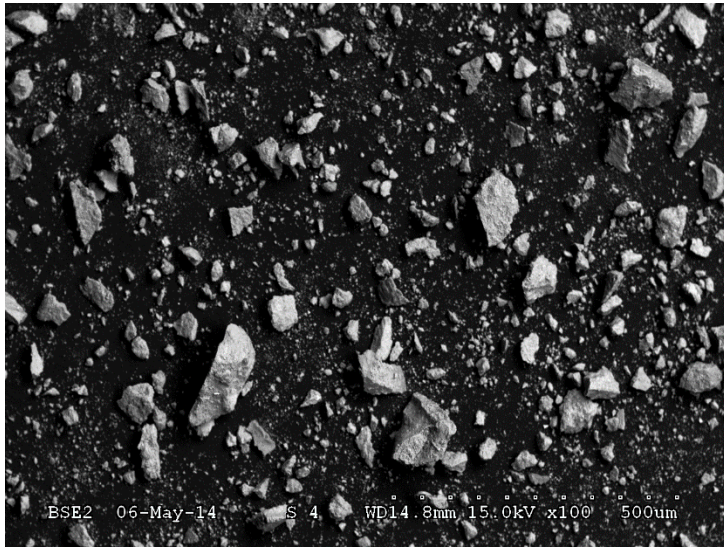
Figure 0.17: PSD of sample 4
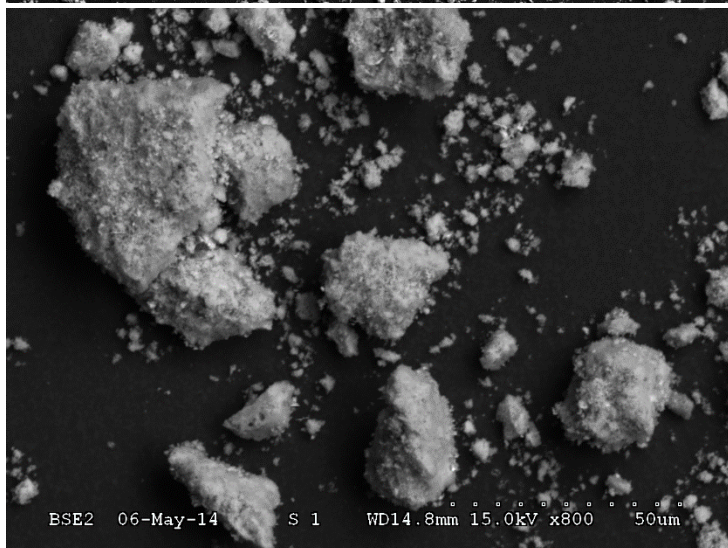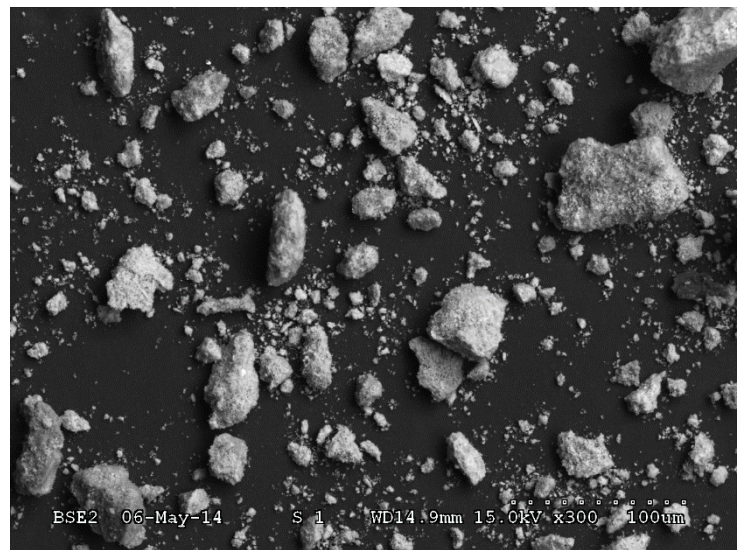
Figure 0.18: Images taken of sample 1 with magnification 100x, 300x, 800x og 1500x using a Scanning Electron Microscope
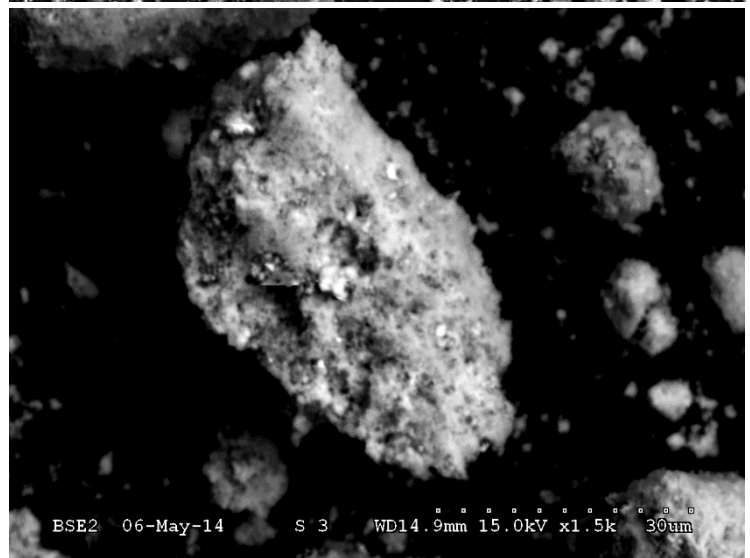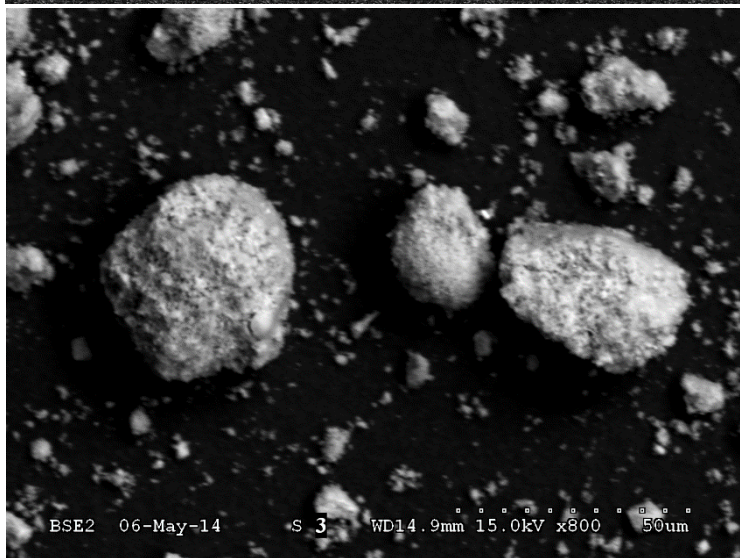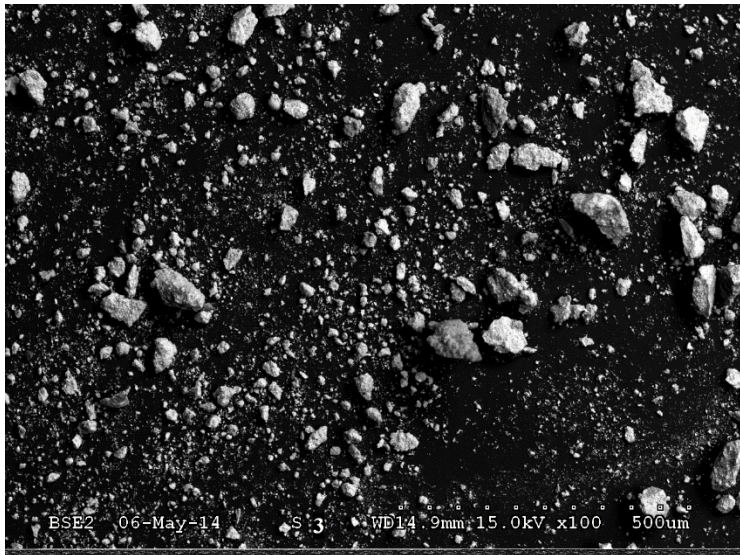
Figure 0.19: Images taken of sample 2 with magnification 100x, 300x, 800x og 1500x using a Scanning Electron Microscope
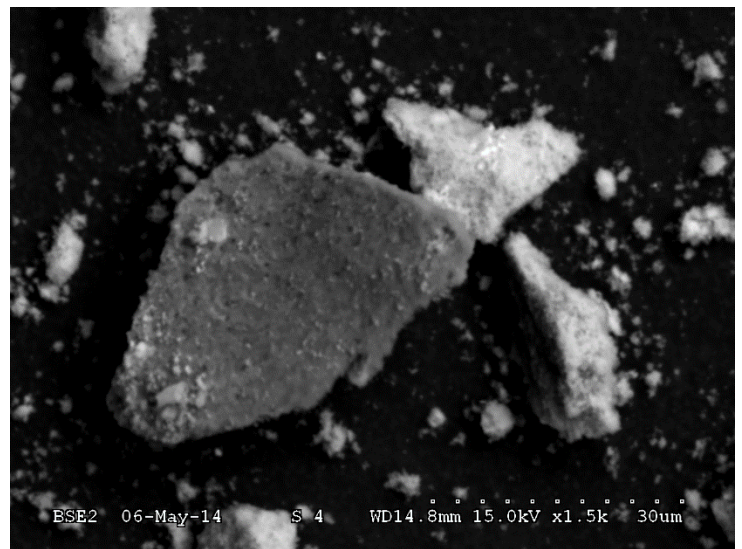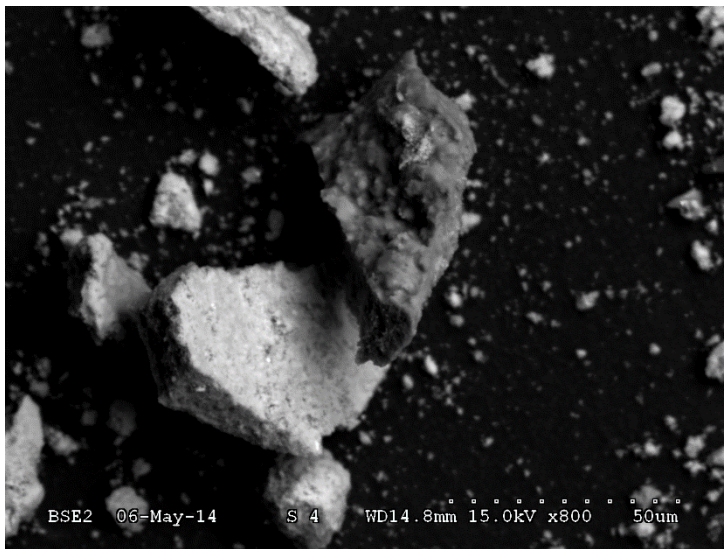
Figure 0.20: Images taken of sample 3 with magnification 100x, 300x, 800x og 1500x using a Scanning Electron Microscope